THÈSE DE DOCTORAT DE
SORBONNE UNIVERSITÉ

Spécialité : Electroniques et Communications

Ecole doctorale : EDITE ED 130

Présentée par

Amel TIBHIRT

Pour obtenir le grade de

DOCTEUR de SORBONNE UNIVERSITE

Mitigation of Cross-link Interference for MIMO TDD Dynamic Systems in 5G+ Networks

---

soutenue le 16 janvier 2024, devant le jury composé de :

Prof. Dirk SLOCK	EURECOM, France	Examinateur, Directeur de thèse
Dr. Yi YUAN-WU	Orange Labs, France	Examinatrice, Co-encadrante de thèse
Dr.Rita IBRAHIM	Orange Labs, France	Examinatrice, Co-encadrante de thèse
Prof. Pascal CHEVALIER	Cnam, France	Examinateur, Raporteur
Prof. Assaad MOHAMAD	CentraleSupélec, France	Examinateur, Rapporteur
Prof. Lina MROUEH	ISEP, France	Examinatrice, Présidente du jury
Dr. Raphaël VISOZ	Orange Labs, France	Examinateur

Titre : Réduction de l'Interférence des Liens Croisés pour les Systèmes MIMO TDD Dynamique dans les Réseaux 5G+.

Mots-clés : TDD dynamique, Interférence des liens croisés, rang réduit, MIMO, beamforming, degré de liberté, somme des débits.

Résumé : Le TDD dynamique joue un rôle crucial dans les réseaux 5G, adaptant les ressources aux besoins variés. Il améliore l'éfficacité spectrale en allouant dynamiquement des créneaux horaires pour les transmissions montantes et descendantes en fonction de la demande de trafic et des conditions de canal. Cette allocation dynamique de fréquence assure une utilisation efficace du spectre et prend en charge une connectivité massive, une latence faible et les exigences de la qualité de service. Son rôle dans l'agrégation de porteuses maximise les débits de données et la capacité du réseau, soulignant son importance dans les technologies de communication sans fil avancées. Cependant, le TDD dynamique est confronté à un défi majeur : l'Interférence des liens croisés. Ce type d'interférence se produit lorsque les transmissions montantes et descendantes partagent les mêmes bandes de fréquences, provoquant des interférences. Cette interférence comprend l'interférence de Station de Base à Station de Base (BS-to-BS) ou du lien descendant au lien montant (DL-to-UL) ainsi que l'interférence d'Équipement Utilisateur à Équipement Utilisateur (UE-to-UE) ou du lien montant vers le lien descendant (UL-to-DL). Dans l'interférence DL-to-UL, les transmissions descendantes débordent dans les bandes des transmissions montantes, dégradant la communication montante. À l'inverse, l'interférence UL-to-DL se produit lorsque les transmissions montantes interfèrent avec la réception des transmissions descendantes. Gérer efficacement ces interférences est crucial pour la performance et la fiabilité d'un système TDD dynamique.

Ce mémoire vise à libérer tout le potentiel du TDD dynamique en surmontant les défis posés par les interférence des liens croisés grâce à une analyse rigoureuse et des méthodologies innovantes. La recherche ne se contente pas de faire progresser la technologie TDD dynamique, elle pionnière des solutions applicables à divers contextes de communication, stimulant des stratégies innovantes d'alignment d'interférence dans des scénarios variés.
Le mémoire se divise en plusieurs parties. La première pose les bases avec la définition du problème et les concepts théoriques essentiels. La deuxième partie examine les conditions de faisabilité de l'alignement des interférences. Ces conditions sont exprimées en fonction de la dimension du problème et établissent le degré de liberté (DoF) atteignable, représentant le nombre de flux de données possible. Elle explore l'alignement d'interférence dans des scénarios centralisés, en considérant à la fois les canaux MIMO en rang complet et réduit, et aborde des complexités du monde réel. De plus, elle étend l'exploration à un scénario distribué, offrant

une compréhension réaliste des complexités de la communication. La troisième partie se concentre sur les techniques d'optimisation, en particulier le beamforming. Elle introduit le zeroforcing beamforming pour les utilisateurs, alignant l'interférence dans les systèmes TDD dynamique. Elle met l'accent sur l'impact de l'interférence des liens croisés entre utilisateurs et présente les améliorations apportées par les algorithmes WMMSE. De plus, elle explore l'optimisation de l'allocation de puissance en utilisant l'algorithme water-filling, évaluant la performance de zeroforcing beamforming et l'agorithme WMMSE en fonction de cette approche d'optimisation de puissance.

Title: Mitigation of crosslink interference for MIMO TDD Dynamic Systems in 5G+ Networks.

Keywords: Dynamic Time Division Duplexing (DynTDD), Cross Link Interference (CLI), rank deficient, MIMO, beamforming, Degree of Freedom (DoF), sum rate.

Abstract: Dynamic Time Division Duplexing (DynTDD) is pivotal in 5^{th} generation (5G) networks, adapting resources to diverse needs. It enhances Spectral Efficiency (SE) by dynamically allocating time slots for Uplink (UL) and Downlink (DL) transmissions based on traffic demand and channel conditions. This dynamic frequency allocation ensures efficient spectrum use and supports massive connectivity, low latency, and Quality-of-Service (QoS) requirements. Its role in carrier aggregation maximizes data rates and capacity, highlighting its importance in advanced wireless communication technologies. However, DynTDD faces a significant challenge: cross-link interference (CLI). CLI occurs when UL and DL transmissions share the same frequency bands, leading to interference. CLI comprises base station to base station (BS-to-BS) or downlink to uplink (DL-to-UL) interference and user equipment to user equipment (UE-to-UE) or uplink to downlink (UL-to-DL) interference. In DL-to-UL interference, DL transmissions spill into UL bands, degrading UL communication. Conversely, UL-to-DL interference occurs when UL transmissions interfere with DL reception. Effectively managing CLI is crucial for DynTDD's performance and reliability.

This thesis aims to unleash the full potential of DynTDD by overcoming CLI challenges through rigorous analysis and innovative methodologies. The research not only advances DynTDD technology but also pioneers solutions applicable to various communication contexts, driving innovative interference alignment strategies across diverse scenarios. The study in this thesis is divided into multiple segments. The first part establishes the foundation with the problem definition and essential theoretical concepts. The second part delves into the conditions determining the feasibility of interference alignment. These conditions are expressed in terms of the problem dimension and establish the achievable Degree of Freedom (DoF), representing the number of data streams. It explores interference alignment in centralized scenarios, considering both full-rank and reduced-rank Multiple-Input Multiple-Output (MIMO) Interference Broadcast Multiple Access Channel-Interference Channel (IBMAC-IC), addressing real-world complexities. Additionally, it extends the exploration to a distributed scenario, providing a realistic understanding of communication complexities. The third part focuses on optimization techniques, specifically beamforming. It introduces Zero Forcing (ZF) beamforming for both DL and UL User Equipement (UE)s to align CLI in DynTDD systems. It emphasizes the impact of UE-to-UE interfer-

ence and presents improvements brought by the Weighted Minimum Mean Square Error (WMMSE) algorithms. Furthermore, it explores power allocation optimization using the water-filling algorithm.

"Live as if you were to die tomorrow. Learn as if you were to live forever."

M. Gandhi

Acknowledgments

This PhD was a rich journey for me. A journey that I have not accomplish alone. I would like to express my deepest and sincere thanks to:

... **Dirk Slock**, my supervisor, for his never-ending guidance, inspiring thoughts, boundless help and assistance; I am honored to do my thesis under his supervision and fortunate to learn from his constructive criticism and scientific rigor; to **Yi Yuan-Wu**, my co-supervisor, for always being there to advise me, for her constant technical guidance and kind attitude; to **Rita Ibrahim** for joining me on this journey as a co-supervisor, your valuable advice, unwavering support, and expertise have greatly enriched this research endeavor; to **Raphaël Visoz** and **Lina Mroueh**, my jury members who have closely followed the progress of my thesis since the very first year, for their positive comments to my work; to **Pascal Chevalier** and **Mohamad Assaad**, for taking part of the jury members, and for the time they will spend to evaluate my works.

... all the members of Orange Labs RAP team, namely, the team manager **Pierre Dubois**, for providing an adequate working environment and support; my dear colleagues/friends, **Imène**, **Meriem**, **Youssef**, **Demba**, **Julien**, **Ali**, **Nathalie**, **Joe**, **Lucas**, **Thierry**, and **Stephan**, for the constructive exchanges and the memorable time we spent together; to my colleagues in EURECOM, namely, **Robert**, **Roya**, **Alireza** and **Sophia** for being supportive.

... all my friends, who always believed in me, for their encouragement and support, especially, **Étienne**, **Kary**, **Rahma**, **Imène**, **Mimi**, **Ahmad**, **Tanguy**, **Yi**, **Maya** and **Nicolas**, and for all the fun and positive vibes we shared together.

Last but not least, to my parents, my everything, for their advice, encouragement and moral support throughout my existence; to my wonderful sisters **Soumeya**, **Lynda**, **Souad**, **Wissem**, and my brother **Ibrahim**, for always motivating me and being there for me, for their good influence and positiveness; to **Ayla** my niece; to all my relatives.

Thank you all.

Contents

Acronyms

3GPP	3rd Generation Partnership Project.
5G	5^{th} generation.
BS	Base Station.
BS-to-BS	base station to base station.
CLI	cross-link interference.
CSI	Channel State Information.
CSIT	Channel State Information at the Transmitter.
D2D	device-to-device.
DAA	Distributed Antenna Array.
DIA	Distributed Interference Alignment.
DL	Downlink.
DL-to-UL	downlink to uplink.
DoF	Degree of Freedom.
DUDe	downlink/uplink decoupling.
DynTDD	Dynamic Time Division Duplexing.

HetNets	Heterogeneous Networks.
i.i.d.	independent and identically distributed.
IBC	Interfering Broadcast Channel.
IBMAC	Interference Broadcast Multiple Access Channel.
IBMAC-IC	Interference Broadcast Multiple Access Channel-Interference Channel.
IC	Interference Channel.
LHS	Left Hand Side.
ma-MIMO	Massive MIMO.
MIMO	Multiple-Input Multiple-Output.
mMTC	massive Machine-Type Communication.
MS	Mobile Station.
QoS	Quality-of-Service.
RHS	Right Hand Side.
Rx	Receiver.
SE	Spectral Efficiency.
SINR	Signal-to-Interference-plus-Noise Ratio.
SNR	Signal-to-Noise Ratio.
SU	Single User.
SVD	Singular Value Decomposition.

TDD	Time Division Duplexing.
Tx	Transmitter.
UDNs	ultra-densely deployed networks.
UE	User Equipement.
UE-to-UE	user equipment to user equipment.
UL	Uplink.
UL-to-DL	uplink to downlink.
WMMSE	Weighted Minimum Mean Square Error.
ZF	Zero Forcing.

List of Figures

List of Tables

List of Algorithms

Part I

Introduction

Chapter 1

Motivation and Related Works

1.1 Motivation

Dynamic Time Division Duplexing (DynTDD) is a communication technique used in wireless networks to enhance Spectral Efficiency (SE) by dynamically allocating time slots for Uplink (UL) and Downlink (DL) transmissions based on the traffic demand and channel conditions. Unlike traditional Time Division Duplexing (TDD) where UL and DL transmissions share the same frequency band and are separated by time slots, DynTDD adapts the allocation of time slots according to the varying communication requirements of users and the changing radio channel characteristics. In DynTDD, the allocation of time slots for UL and DL transmissions is not fixed but is adjusted dynamically in response to the network traffic and channel quality. The DynTDD system offers seven distinct DL/UL configurations, as depicted in Fig. 1.1. Base Station (BS)s dynamically choose appropriate configurations to accommodate the traffic requirements. This dynamic allocation is based on real-time measurements of the channel conditions and the data traffic load. By allowing flexible adjustment of the UL and DL time slots, DynTDD optimizes the utilization of the available spectrum, leading to improved overall system capacity and efficiency.

The key components of DynTDD include:

- **Channel Sensing:** DynTDD systems employ channel sensing techniques to assess the quality of the radio channel. This involves measuring parameters such as signal strength, interference levels, and noise to determine the current channel conditions.
- **Traffic Monitoring:** Network operators continuously monitor the traffic patterns and demand from users. This information is crucial for dynamically adjusting the allocation of time slots to accommodate varying communication needs.
- **Dynamic Allocation Algorithm:** DynTDD systems use intelligent algorithms to dynamically allocate time slots for UL and DL transmissions. These algorithms take

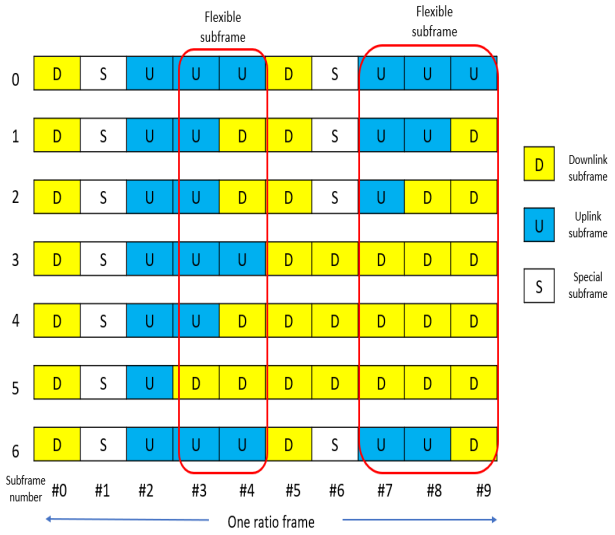

Figure 1.1: Dynamic TDD DL/UL configurations

into account the real-time channel measurements and traffic demand to optimize the allocation, ensuring efficient use of the available spectrum.

- **Adaptive Modulation and Coding:** DynTDD systems often employ adaptive modulation and coding schemes, where the modulation scheme and error correction coding rate are adjusted based on the channel quality. This ensures that data is transmitted at the highest possible rate while maintaining reliable communication under varying channel conditions.

- **Quality-of-Service (QoS) Considerations**: DynTDD implementations consider the QoS requirements of different services and applications. By dynamically adjusting the time slot allocation, DynTDD can prioritize certain types of traffic, ensuring that high-priority applications receive the necessary resources for smooth operation.

DynTDD revolutionizes wireless communication by dynamically allocating time slots for UL and DL transmissions, adapting to changing demands and channel conditions. While this flexibility significantly enhances spectrum efficiency, it brings forth a crucial challenge: the management of interference. In DynTDD systems, where UL and DL transmissions share the same frequency bands, ensuring that signals don't collide or degrade each other's quality is paramount. This challenge, known as cross-link interference (CLI), arises due to the overlapping nature of these transmissions, impacting the integrity of data being sent and received. Effectively addressing CLI becomes pivotal to maintaining the high performance and reliability that DynTDD promises. This interference comprises two types: between the BSs, which is known as base station to base station (BS-to-BS) or downlink to uplink (DL-to-UL) interference, and between User Equipement (UE) known as user equipment to user equipment (UE-to-UE) or uplink to downlink (UL-to-DL) interference. In the UL-to-DL scenario, interference from UL transmissions affects DL recep-

tions. When devices transmit data in the UL direction, signals may leak or spill over into the DL frequency bands. This leakage can occur due to various factors, such as imperfect isolation between the UL and DL frequency bands, hardware limitations, or multi-path propagation. As a result, DL communications can experience interference, leading to reduced signal quality, decreased data rates, and increased error rates. Conversely, in the DL-to-UL scenario, interference from DL transmissions affects UL receptions. DL transmissions can cause interference in the UL direction if signals from the DL transmissions spill over into the UL frequency bands. This interference can occur due to similar reasons as the UL to DL interference, including imperfect isolation and multi-path propagation. DL-to-UL interference can impact the ability of UL transmissions to be received accurately, leading to degraded communication quality and reduced system performance. In Fig. 1.2, we depict the two types of interference encountered in a DynTDD system.

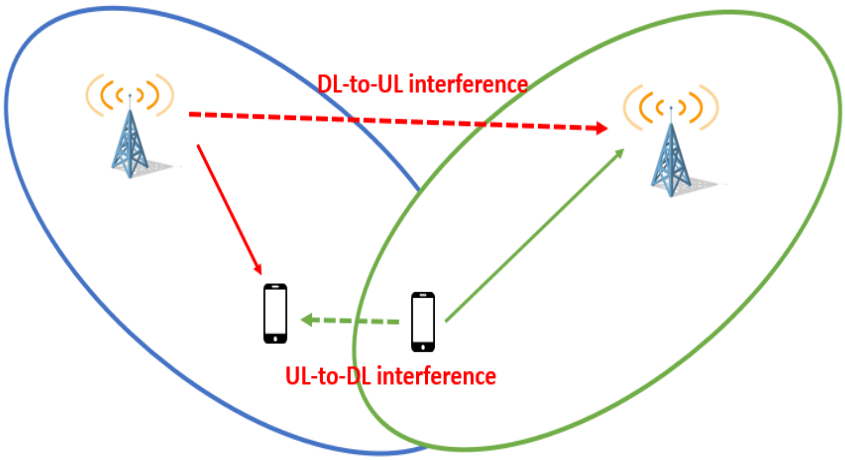

Figure 1.2: Cross Link Interference

DynTDD is a concept that can be applied in various wireless communication technologies, including 5^{th} generation (5G). In the context of 5G networks, DynTDD is an essential feature that allows for flexible allocation of UL and DL resources, adapting to the varying communication needs and channel conditions of users. One of the defining features of 5G technology is its ability to support a wide range of use cases with varying requirements, such as high data rates, low latency, massive connectivity, and energy efficiency. To meet these diverse demands, $5G^{+}$ networks need the utilization of a combination of different technologies, including DynTDD, to optimize the utilization of the available spectrum and enhance overall network efficiency. Here's how DynTDD relates to 5G:

- **Spectral Efficiency:** 5G networks leverage DynTDD to enhance SE. By dynamically adjusting the allocation of time slots for UL and DL transmissions based on real-time channel conditions and traffic demand, 5G systems can maximize the utilization of the available spectrum, leading to higher data rates and increased capacity.

- **Massive Connectivity:** 5G aims to support massive Machine-Type Communication (mMTC) scenarios where a large number of devices are connected simultaneously. DynTDD allows 5G networks to efficiently manage UL and DL communications for a massive number of devices, ensuring that resources are allocated where they are needed the most.

- **Low Latency:** For applications requiring low latency, such as autonomous driving and real-time remote control, DynTDD in 5G networks enables quick adaptation of time slot allocations. This flexibility reduces communication delays, ensuring a timely exchange of information between devices and the network.

- **QoS:** DynTDD in 5G networks allows for the prioritization of specific types of traffic. Critical applications, such as emergency services or mission-critical industrial automation, can be given higher priority in resource allocation, ensuring that they receive the necessary resources for reliable and low-latency communication.

- **Carrier Aggregation:** 5G networks often utilize carrier aggregation techniques, where multiple frequency bands are combined to increase data rates and capacity. DynTDD plays a crucial role in carrier aggregation scenarios, allowing efficient allocation of UL and DL resources across different frequency bands.

The rapid evolution of wireless communication technologies, particularly in the realm of 5G networks, has ushered in an era of unprecedented connectivity and efficiency. DynTDD's adaptive nature optimizes spectrum utilization, leading to enhanced data rates, improved capacity, and reduced latency, addressing the diverse demands of modern wireless applications. In our pursuit of advancing this transformative technology, our motivation stems from the pivotal challenges faced in the mitigation of interference, specifically CLI. The essence of our research lies in comprehensively understanding and effectively managing CLI in DynTDD systems. By delving deep into the complexities of interference alignment, we aim to devise innovative solutions to ensure seamless communication.
Our motivation stems from the critical need to unlock the true capabilities of DynTDD by addressing CLI challenges. Through rigorous analysis, innovative methodologies, and a commitment to pushing the boundaries of current knowledge, our thesis aims to contribute significantly to the field. By mitigating CLI, we not only enhance the efficiency of DynTDD but also pave the way for more robust, reliable, and high-performing wireless networks, shaping the future of communication technology.
Moreover, our study's impact transcends the confines of DynTDD systems. While our focus is on mitigating CLI within DynTDD, the methodologies, insights, and innovative solutions derived from our research possess broader applicability. DynTDD serves as a specific use case, showcasing the versatility of our methods. By addressing interference challenges within DynTDD, we pioneer solutions applicable to a spectrum of Interference Channel (IC)s across diverse communication contexts. Our research thus stands not only as an advancement in DynTDD technology but also as a catalyst for innovative interference management strategies in various communication scenarios.

1.2 Related Work

Interference Alignment and DynTDD systems are areas that generate significant interest.

Multiple-Input Multiple-Output (MIMO) technology is a promising solution for achieving high throughput in wireless communication systems [1]. In DL communication, if the transmitter has certain knowledge of the Channel State Information (CSI), the system throughput can be maximized. In this study, we focus on DynTDD systems, which have the potential to significantly improve overall resource utilization [2] and reduce latency [3]. [4] demonstrated that Distributed Antenna Array (DAA) Massive MIMO (ma-MIMO) system enabled by DynTDD significantly enhances the spectral efficiency in the sum of UL-DL compared to TDD DAA and TDD Cellular ma-MIMO systems.
Mobile broadband applications and multimedia services commonly found in ultra-densely deployed networks (UDNs) exhibit intermittent and bursty behavior. Consequently, the transmission bandwidth in UL and DL directions becomes asymmetric and fluctuates based on traffic patterns. To better handle this bursty nature, DynTDD is viewed as an intriguing solution [5–7]. In [8] an evaluation of the balance between throughput and energy efficiency was conducted for static and dynamic TDD schemes, with and without downlink/uplink decoupling (DUDe). The results indicate thatDynTDD with DUDe outperforms static TDD without DUDe, achieving higher throughput (52.45%) with only a slight reduction (2.3%) in energy efficiency. Likewise, compared to a static TDD system with DUDe, DynTDD with DUDe demonstrates a throughput increase (28.54%) while maintaining consistent energy efficiency. In a concurrent initiative, the enhancement in performance resulting from full-duplex access points, in comparison to the conventional TDD-based cell-free ma-MIMO, was measured in studies [9–11]. It's worth noting that both DynTDD and full duplex share the common goal of serving both UL and DL users simultaneously, albeit through distinct methods.
However, DynTDD also presents new challenges due to the introduction of CLI, including DL-to-UL and UL-to-DL interference. Previous studies have mainly focused on resolving the BS-to-BS interference problem, while interference between UE has been less explored. This is because, during UL transmission, DL-to-UL interference can cause substantial performance degradation, unlike during DL transmission where DynTDD is used in its favor [12]. However, as reported in [13], UE-to-UE interference is low for UEs in the center of the cell region, but very high for UEs at the cell edge. [14] includes simulation results demonstrating the performance improvements with flexible duplex and the efficacy of CLI management techniques. The results emphasize the pivotal importance of managing cross-link interference for the system performance of both flexible duplex and full duplex setups. This observation underscores the necessity for future research efforts to explore this aspect further.
To improve network capacity significantly and ensure network stability, it is necessary to handle UE-to-UE interference of edge UEs. Therefore, concurrent transmission techniques, such as Zero Forcing (ZF), Interference Alignment, and distributed MIMO, have

been proposed, in which multiple senders jointly encode signals to multiple receivers so that interference is aligned or canceled, and each receiver can decode its desired information. The scenario of a two-user IC with mixed interference is prevalent in various network types such as device-to-device (D2D), ad-hoc, and homogeneous/heterogeneous cellular networks. Employing successive interference cancellation (SIC) in these scenarios effectively enhances concurrent connections and network throughputs, as demonstrated in previous studies [15–19]. Nevertheless, in the case of a general K-user IC with partial unidirectional strong interference where $K \geq 3$, determining the achievable capacity becomes significantly more complex.

The feasibility conditions of interference alignment have been analyzed in various studies, such as [20–26]. In [20] the authors analyze the feasibility of linear interference alignment for the MIMO-Interfering Broadcast Channel (IBC) with constant coefficients. They pose and prove the necessary conditions of linear interference alignment feasibility for general MIMO-IBC. Except for the proper condition, they find another necessary condition to ensure a kind of irreducible interference to be eliminated. Then they prove the necessary and sufficient conditions for a special class of MIMO-IBC, where the number of antennas is divisible by the number of data streams per user. [26] established a necessary and sufficient condition on interference alignment feasibility for the (full rank) MIMO Interference Broadcast Multiple Access Channel (IBMAC), which characterizes the optimal sum of Degree of Freedom (DoF) for various practical network configurations, A MIMO IBMAC model is illustrated in Fig. 1.3. In the realm of IBMAC, several interference mitigation techniques have been extensively explored in existing literature, as referenced in [27–34] and the sources cited therein. For example, research efforts in Heterogeneous Networks (HetNets) have focused on interference management techniques to enhance area spectral efficiency [27] or improve throughputs [28–30]. Additionally, scheduling policies have been investigated in [32–34] to curb significant interferences from neighboring users. [35] addresses (centralized) attainable DoF for general interference networks with general channel rank conditions. The multiple antennas give each node a certain ZF budget that for a given DoF distribution needs to be coordinated between all nodes to handle all interference. [36] has mathematically characterized the achievable DoF of their proposed Distributed Interference Alignment (DIA) technique for a given number of antennas at the BS/Mobile Station (MS).

Additionally [37] proposes an interference neutralization scheme to eliminate the inter-user interference with the help of partial Channel State Information at the Transmitter (CSIT). CLI cancellation methods have been studied in [38], where a joint user scheduling and transceiver design-based CLI suppression scheme is investigated in multi-cell multi-user MIMO DynTDD systems to eliminate UL-to-DL interference. An algorithm is designed to avoid scheduling DL UEs which will be interfered by neighboring UL UEs. To suppress DL-to-UL interference, the DL-to-UL IC is divided into several interference sub-channels, and a novel precoding and detection design is provided to make the wanted signal channel orthogonal to these interference sub-channels. [39] gives also an approach to finding the spatial filter matrices that offer the desired DoF scheduling and reduce the unwanted interference signal strength to close to zero (rather than absolute zero).

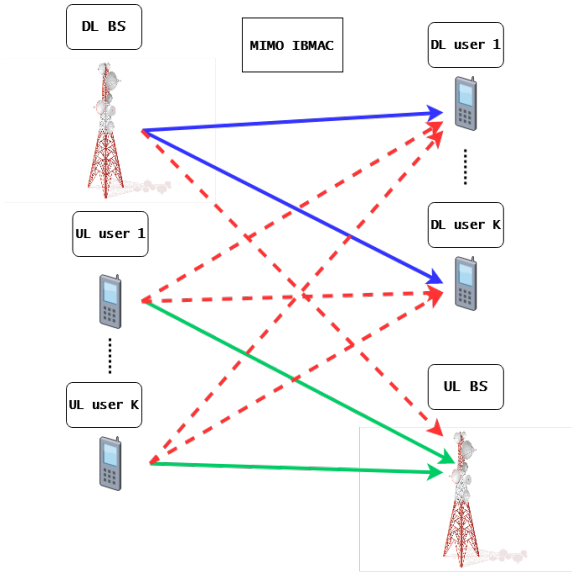

Figure 1.3: MIMO Interfering broadcast-multiple-access channel (IBMAC)

1.3 Thesis Outline

This thesis is structured into four distinct parts. In Part I, the groundwork is laid with an introduction followed by Chapter 2, delving into the problem definition and essential theoretical foundations.
Part II focuses on the feasibility of interference alignment for DynTDD UE-to-UE IC. In particular:
Chapter 3 explores interference alignment feasibility in a centralized scenario, considering a full-rank MIMO IBMAC IC. This analysis establishes conditions crucial for system sizing.
In Chapter 4, the study extends to a centralized scenario with reduced rank MIMO IBMAC IC, accommodating real-world complexities like absorption and scattering.
Chapter 5 takes the exploration further into a distributed scenario, allowing for a more realistic understanding of communication complexities.

Part III delves into optimization techniques, specifically focusing on beamforming. In particular:
Chapter 6 introduces a design for ZF beamformers for both DL and UL UEs, ensuring CLI alignment. To enhance sum rates, we define Weighted Minimum Mean Square Error (WMMSE) beamformers at the DL BS and UL and DL UEs. The chapter includes simulations of sum rates at DL and UL users based on Signal-to-Interference-plus-Noise Ratio (SINR). It emphasizes the impact of UE-to-UE interference in DynTDD systems and showcases the improvements brought by the WMMSE algorithms. In this chapter, we explore also the power allocation optimization using the water-filling algorithm within our model. Then we evaluate the performance behavior of both ZF and WMMSE beamformers concerning this power optimization approach.

Finally, Part IV includes our conclusions and outlines future work based on the presented findings in this thesis.

1.4 Contributions

The results obtained during this Ph.D. are published in the following

- A. Tibhirt, D. Slock, and Y. Yuan-Wu, "Interference in dynamic TDD: effect of MIMO rank on DoF and transceiver design," in the International Journal of Mobile Network Design and Innovation (IJMNDI2023).
- A. Tibhirt, D. Slock, and Y. Yuan-Wu, "Beamforming for Reduced-Rank MIMO Interference Channels in Dynamic TDD Systems," in the Fourteenth International Conference on Ubiquitous and Future Networks (ICUFN2023), Paris, France, July 2023.
- A. Tibhirt, D. Slock, and Y. Yuan-Wu, "Transceiver design in dynamic TDD with reduced-rank MIMO interference channels," in the 22nd Annual Wireless Telecommunications Symposium (WTS2023), Boston, MA, USA, April 2023.
- A. Tibhirt, D. Slock, and Y. Yuan-Wu, "Interference Mitigation in Dynamic TDD MIMO Interference Channels," in IEEE 27th International Workshop on Computer Aided Modeling and Design of Communication Links and Networks (CAMAD2022), Paris, France, November 2022.
- A. Tibhirt, D. Slock, and Y. Yuan-Wu, "Interference Alignment in Reduced-Rank MIMO Networks with Application to Dynamic TDD," in the 20th International Symposium on Modeling and Optimization in Mobile, Ad hoc, and Wireless Networks (WiOpt2022), Turin, Italy, September 2022.
- A. Tibhirt, D. Slock, and Y. Yuan-Wu, "Distributed Beamforming Design in Reduced-Rank MIMO Interference Channels and Application to Dynamic TDD," in 25th International ITG Workshop on Smart Antennas (WSA2021), French Riviera, France, November 2021.

Chapter 2

Problem Definition and Background Theory

2.1 Overview

Dynamic Time Division Duplexing (DynTDD) represents a significant advancement in wireless communication networks. Unlike traditional Time Division Duplexing (TDD), DynTDD dynamically allocates time slots for uplink and downlink transmissions based on changing traffic demands and channel conditions. This adaptive approach optimizes spectrum utilization, enhancing overall system capacity and efficiency. DynTDD relies on key components such as channel sensing, traffic monitoring, dynamic allocation algorithms, adaptive modulation, and Quality-of-Service considerations. However, the dynamic nature of DynTDD introduces challenges, cross-link interference (CLI). Managing CLI is crucial to maintaining high performance. In the context of 5G networks, DynTDD is pivotal, enhancing spectral efficiency, supporting massive connectivity, minimizing latency, ensuring Quality-of-Service, and enabling carrier aggregation across multiple frequency bands. DynTDD stands at the forefront of 5G technology, revolutionizing wireless communication capabilities to meet diverse and evolving demands.

2.2 Problem Definition

CLI in DynTDD systems refers to the unwanted interference that occurs between uplink and downlink transmissions, impacting the integrity of the data being sent and received. In DynTDD, both uplink (UL) and downlink (DL) transmissions share the same frequency bands, but their time slots are dynamically allocated based on changing traffic demands and channel conditions. Due to the overlapping nature of these transmissions, signals from one direction can spill over or interfere with signals in the opposite direction.

In our study, we examine the interaction among users in different cells. Specifically,

we focus on User Equipement (UE)s in Uplink (UL) cells transmitting data to their respective Base Station (BS). Additionally, due to their proximity to Downlink (DL) UEs in neighboring cells, these UL UEs inadvertently introduce interference to these DL UEs.

The l^{th} UL user transmits $d_{ul,l}$ independent streams to the UL BS, where $p_{ul,l}$ represents the non-negative UL power at user l. At the same time, the k^{th} DL user receives $d_{dl,k}$ independent streams from the DL BS, with non-negative DL power allocation $p_{dl,k}$.
Let $\boldsymbol{V}_{dl,k} \in \mathbb{C}^{M_{dl} \times d_{dl,k}}$ denote the beamformer used by the DL BS to transmit the signal $s_{dl,k} \in \mathbb{C}^{d_{dl,k} \times 1}$ to the k^{th} DL UE, and $\boldsymbol{V}_{ul,l} \in \mathbb{C}^{N_{ul,l} \times d_{ul,l}}$ denote the beamformer used by the l^{th} UL UE to transmit the signal $s_{ul,l} \in \mathbb{C}^{d_{ul,l} \times 1}$ to the UL BS. We assume that $E[\boldsymbol{s}_{dl,k}\boldsymbol{s}_{dl,k}^H] = \boldsymbol{I}$ and $E[\boldsymbol{s}_{ul,l}\boldsymbol{s}_{ul,l}^H] = \boldsymbol{I}$. Furthermore, we consider $\boldsymbol{U}_{dl,k} \in \mathbb{C}^{N_{dl,k} \times d_{dl,k}}$ and $\boldsymbol{U}_{ul,l} \in \mathbb{C}^{M_{ul} \times d_{ul,l}}$ as the Rx beamforming matrices at the k^{th} DL UE and UL BS (from the l^{th} UL UE), respectively.
The received signal at the k^{th} DL UE is given by $\boldsymbol{y}_{dl,k}$:

$$\boldsymbol{y}_{dl,k} = \underbrace{\boldsymbol{H}_k^{DL}\boldsymbol{V}_{dl,k}\boldsymbol{s}_{dl,k}}_{\text{desired signal}} + \underbrace{\sum_{j=1,j\neq k}^{K_{dl}} \boldsymbol{H}_k^{DL}\boldsymbol{V}_{dl,j}\boldsymbol{s}_{dl,j}}_{\text{intracell interference}} + \underbrace{\sum_{l=1}^{K_{ul}} \boldsymbol{H}_{k,l}\boldsymbol{V}_{ul,l}s_{ul,l}}_{\text{UL To DL interference}} + \underbrace{\boldsymbol{n}_{dl,k}}_{\text{noise}}, \tag{2.1}$$

this implies that the estimated signal for the k^{th} DL UE is determined by $\hat{\boldsymbol{s}}_{dl,k} = \boldsymbol{U}_{dl,k}\boldsymbol{y}_{dl,k}$, where the matrix $\boldsymbol{H}_k^{DL} \in \mathbb{C}^{N_{dl,k} \times M_{dl}}$ represents the channel from the DL BS to the k^{th} DL UE. And $\boldsymbol{H}_l^{UL} \in \mathbb{C}^{M_{ul} \times N_{ul,l}}$ in (6.1) is the matrix of the channel from the l^{th} UL UE to the UL BS. We call $\boldsymbol{H}_k^{DL}$ and $\boldsymbol{H}_l^{UL}$ the direct channels. The Interference Channel (IC) between the l^{th}UL and the k^{th} DL UEs is denoted as $\boldsymbol{H}_{k,l} \in \mathbb{C}^{N_{dl,k} \times N_{ul,l}}$. $\boldsymbol{n}_{dl,k} \in \mathbb{C}^{N_{dl,k} \times 1}$ denotes the additive white Gaussian noise with distribution $\mathcal{CN} \in (0, \sigma_{dl,k}^2\boldsymbol{I})$ at the k^{th} DL UE. ZF from UL UE l to the DL UE k requires:

$$\boldsymbol{U}_{dl,k}^H\boldsymbol{H}_{k,l}\boldsymbol{V}_{ul,l} = \boldsymbol{0}, \forall k \in \{1, ..., K_{dl}\}, \forall l \in \{1, ..., K_{ul}\}\,. \tag{2.2}$$

Fig. 2.1 visually represents our problem and delineates the different dimensions involved.

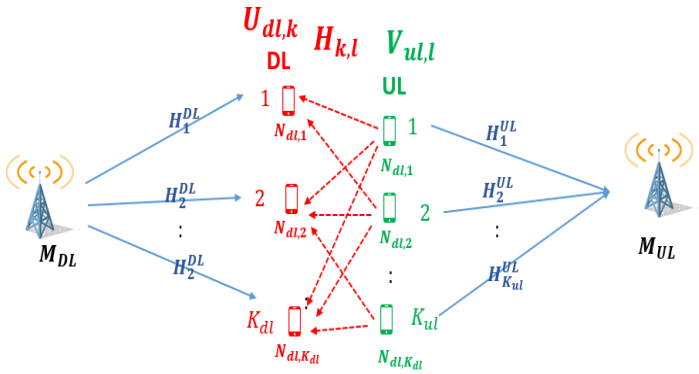

Figure 2.1: Key Dimensions in Problem Statement

Our challenge lies in solving equation (2.2). To do so, we must first determine the conditions for the dimensions and ranks of the matrices within this equation. This step is vital to ensure the existence of a solution and is referred to as the interference alignment feasibility condition. These matrices' dimensions correspond to the system parameters, including the number of antennas, data streams at transmission and reception, as well as the count of UL and DL users. Meeting this condition provides valuable insights for selecting the appropriate system dimensions. Once these conditions are established, our focus shifts to designing beamformers at the $\boldsymbol{U}_{dl,k}$ and $\boldsymbol{V}_{ul,l}$ that satisfy this equation with the correct dimensions, and increase the total sum rates at the UL and DL UEs.
Table 2.1 and Table 2.2 below present a summary of the notations used in this manuscript, and a summary of all variables dimensions respectively, to facilitate easy reference and understanding:

notation	references
$d_{dl,k}$, $d_{ul,l}$	number of data streams at the k^{th} DL UE, at the l^{th} UL UE respectively
$N_{dl,k}$, $N_{ul,l}$	number of antennas at the k^{th} DL UE, at the l^{th} UL UE respectively
K_{dl}, K_{ul}	number of DL UEs, of UL UEs respectively
M_{dl}, M_{ul}	number of antennas at the DL BS, at the UL BS respectively
$p_{dl,k}$, $p_{ul,l}$	the power at DL BS for the k^{th} DL UE, at the l^{th} UL UE respectively
$s_{dl,k}$, $s_{ul,l}$	Tx signal from DL BS to the k^{th} DL UE, from the l^{th} UL UE respectively
$\boldsymbol{H}_k^{DL}$,$\boldsymbol{H}_l^{UL}$	direct channel from the DL BS to the k^{th} DL UE, from the l^{th} UL UE to the UL BS respectively
$\boldsymbol{H}_{k,l}$	IC between the l^{th} UL UE and the k^{th} DL UE
$\boldsymbol{V}_{dl,k}$, $\boldsymbol{V}_{ul,l}$	Tx beamforming at the DL BS for the k^{th} DL UE, at the l^{th} UL UE respectively
$\boldsymbol{U}_{dl,k}$, $\boldsymbol{U}_{ul,l}$	Rx beamforming at the k^{th} DL UE, at the UL BS

Table 2.1: Notation.

Variable	Dimension
$s_{dl,k}$	$\mathbb{C}^{d_{dl,k}\times 1}$
$s_{ul,l}$	$\mathbb{C}^{d_{ul,l}\times 1}$
$\boldsymbol{H}_k^{DL}$	$\mathbb{C}^{N_{dl,k}\times M_{dl}}$
$\boldsymbol{H}_l^{UL}$	$\mathbb{C}^{M_{ul}\times N_{ul,l}}$
$\boldsymbol{H}_{k,l}$	$\mathbb{C}^{N_{dl,k}\times N_{ul,l}}$
$\boldsymbol{V}_{dl,k}$	$\mathbb{C}^{M_{dl}\times d_{dl,k}}$
$\boldsymbol{V}_{ul,l}$	$\mathbb{C}^{N_{ul,l}\times d_{ul,l}}$
$\boldsymbol{U}_{dl,k}$	$\mathbb{C}^{N_{dl,k}\times d_{dl,k}}$
$\boldsymbol{U}_{ul,l}$	$\mathbb{C}^{M_{ul}\times d_{ul,l}}$

Table 2.2: Variabels Dimensions.

2.3 Closing Remarks

In summary, our investigation into CLI in DynTDD systems has uncovered the intricate challenges posed by simultaneous UL and DL transmissions sharing the same frequency bands. As UL UEs communicate with their respective BS, the proximity of DL UEs in neighboring cells introduces unintended interference. This complexity is encapsulated in Equation (2.1), illustrating the interplay of desired signals, intracell and intercell interference, and noise.
Central to our study is the resolution of equation (2.2), a task demanding a meticulous consideration of matrix dimensions and ranks. These considerations form the cornerstone of the interference alignment feasibility condition, shaping the foundational parameters of our system. The careful establishment of these conditions provides crucial guidelines for selecting the appropriate system dimensions, ensuring the viability of our solutions.

As we move forward, our focus sharpens on the design of the different beamformers, meticulously crafted to meet these conditions while maximizing the total sum rates at the UL and DL UEs. This intricate balance between interference management and signal optimization lies at the heart of our research, promising to unveil innovative solutions that elevate the efficiency and reliability of DynTDD systems. In the chapters that follow, we delve deeper into these challenges, exploring novel methodologies, and innovative strategies to overcome CLI complexities. Our endeavor not only expands the realm of interference alignment but also contributes significantly to the advancement of DynTDD technology, paving the way for more robust and high-performing wireless networks.

Part II

Feasibility condition of Interference Alignment for the Dynamic TDD UE-to-UE Interference channel

Chapter 3

Centralized Case Full Rank MIMO IBMAC IC Analysis

3.1 Overview

In this chapter, we focus on a centralized design for interference channel matrices of full rank. Our objective is to establish various conditions regarding the system dimensions that facilitate the feasibility of interference alignment in DynTDD systems. In the centralized case, we consider a central design unit disposes of the knowledge of all channels involved. The channel matrix in wireless communication serves as a description of how the channel affects the transmitted signal. It is instrumental in modeling the signal's interactions with the atmospheric or underwater conditions, including absorption, reflection, and scattering caused by surrounding objects. In Multiple-Input Multiple-Output (MIMO) communication, the channel matrix's rank indicates the number of data streams that can be transmitted between the Transmitter (Tx) and Receiver (Rx), i.e, of how many data streams can be spatially multiplexed on the MIMO channel. Mathematically the rank of this matrix is the number of singular values not equal to zero. The rank of the channel matrix is thus an indicator of how many data streams can be spatially multiplexed on the MIMO channel. When the channel matrix is full rank, it implies that the communication system is operating at its maximum potential. In the context of data transmission, having a full-rank channel matrix means that you can exploit all available antennas fully. Each antenna contributes an independent data stream that can be transmitted simultaneously without interference.
To address the problem of the CLI, it is crucial to determine the conditions on the system dimensions as they enable us to ascertain the system dimensions ensuring the feasibility of interference alignment. We will introduce several conditions, including the proper (necessary), the necessary and sufficient condition, as well as sufficient conditions. Throughout this chapter, we will highlight the distinctions between these conditions as we progress. This comparative analysis will provide valuable insights into the specific requirements for interference alignment, offering a comprehensive understanding of the system's design

parameters necessary for optimal performance.

3.2 System Model

Let's consider a MIMO system that consists of two cells, with each cell containing one base station (BS). One cell operates in the DL mode, while the other cell operates in the UL mode. The UL and DL cells are equipped with M_{ul} and M_{dl} antennas, respectively, and there are K_{ul} and K_{dl} interfering or interfered users in the UL and DL cells, respectively. The k^{th} DL UE and the l^{th} UL UE are equipped with $N_{dl,k}$ and $N_{ul,l}$ antennas, respectively. Due to the different configurations in DynTDD between neighboring cells, two types of interference arise the user equipment to user equipment (UE-to-UE) interference between the UEs located at the edge of the two cells, and the base station to base station (BS-to-BS) interference.
Our system featuring two cells—one operating in DL and the other one in the UL, as shown in Fig. 3.1, is known as IBMAC (Interfering Broadcast-Multiple Access Channel) in [26]. It represents a two-cell system, with one cell in DL mode (broadcast) and the other in UL mode (multiple access), with interference between the two cells. For this study, we assume that the number of BS antennas is large enough to support all UL or DL UE streams and that the BS-to-BS interference can be mitigated by utilizing a limited rank BS-to-BS channel [36]. As a result, the IBMAC problem is then limited to interference from UL UEs to DL UEs, which we refer to as Interference Broadcast Multiple Access Channel-Interference Channel (IBMAC-IC). In terms of the number of data streams at the Tx and Rx, we make the following assumptions:

$$d_{dl,k} \geq 1 \quad and \quad d_{ul,l} \geq 1. \tag{3.1}$$

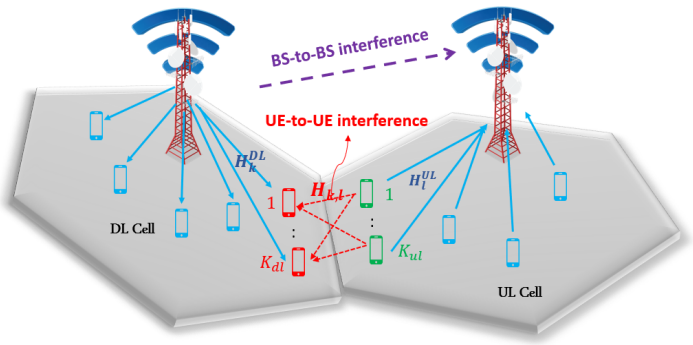

Figure 3.1: DynTDD system Model

In Section 2.2, it was noted that interference alignment requires a solution for equation (2.2) to exist. In this system model, the interference channel matrix $\boldsymbol{H}_{k,l}$ is full rank. In

the context of our centralized design approach, the central design unit possesses knowledge about all the channels involved.
The comprehensive details of the notations employed in the study can be found in Table 2.1, while a succinct summary of the dimensions of all variables is provided in Table 2.2.

3.3 Proper Condition for interference alignment Feasibility

We initiate our analysis by laying the foundation through the proper conditions initially introduced in the reference [40]. These conditions play a pivotal role in the context of full-rank MIMO channels. The essence of these proper conditions revolves around a fundamental principle: for a given set of variables to possess the capacity to fulfill a set of non-linear equations, particularly of a bilinear nature here, a critical criterion must be met. This criterion signifies that the count of variables engaged in the equations must be no less than the count of equations themselves, which are effectively constraints. The fulfillment of the proper condition implies that the system at hand could potentially exhibit feasibility, but it also acknowledges the possibility that the system might still turn out to be infeasible depending on other factors or constraints. On the other hand, if the proper condition is not satisfied, it unequivocally indicates that interference alignment cannot be achieved for the given system configuration. In such cases, interference alignment strategies would not lead to effective interference management, and alternative approaches or techniques may need to be considered to handle the interference and improve system performance.

In the following, we will delve into an analysis aimed at quantifying both the variables and constraints inherent within the system. This examination serves as proof for Theorem 1, which constitutes the global proper condition:

- The total number of variables in $\boldsymbol{V}_{ul,l}$ is $d_{ul,l}(N_{ul,l} - d_{ul,l})$, since only the column space of $\boldsymbol{V}_{ul,l}$ counts. Hence for ZF, $\boldsymbol{V}_{ul,l}$ is determined up to a $d_{ul,l} \times d_{ul,l}$ mixture matrix.

- The total number of variables in $\boldsymbol{U}_{dl,k}$ is $d_{dl,k}(N_{dl,k} - d_{dl,k})$, since again only the column space of $\boldsymbol{U}_{dl,k}$ counts. $\boldsymbol{U}_{dl,k}$ is determined up to a $d_{dl,k} \times d_{dl,k}$ mixture matrix, more details of how we obtain these numbers of variables can be found in Appendix A.

- Equation (2.2) represents $d_{ul,l}d_{dl,k}$ constraints for the cross (interfering) link from UL UE l to DL UE k [40].

- The total number of cross-links is $K_{dl}K_{ul}$.

Now, with the variables and constraints of our system duly ascertained, we proceed to enunciate the proper condition within the subsequent theorem:

Theorem 1. ***Global Proper Condition for interference alignment Feasibility in a Regular MIMO IBMAC-IC*** *For full-rank MIMO channels, if the tuple of Degree of Freedom (DoF)* $(d_{ul,1}, ..., d_{ul,K_{ul}}, d_{dl,1}, ..., d_{ul,K_{dl}})$ *is achievable through interference alignment, then it must satisfy the global proper condition:*

$$\sum_{l=1}^{K_{ul}} d_{ul,l}(N_{ul,l} - d_{ul,l}) + \sum_{k=1}^{K_{dl}} d_{dl,k}(N_{dl,k} - d_{dl,k}) \geq \sum_{l=1}^{K_{ul}} \sum_{k=1}^{K_{dl}} d_{ul,l} d_{dl,k} \,. \tag{3.2}$$

Note that this condition subsumes the Single User (SU) MIMO conditions $d_{ul,l} \leq N_{ul,l}$, $d_{dl,k} \leq N_{dl,k}$ so that the number of variables on the Left Hand Side (LHS) is non-negative. Apart from this proper condition for the overall system, we get an overall set of proper conditions by considering all subsystems. The global proper condition accounts for all interference links simultaneously, considering their collective impact. Conversely, the overall proper condition evaluates each subsystem's feasibility within the larger system. This granular approach makes the overall condition more restrictive than the global condition, ensuring thorough subsystem feasibility.

Theorem 2. ***Overall Proper Conditions for interference alignment Feasibility in a Regular MIMO IBMAC-IC***
The conditions in (3.2) *should be satisfied also by any subsystem, i.e., the IBMAC-IC formed by any subset of the UL users and any subset of the DL users.*

The proof of Theorem 2 is identical to the global proper condition stated in Theorem 1, with the only difference being that it must be applied to all subsystems relative to the number of users in both the UL and DL.

3.4 Necessary and Sufficient Condition for interference alignment Feasibility

A necessary and sufficient condition for interference alignment feasibility embodies a dual-purpose criterion. It encompasses a set of prerequisites that are indispensable (necessary) to establish the alignment of interfering signals, ensuring that certain foundational elements are in place. Moreover, this condition extends its significance by also ensuring that once these prerequisites are met, the feasibility of interference alignment is unequivocally guaranteed (sufficient). This condition stands as a precise characterization of the feasible DoF.

The precise characterization of the feasibility of interference alignment is presented through Theorem 3, which provides a necessary and sufficient condition:

Theorem 3. ***Necessary and Sufficient Condition for interference alignment Feasibility in a Regular MIMO IBMAC-IC***

For a full rank MIMO IBMAC-IC, the DoF tuple $(d_{ul,1}, ..., d_{ul,K_{ul}}, d_{dl,1}, ..., d_{ul,K_{dl}})$ *is feasible almost surely if and only if* $\boldsymbol{J}$ *as defined in* (B.11) *has full row rank.*

The comprehensive demonstration of Theorem 3 can be found in meticulous detail within Appendix B.

3.5 Sufficient Condition for interference alignment Feasibility

In this section, we focus on the sufficient condition of interference alignment feasibility in a full-rank MIMO IBMAC-IC. A sufficient condition can be briefly defined as a subset encompassing various scenarios that meet the prerequisites for successful interference alignment. Unlike the exhaustive criteria provided by the "necessary and sufficient condition," which outlines all instances of feasibility, a sufficient condition constitutes a subset of the feasible cases. When a given system adheres to this condition, the feasibility of interference alignment is certain. However, it's important to note that the application of this condition does not guarantee universal feasibility; rather, it acts as a reliable indicator of alignment potential. In cases where the sufficient condition is not met, the system's feasibility remains uncertain, highlighting the nuanced spectrum between possible feasibility and in-feasibility.

The aim here is to give an easy formulation of a sufficient condition, in terms of the problem dimensions: the number of antennas at UL and DL UEs, the number of data streams, and the number of users that are included in the UE-to-UE interference, rather than the sufficient and necessary condition in Theorem 3 given by a Jacobian matrix row rank. [26] finds sufficiency in the limited scenario in which all DL UEs and UL UEs have the same number of data streams $d_{dl,k} = d_{dl}, d_{ul,l} = d_{ul}$, for this assumption the number of antennas at DL $N_{dl,k}$ and at UL $N_{ul,l}$ must satisfy $mod(N_{dl,k} - d_{dl}, d_{ul}) = mod(N_{ul,l} - d_{ul}, d_{dl}) = 0$ so the interference alignment is feasible. Within this scope, we establish a sufficient condition for interference alignment feasibility given by our following Theorem 4, which gives a much greater DoF than the recent work in [26].

Theorem 4. ***Sufficient Condition for interference alignment Feasibility in a Regular MIMO IBMAC-IC***
For a full rank MIMO IBMAC-IC, respecting the proper condition of Theorem 1 and Theorem 2 , and if:

$$\forall k, l : (N_{ul,l} - d_{ul,l}) \geq d_{dl,k} \ \textit{and} \ (N_{dl,k} - d_{dl,k}) \geq d_{ul,l} \tag{3.3}$$

then $(d_{ul,1}, ..., d_{ul,K_{ul}}, d_{dl,1}, ..., d_{ul,K_{dl}})$ *is feasible.*

The equation in (3.3) means that both the block matrix $\boldsymbol{I}_{d_{ul,l}} \otimes \boldsymbol{H}_{kl}^{(2)}$ of $\boldsymbol{J}_G$ and the block matrix $(\boldsymbol{H}_{kl}^{(3)})^T \otimes \boldsymbol{I}_{d_{dl,k}}$ of $\boldsymbol{J}_F$ in equation (B.11) should be full row rank. The proof for Theorem 4 is provided in extensive detail within Appendix C.

In the following, we introduce three conjectures that represent another sufficient condition and two tighter necessary conditions for interference alignment feasibility in regular MIMO IBMAC-IC.

Conjecture 1. ***Sufficient Condition for interference alignment Feasibility in a Regular MIMO IBMAC-IC***
For a full rank MIMO IBMAC-IC, respecting the proper condition of Theorem 1 and Theorem 2, and if:

$$\forall k, l : (N_{ul,l} - d_{ul,l}) \geq d_{dl,k} \;\; or \;\; (N_{dl,k} - d_{dl,k}) \geq d_{ul,l} \tag{3.4}$$

and:

$$\begin{aligned} &\sum_{k=1}^{K_{dl}} d_{dl,k} \, \min(N_{dl,k} - d_{dl,k}, \sum_{l} d_{ul,l} - \max_{i}(d_{ul,i})) + \\ &\sum_{l=1}^{K_{ul}} d_{ul,l} \, \min(N_{ul,l} - d_{u,l}, \sum_{k} d_{dl,k} - \max_{i}(d_{dl,i})) \\ &\geq \sum_{k=1}^{K_{dl}} \sum_{l=1}^{K_{ul}} d_{dl,k} d_{ul,l} \end{aligned} \tag{3.5}$$

then $(d_{ul,1}, ..., d_{ul,K_{ul}}, d_{dl,1}, ..., \, d_{ul,K_{dl}})$ *is feasible.*

The equation in (3.4) means that either the block matrix $\boldsymbol{I}_{d_{ul,l}} \otimes \boldsymbol{H}_{kl}^{(2)}$ of $\boldsymbol{J}_G$ or the block matrix $(\boldsymbol{H}_{kl}^{(3)})^T \otimes \boldsymbol{I}_{d_{dl,k}}$ of $\boldsymbol{J}_F$ in equation (B.11) should be full row rank. The equation in (3.5) represents the tighter necessary version of the proper condition in (3.2).

A "tighter necessary condition" is a specific rule that has a similar quality to the necessary condition. It signifies that a given system that fulfills this condition might be feasible, yet its feasibility remains uncertain. However, if the system fails to meet the criteria, its in-feasibility is definitive. The uniqueness of the tighter necessary condition lies in its propensity to approach the rigor of the necessary and sufficient condition. As such, the tighter necessary condition encapsulates fewer scenarios of in-feasibility, resulting in a more precise estimation of the entire range.

The forthcoming pair of conjectures introduces tighter necessary conditions, addressing interference alignment feasibility. These conditions aim to refine our understanding of interference alignment feasibility by offering specific criteria that, if satisfied, suggest potential feasibility. These conjectures represent significant strides toward attaining a deeper understanding of the complex terrain that characterizes interference alignment.

Conjecture 2. ***Tighter Necessary Condition for interference alignment Feasibility in a Regular MIMO IBMAC-IC***
For full-rank MIMO channels, if the tuple of DoF $(d_{ul,1}, ..., d_{ul,K_{ul}}, d_{dl,1}, ..., d_{ul,K_{dl}})$ *respects*

the proper condition of Theorem 1 and Theorem 2, and is feasible, then it may satisfy the following necessary condition:

$$\begin{aligned}&\sum_{k=1}^{K_{dl}} d_{dl,k}\ \min(N_{dl,k}-d_{dl,k}, \max_{l}(d_{ul,l}))+\\&\sum_{l=1}^{K_{ul}} d_{ul,l}\ \min(N_{ul,l}-d_{ul,l}, \max_{k}(d_{dl,k}))\\&\geq \sum_{l=1}^{K_{ul}}\sum_{k=1}^{K_{dl}} d_{ul,l}d_{dl,k}\end{aligned} \tag{3.6}$$

The LHS of equation (3.6) represents the number of non-zero columns of the Jacobian matrix $\boldsymbol{J}$ in equation (B.11), and the Right Hand Side (RHS) is the number of rows of $\boldsymbol{J}$.

Conjecture 3. ***Tighter Necessary Condition for interference alignment Feasibility in a Regular MIMO IBMAC-IC***
For full-rank MIMO channels, if the tuple of DoF $(d_{ul,1},...,d_{ul,K_{ul}},d_{dl,1},...,d_{ul,K_{dl}})$ *respects the proper condition of Theorem 1 and Theorem 2, and is feasible, then it may satisfy the following necessary condition:*

$$\begin{aligned}&\forall k,l : (N_{ul,l}-d_{ul,l}) \geq d_{dl,k}\\&\qquad or\\&\forall k,l : (N_{dl,k}-d_{dl,k}) \geq d_{ul,l}\end{aligned} \tag{3.7}$$

The conjecture 3 means that either $\boldsymbol{J}_G$ or $\boldsymbol{J}_F$ in equation (B.11) is full row rank.

3.6 Numerical Results

In this section, we undertake a comprehensive assessment of the various conditions pertinent to the feasibility of interference alignment. Presented herein are the empirical findings, meticulously tabulated in Table 3.1 and Table 3.2, which are essential for our analysis. These results serve two main purposes: first, they carefully look at and establish the definitions of different conditions, showing how they're an improvement over the existing methods. Second, it enables us to define the realm of feasible DoF, encompassing the cumulative data streams at both DL users ($\sum_{k=1}^{K_{dl}} d_{dl,k}$) and UL users ($\sum_{l=1}^{K_{ul}} d_{ul,l}$). The inherent value of these conditions lies in their capacity to guide us, for a given number of antennas at the Tx and Rx, in determining the permissible count of data streams that can be transmitted and received ensuring the realization of interference alignment feasibility.

In Table 3.1, we compare the various combinations (combinations being specific numbers of data streams for each UL and DL UE) for different total DoF values. This comparison involves taking into account the proper condition described in Theorem 1,

the necessary and sufficient condition outlined in Theorem 3, the sufficient condition presented in Theorem 4, and the sufficient condition provided in [26, Theorem 3]. We use an example where there are $K_{ul} = 2$ and $K_{dl} = 3$, and this applies to the following three systems:

- System 1: $N_{ul,1} = 3, N_{ul,2} = 7, N_{dl,1} = 2, N_{dl,2} = 3$ and $N_{dl,3} = 8$, which is the system that has been chosen in [26],
- System 2: $N_{ul,1} = 4, N_{ul,2} = 7, N_{dl,1} = 4, N_{dl,2} = 5$ and $N_{dl,3} = 6$,
- System 3: $N_{ul,1} = 7, N_{ul,2} = 7, N_{dl,1} = 6, N_{dl,2} = 5$ and $N_{dl,3} = 6$.

We get the following numerical results by doing an exhaustive search for all the possible combinations that satisfy each given theorem in Table 3.1, and this process is repeated for different sum DoF. This comprehensive exploration involves attempting all potential combinations of UL and DL user data streams, corresponding to a specific interference alignment condition, for a given number of antennas at both the DL and UL sides. The goal is to verify the feasibility of interference alignment under these conditions. We give here an example to better understand the meaning of a combination, for System 1 when $SumDoF = 6$, the different possible combinations that respect the proper condition in Theorem 1 are:

- $d_{ul,1} = 2, d_{ul,2} = 1, d_{dl,1} = 1, d_{dl,2} = 1$ and $d_{dl,3} = 1$
- $d_{ul,1} = 1, d_{ul,2} = 2, d_{dl,1} = 1, d_{dl,2} = 1$ and $d_{dl,3} = 1$
- $d_{ul,1} = 1, d_{ul,2} = 1, d_{dl,1} = 2, d_{dl,2} = 1$ and $d_{dl,3} = 1$
- $d_{ul,1} = 1, d_{ul,2} = 1, d_{dl,1} = 1, d_{dl,2} = 2$ and $d_{dl,3} = 1$
- $d_{ul,1} = 1, d_{ul,2} = 1, d_{dl,1} = 1, d_{dl,2} = 1$ and $d_{dl,3} = 2$

In Algorithm 1, we provide a pseudo-code offering a thorough outline of the exhaustive search procedure conducted to generate the numerical results showcased in Tables 3.1 and 3.2.

Algorithm 1 Pseudo code for the exhaustive search

For $K_{dl} = 3$ and $K_{ul} = 2$:

1) For a given system dimension $N_{dl,1}$, $N_{dl,2}$, $N_{dl,3}$, $N_{ul,1}$ and $N_{ul,2}$

I) For each $sumDoF = d_{dl,1} + d_{dl,2} + d_{dl,3} + d_{ul,1} + d_{ul,2}$

i) Define all the possible combinations of data streams $(d_{dl,1}, d_{dl,2}, d_{dl,3}, d_{ul,1}, d_{ul,2})$ that satisfy the proper condition:

a) Test for each combination if the following condition are satisfied:

The necessary and sufficient condition Theorem 3
Our proved sufficient condition in Theorem 4
The state-of-the-art sufficient condition

b) Count the number of combination that satisfy each condition

Table 3.1: Number of combinations for different Sum DoF in a full rank interference channel, $K_{ul} = 2$ and $K_{dl} = 3$

Interference Alignment	Sum DoF										
Feasibility Condition	5	6	7	8	9	10	11	12	13	14	15
Proper Theorem 1_{SYS1}	1	5	10	15	20	21	19	5	0	0	0
Theorem 3_{SYS1}	1	5	10	15	20	21	16	3	0	0	0
Theorem 4_{SYS1}	1	2	1	0	0	0	0	0	0	0	0
[26, Theorem 3]$_{SYS1}$	1	0	0	1	0	0	0	0	0	0	0
Proper Theorem 1_{SYS2}	1	5	15	33	58	83	80	26	4	0	0
Theorem 3_{SYS2}	1	5	15	31	50	67	60	21	4	0	0
Theorem 4_{SYS2}	1	5	15	22	20	9	2	0	0	0	0
[26, Theorem 3]$_{SYS2}$	1	0	0	0	0	0	1	0	0	0	0
Proper Theorem 1_{SYS3}	1	5	15	35	70	125	189	241	187	51	8
Theorem 3_{SYS3}	1	5	15	35	70	125	173	197	167	51	8
Theorem 4_{SYS3}	1	5	15	35	61	76	72	52	28	12	3
[26, Theorem 3]$_{SYS3}$	1	0	0	1	0	0	1	0	0	0	0

From these results, we can conclude that:

- The gap in terms of the number of combinations between the proper (Theorem 1) and the necessary and sufficient condition (Theorem 3) is not negligible, and it is proportional to the number of antennas. Thus a feasible Sum DoF needs to be associated with feasible combinations (distribution of the DoF at UL and DL UE), so the interference alignment is feasible,

- All the feasible cases are given by the necessary and sufficient condition (Theorem 3), our sufficient condition (Theorem 4) comes to cover a subset of these feasible cases, the size of this subset is quite interesting, since Theorem 4 is written in term of the problem dimension, and does not need the full row rank test on $\boldsymbol{J}$.

- When considering our sufficient condition (Theorem 4) with the sufficient condition mentioned before in the state of the art [26, Theorem 3], we notice how much our sufficient condition outperforms and improves the available state of the art.

In Table 3.2 we give some numerical results for the three systems mentioned before, to evaluate the gap between the given conjectures and the necessary and sufficient condition in Theorem 3.

From these results, we can notice that:

- Conjecture 1 is another sufficient condition for interference alignment feasibility that gives more feasible combinations compared to Theorem 4, from our observation, Conjecture 1 can find some combinations which are not found by Theorem 4, so Conjecture 1 and Theorem 4 can be complementary,

- Conjecture 2 and Conjecture 3 are very close to the necessary and sufficient conditions in Theorem 3, but at some DoF, these conditions give some combinations (at most two combinations) that are proper but not feasible, it is for this reason that these conditions are mentioned as a tighter necessary condition.

Table 3.2: Number of combinations for different Sum DoF in a full rank interference channel, $K_{ul} = 2$ and $K_{dl} = 3$

Interference Alignment	Sum DoF										
Feasibility Condition	5	6	7	8	9	10	11	12	13	14	15
Proper Theorem 1_{SYS1}	1	5	10	15	20	21	19	5	0	0	0
Theorem 3_{SYS1}	1	5	10	15	20	21	16	3	0	0	0
Theorem 4_{SYS1}	1	2	1	0	0	0	0	0	0	0	0
Conjecture 1_{SYS1}	1	3	1	0	0	0	0	0	0	0	0
Conjecture 2_{SYS1}	1	4	6	8	12	14	8	2*	0	0	0
Conjecture 3_{SYS1}	1	5	9	11	11	7	2	0	0	0	0
Proper Theorem 1_{SYS2}	1	5	15	33	58	83	80	26	4	0	0
Theorem 3_{SYS2}	1	5	15	31	50	67	60	21	4	0	0
Theorem 4_{SYS2}	1	5	15	22	20	9	2	0	0	0	0
Conjecture 1_{SYS2}	1	5	4	11	11	4	1	0	0	0	0
Conjecture 2_{SYS2}	1	5	15	31	50	66	57	11	1	0	0
Conjecture 3_{SYS2}	1	5	15	31	49	61	46*	14*	3	0	0
Proper Theorem 1_{SYS3}	1	5	15	35	70	125	189	241	187	51	8
Theorem 3_{SYS3}	1	5	15	35	70	125	173	197	167	51	8
Theorem 4_{SYS3}	1	5	15	35	61	76	72	52	28	12	3
Conjecture 1_{SYS3}	1	5	4	12	14	30	24	38	28	10	0
Conjecture 2_{SYS3}	1	5	15	35	69	119	160	161	85	12	0
Conjecture 3_{SYS3}	1	5	15	35	70	125	173	197	167	51	8

(*): the given condition gives some combinations that are proper but not feasible. (Feasible = Theorem 3 is satisfied).

3.7 Closing Remarks

In conclusion, this chapter focuses on a centralized design approach and assumes a full-rank interference channel matrix. Through rigorous analysis, we explored the feasibility conditions necessary for interference alignment between UL UEs and DL UEs. This

exploration provided crucial insights into determining the optimal sizing of our systems in terms of the number of antennas and data streams, ensuring the discovery of zero-forcing filters. By establishing the proper conditions, which serve as an upper bound for the feasible DoF, we laid a solid foundation. Building upon this foundation, we went a step further to identify precise characterizations of the feasible DoF. This endeavor led us to essential necessary and sufficient conditions, enabling us to gain a comprehensive understanding of interference alignment.

In our pursuit of refining these conditions, we devised a significant subset of feasible cases for interference alignment as a sufficient condition. This breakthrough not only alleviates the complexity associated with the necessary and sufficient conditions but also advances the existing state-of-the-art substantially. Moreover, we presented thought-provoking conjectures, offering tighter necessary conditions and another sufficient condition. These conjectures serve as valuable tools, aiding us in comprehending the nuances of interference alignment across various system dimensions.

In essence, this chapter offers a detailed and comprehensive study of the conditions of interference alignment in a centralized scenario with full-rank interference channel matrices. Through meticulous analysis, we have illuminated the intricate pathways of interference alignment, providing invaluable insights that will undoubtedly shape the future landscape of interference alignment. Furthermore, the knowledge gleaned from this chapter serves as a critical foundation for our upcoming endeavors. Understanding the intricacies of interference alignment in the context of full-rank interference channel matrices paves the way for our exploration of reduced-rank interference channels in the next chapter.

Chapter 4

Centralize case Reduced Rank MIMO IBMAC IC Analysis

4.1 Overview

In this chapter, with a centralized scenario, we're focusing on a reduced rank interference channel matrix between UL and DL users. This consideration is important because, the full-rank channel matrix assumption is not always met in practical scenarios, due to the interaction with the environment including absorption, reflection, and scattering caused by surrounding objects. So, we're considering a situation where the available antennas aren't used to their full capacity, making our study more practical and applicable to every communication system. This approach helps us understand how wireless systems behave, where signals often have to navigate around obstacles, providing insights that can be useful for practical applications.

Initiating our study with a comprehensive analysis of full-rank channel matrices, although it represents a specific case within the realm of reduced-rank channel matrices, holds paramount importance. Despite being a simplified scenario, examining full-rank matrices offers a foundational understanding that is less intricate than delving directly into the complexities of reduced-rank matrices. By starting with the full rank analysis, we gain valuable insights into the fundamental principles governing the system. Therefore, commencing our study with the full rank channel matrices equips us with essential knowledge, enabling a smoother transition into the complexities of the reduced rank matrices, ensuring a more comprehensive and insightful exploration of the subject matter.

Existing work on interference alignment feasibility assumes only the full rank channel model [22], [21], and [20], but in many practical propagation environments such as the number of surrounding scatterers which is finite and limited, the MIMO channel matrix is likely to have reduced rank [41], [42], so thus designs based on full rank channels become inefficient. In this chapter, we investigate feasibility conditions for interference alignment designed specifically for the reduced rank MIMO IBMAC-IC system. Our analysis extends the foundational work established in Chapter 3, where similar conditions were developed

for the full-rank case.

4.2 System Model

In our study of the MIMO DynTDD system outlined in Chapter 3, we maintain consistency in the system setup involving DL and UL cells, as well as interfered and interfering users and base stations. However, a notable development occurs when we examine the interference channel between UL and DL users. Here, we shift our focus to a realistic approach by considering a reduced rank MIMO IBMAC-IC model. This change allows for a more detailed exploration of UL and DL interactions within the MIMO DynTDD framework. The rank of the UE-to-UE interference channel is denoted as $r_{k,l}$, indicating the presence of $r_{k,l}$ distinguishable significant propagation paths contributing to $\boldsymbol{H}_{k,l}$. Then we can factorize $\boldsymbol{H}_{k,l}$ as:

$$\boldsymbol{H}_{k,l} = \boldsymbol{B}_{k,l}\boldsymbol{A}_{k,l}^{H} \tag{4.1}$$

with a full rank matrices $\boldsymbol{B}_{k,l} \in \mathbb{C}^{N_{dl,k}\times r_{k,l}}$ and $\boldsymbol{A}_{k,l} \in \mathbb{C}^{N_{ul,l}\times r_{k,l}}$. We have $\boldsymbol{r}_{k,l}$ distinguishable significant paths contribute to $\boldsymbol{H}_{k,l}$, where distinguishable means with linearly independent antenna array responses from other paths, at both the Tx side and the Rx side.

4.3 Proper Condition for interference alignment Feasibility

As for the full-rank inference channel, the requisite condition states that, for a given set of non-linear (specifically bilinear) equations to be specifiable by a set of variables, the number of variables involved must be equal to or greater than the number of equations (constraints). The number of variables is as expressed in the full rank $\sum_{l=1}^{K_{ul}} d_{ul,l}(N_{ul,l} - d_{ul,l}) + \sum_{k=1}^{K_{dl}} d_{dl,k}(N_{dl,k} - d_{dl,k})$, and the number of constraints is derived from equation (2.2) which represents $\min(d_{dl,k}r_{k,l}, d_{ul,l}r_{k,l}, d_{ul,l}d_{dl,k})$ constraints for the cross (interfering) link from UL UE l to DL UE k [40], with a total number of cross-links equal to $K_{dl}K_{ul}$. The global proper (necessary) condition for a reduced rank interference channel is then given by the following theorem:

Theorem 5. ***Global Proper Condition for interference alignment Feasibility in a Reduced rank MIMO IBMAC-IC*** *For reduced-rank MIMO channels, if the tuple of DoF* $(d_{ul,1}, ..., d_{ul,K_{ul}}, d_{dl,1}, ..., d_{ul,K_{dl}})$ *is achievable through interference alignment, then it must satisfy the proper condition:*

$$\begin{aligned}&\sum_{l=1}^{K_{ul}} d_{ul,l}(N_{ul,l} - d_{ul,l}) + \sum_{k=1}^{K_{dl}} d_{dl,k}(N_{dl,k} - d_{dl,k}) \\ &\geq \sum_{l=1}^{K_{ul}}\sum_{k=1}^{K_{dl}} \min(r_{k,l}d_{dl,k}, r_{k,l}d_{ul,l}, d_{ul,l}d_{dl,k})\,.\end{aligned} \tag{4.2}$$

In the following, we aim to define the specific local conditions necessary for interference alignment by introducing a collaborative Zero Forcing (ZF) technique among both UL and DL users. To delve into this topic, it is advisable to review the work presented in [35]. For the ZF conditions in interference networks, [35] introduces binary variables $\mathbf{1}^T_{k,l}$ and $\mathbf{1}^R_{k,l}$ with the following definition:

$$\mathbf{1}^T_{k,l} = \begin{cases} 1 \text{ if Tx node } l \text{ is active for ZF from } l \text{ to } k, \\ 0 \text{ otherwise} \end{cases} \tag{4.3}$$

$$\mathbf{1}^R_{k,l} = \begin{cases} 1 \text{ if Rx node } k \text{ is active for ZF from } l \text{ to } k, \\ 0 \text{ otherwise} \end{cases} \tag{4.4}$$

We denote by $\boldsymbol{z}^R_{k,l}$ (resp. $\boldsymbol{z}^T_{k,l}$) the number of ZF constraints satisfied by the Rx (resp. the Tx). To cancel all interference from the UL UEs to the DL UEs, according to [35, Theorem 1], the following conditions should be satisfied (here formulated for the uplink to downlink (UL-to-DL) interference in the DynTDD problem considered):

$$\boldsymbol{z}^R_{k,l}\mathbf{1}^R_{k,l} + \boldsymbol{z}^T_{k,l}\mathbf{1}^T_{k,l} = \min(\mathbf{1}^R_{k,l}d_{ul,l} + \mathbf{1}^T_{k,l}d_{dl,k}, r_{k,l}) \tag{4.5a}$$

$$(\mathbf{1}^R_{k,l}, \mathbf{1}^T_{k,l}) \neq (0,0) \tag{4.5b}$$

$$d_{dl,k} + \textstyle\sum_{l\in\boldsymbol{I}_{dl,k}} \boldsymbol{z}^R_{k,l} \leq N_{dl,k} \tag{4.5c}$$

$$d_{ul,l} + \textstyle\sum_{k\in\boldsymbol{I}_{ul,l}} \boldsymbol{z}^T_{k,l} \leq N_{ul,l} \tag{4.5d}$$

where $\boldsymbol{I}_{dl,k}$ denotes the set of UL UEs for which the CLI is zero-forced at the kth DL UE, and $\boldsymbol{I}_{ul,l}$ denotes the set of DL UEs for which the CLI is zero-forced at the lth UL UE.

Equation (4.5c) means that DL UE k has $N_{dl,k}$ antennas to receive $d_{dl,k}$ streams while performing ZF to the CLI coming from a certain number of UL UEs. And similarly for an UL UE in (4.5d). $(\mathbf{1}^R_{k,l}, \mathbf{1}^T_{k,l}) = (1,0)$ or $(0,1)$ or $(1,1)$ means that in this link, the ZF is performed by the Rx or the Tx or by both in a shared fashion. [35] believes that these conditions are sufficient (i.e. correspond to a feasible design of Tx/Rx filters) but actually they are necessary conditions. Furthermore, the first term on the RHS of (4.5a) is suboptimal in the case $(\mathbf{1}^R_{k,l}, \mathbf{1}^T_{k,l}) = (1,1)$, when the minimum corresponds to the first argument.
The work here is inspired by the ideas of [35], which at first sight appears to introduce an elegant and simplified approach to DoF analysis in general interference networks, furthermore applicable to MIMO channels with general rank conditions. However, [35] does not seem to be aware of the vast body of work on interference alignment, and believes that the state of the art corresponds to one-sided ZF. As a result, they e.g. believe that the DoF region in [35, Fig. 1] represents an improvement w.r.t. their assumed state of the art, but actually the point $(8,8)$ is also achievable in the DoF region of [35, Fig. 1].

But due to the suboptimality of (4.5a), [35] does not capture this. On the other hand, in other scenarios, some DoF distributions that are assumed to be feasible by [35] will in reality not be.

Now, inspired by the work in [35], we shall investigate localized instances of the proper condition, or stated differently, we shall consider a distribution of the roles of the Tx/Rx variables in satisfying the ZF conditions. Actually, we had already considered such a role distribution perspective in [25], which in general can go beyond the global proper condition. But in the scenario considered here, in which each DL UE receives interference from each UL UE (at least if all channel ranks are positive), the ensemble of local proper conditions adds up to the single global proper condition. In any case, for the local version, consider first a somewhat simplified scenario in which the cross-link ZF in (2.2) is either handled completely by the corresponding Rx $\boldsymbol{U}_{dl,k}$ or completely by the corresponding Tx $\boldsymbol{V}_{ul,l}$. For the links (k,l) handled by the Rx, i.e. $(\mathbf{1}^R_{k,l}, \mathbf{1}^T_{k,l}) = (1,0)$, then (2.2) represents a *linear* ZF equation in $\boldsymbol{U}_{dl,k}$ which represents $z^R_{k,l} = \text{rank}(\boldsymbol{H}_{k,l}\boldsymbol{V}_{ul,l}) = \min(d_{ul,l}, r_{k,l})$ constraints [35, Lemma 1]. These constraints can actually be interpreted as applying to each column of $\boldsymbol{U}_{dl,k}$, which is an Rx beamformer for the corresponding stream of user k. For the overall beamforming matrix $\boldsymbol{U}_{dl,k}$, we account for the $d_{dl,k}$ streams and we get a total of $d_{dl,k}z^R_{k,l} = \min(d_{dl,k}d_{ul,l}, d_{dl,k}r_{k,l})$ ZF constraints. If we take into account that Rx $\boldsymbol{U}_{dl,k}$ will handle the ZF for the links in $\boldsymbol{I}_{dl,k}$, then we get the following local proper condition for $\boldsymbol{U}_{dl,k}$:

$$d_{dl,k}(N_{dl,k} - d_{dl,k}) \geq \sum_{l \in \boldsymbol{I}_{dl,k}} d_{dl,k}\boldsymbol{z}^R_{k,l} \tag{4.6}$$

$$\Rightarrow \quad N_{dl,k} - d_{dl,k} \geq \sum_{l \in \boldsymbol{I}_{dl,k}} \boldsymbol{z}^R_{k,l} \tag{4.7}$$

where the last equation corresponds exactly to (4.5c). It can be interpreted as a proper condition per stream, where the subtraction on the LHS makes sure that after the $N_{dl,k}$ antennas are used for ZF of interfering links, $d_{dl,k}$ dimensions are left for receiving that many streams. A completely analogous reasoning can be made for the case $(\mathbf{1}^R_{k,l}, \mathbf{1}^T_{k,l}) = (0,1)$ in which the ZF conditions are handled by the Tx side $\boldsymbol{V}_{ul,l}$, which will lead to (4.5d). The remaining case is $(\mathbf{1}^R_{k,l}, \mathbf{1}^T_{k,l}) = (1,1)$, which is not handled correctly in [35] or in (4.5b). The correct treatment actually corresponds to a finer split between the ZF roles at the Tx and Rx sides of a UE-to-UE link at the stream level. The resulting correct local proper conditions are given by Theorem 6 :

Theorem 6. ***Local Proper Condition for interference alignment Feasibility in a Reduced rank MIMO IBMAC-IC*** *For reduced-rank MIMO channels, if the tuple of DoF* $(d_{ul,1}, ..., d_{ul,K_{ul}}, d_{dl,1}, ..., d_{ul,K_{dl}})$ *is achievable through interference alignment, then*

it must satisfy the following local proper conditions:

$$\forall k,l: \begin{cases} d_{dl,k}\boldsymbol{z}^R_{k,l} + d_{ul,l}\boldsymbol{z}^T_{k,l} = d_{dl,k}d_{ul,l}\,, \\ \qquad \textit{if } r_{k,l} \geq \max(d_{dl,k}\mathbf{1}_{\boldsymbol{z}^R_{k,l}}, d_{ul,l}\mathbf{1}_{\boldsymbol{z}^T_{k,l}}) \\ \boldsymbol{z}^T_{k,l} = \min(d_{dl,k}, r_{k,l} - z^R_{k,l})\,, \\ \qquad \textit{if } d_{dl,k} < r_{k,l} < d_{ul,l} \\ \boldsymbol{z}^R_{k,l} = \min(d_{ul,l}, r_{k,l} - z^T_{k,l})\,, \\ \qquad \textit{if } d_{ul,l} < r_{k,l} < d_{dl,k} \\ \boldsymbol{z}^R_{k,l} + \boldsymbol{z}^T_{k,l} = r_{k,l}\,, \\ \qquad \textit{otherwise} \end{cases} \tag{4.8}$$

$$\forall l: \quad N_{ul,l} - d_{ul,l} \geq \textstyle\sum_{k\in\boldsymbol{I}_{ul,l}} \boldsymbol{z}^T_{k,l}$$

$$\forall k: \quad N_{dl,k} - d_{dl,k} \geq \textstyle\sum_{l\in\boldsymbol{I}_{dl,k}} \boldsymbol{z}^R_{k,l}$$

where $\mathbf{1}_x = 1$ *if* $x > 0$ *and* $\mathbf{1}_x = 0$ *otherwise. One can check easily that the cases* $(\mathbf{1}^R_{k,l}, \mathbf{1}^T_{k,l}) = (1,0), (0,1)$ *discussed above can be recovered from* (4.8).

The proof of (4.8) appears in Appendix D. It turns out that summing up all local conditions in (4.8) leads to the global proper condition (4.2).

4.3.1 Uniform Scenarios

To have a simplified version of the conditions above we define a uniform asymmetric scenario, in which:

$d_{dl,k} = d_{dl}$, $\forall k \in [1, ..., K_{dl}]$

$d_{ul,l} = d_{ul}$, $\forall l \in [1, ..., K_{ul}]$

$N_{dl,k} = N_{dl}$, $\forall k \in [1, ..., K_{dl}]$

$N_{ul,l} = N_{ul}$, $\forall l \in [1, ..., K_{ul}]$

$r_{k,l} = r$, $\forall l \in [1, ..., K_{ul}]$, $\forall k \in [1, ..., K_{dl}]$

Then the centralized proper condition in equation (4.2) becomes:

$$K_{ul}d_{ul}(N_{ul} - d_{ul}) + K_{dl}d_{dl}(N_{dl} - d_{dl}) \geq K_{ul}\,K_{dl}\,\min(rd_{dl}, rd_{ul}, d_{ul}d_{dl}) \tag{4.9}$$

We define also a uniform symmetric case when for $K_{dl} = K_{ul} = K$, $d_{dl} = d_{ul} = d$ and $N_{dl} = N_{ul} = N$, for which (4.9) becomes:

$$d \leq N - \frac{K}{2} \min(d, r) \tag{4.10}$$

Now, consider the local proper conditions and introduce $n_{F,k} = |\boldsymbol{I}_{dl,k}|$, $n_{G,l} = |\boldsymbol{I}_{ul,l}|$. Hence $n_{F,k}$ (resp.$n_{G,l}$) denote the number of UL (resp. DL) UEs for which the CLI is canceled by the kth DL UE (resp. the lth UL UE). For this ZF role distribution to ensure the cancellation of all CLI, we require:

$$\sum_{k=1}^{K_{dl}} n_{F,k} + \sum_{l=1}^{K_{ul}} n_{G,l} \geq K_{ul} K_{dl} \,. \tag{4.11}$$

In the uniform case, $n_{F,k} = n_F, \forall k \in [1, ..., K_{dl}]$ and $n_{G,l} = n_G, \forall l \in [1, ..., K_{ul}]$, equation (4.11) becomes:

$$K_{dl} n_F + K_{ul} n_G \geq K_{ul} K_{dl} \,. \tag{4.12}$$

The optimization of n_F, n_G depends on the desired point (d_{dl}, d_{ul}) in the DoF region. For a uniform asymmetric case, we get on the Rx side $((\mathbf{1}^R_{k,l}, \mathbf{1}^T_{k,l}) = (1, 0))$:

$$d_{dl} \leq N_{dl} - n_F min(d_{ul}, r) \tag{4.13}$$

and on the Tx side $((\mathbf{1}^R_{k,l}, \mathbf{1}^T_{k,l}) = (0, 1))$:

$$d_{ul} \leq N_{ul} - n_G min(d_{dl}, r) \,. \tag{4.14}$$

Equations (4.13) and (4.14) are dubbed as our combined method for interference alignment feasibility, to refer to the shared ZF considerations between Tx and Rx.
Exploring the case $(\mathbf{1}^R_{k,l}, \mathbf{1}^T_{k,l}) = (1, 1)$ only leads to a finer granularity of ZF roles (at stream level instead of user level). For the symmetric case we have $n_F = n_G = \frac{K}{2}$ and we get back (4.10).

We can consider the distributed approaches with fixed Tx/Rx factors (symmetric uniform case):

- $(\mathbf{1}^R_{k,l}, \mathbf{1}^T_{k,l}) = (1, 0)$: applied to all links $n_F = K$:

$$d \leq N - K \min(d, r) \tag{4.15}$$

- $(\mathbf{1}^R_{k,l}, \mathbf{1}^T_{k,l}) = (0, 1)$: applied to all links $n_G = K$:

$$d \leq N - K \min(d, r) \tag{4.16}$$

- $(\mathbf{1}^R_{k,l}, \mathbf{1}^T_{k,l}) = (1, 1)$: considering (4.5a) from [35], applied to all links, we can take $\boldsymbol{z}^R_{k,l} = \boldsymbol{z}^T_{k,l} = \min(2d, r)$ leading to

$$d \leq N - \frac{K}{2} \min(2d, r) \tag{4.17}$$

Which all three yield worse DoF than (4.10).

We analyze the feasibility of the combined method that is given in (4.13) and (4.14). For this, we compare the DoF given by the combined method in (4.13) and (4.14) to the DoF given by the sufficient and necessary condition for a generic rank interference channel in Theorem 7, which is a precise characterization of the feasible DoF. And we make our observation in the following conjecture:

Conjecture 4.
For a DynTDD system, if the DoF tuple $(d_{ul,1}, ..., d_{ul,K_{ul}}, d_{dl,1}, ..., d_{dl,K_{dl}})$ *satisfies the condition for the combined method in equations* (4.13) *and* (4.14)*, then this DoF is almost surely feasible.*

4.4 Necessary and Sufficient Condition for interference alignment Feasibility

The necessary and sufficient condition for interference alignment feasibility for rank deficient interfering channels is given by the following theorem:

Theorem 7. ***Necessary and Sufficient Condition for interference alignment Feasibility in Reduced Rank MIMO IBMAC-IC***
For a deficient rank MIMO IBMAC-IC, the DoF $(d_{ul,1}, ..., d_{ul,K_{ul}}, d_{dl,1}, ..., d_{ul,K_{dl}})$ *are feasible almost surely if and only if*

$$rank(\boldsymbol{J}) = rank(\boldsymbol{J}_J) = rank([\boldsymbol{J} \ \ \boldsymbol{J}_H]) \tag{4.18}$$

i.e., the column space of $\boldsymbol{J}_H$ *should be contained in the column space of* $\boldsymbol{J}$*.*

Appendix E provides the representation of $\boldsymbol{J}$ in equations (E.4) and (E.5), and $\boldsymbol{J}_H$ in equation (E.7), containing interference channel matrices. Note that the result in Theorem 7 is valid for *any* interference network, with appropriately defined matrices $\boldsymbol{J}$, $\boldsymbol{J}_H$.
The detailed proof of Theorem 7 can be found in Appendix E.

Now, we leverage the non-uniform DoF among the DL UEs and the UL UEs, wherein the number of data streams at each DL UE, denoted as $d_{dl,k}$, or each UL UE, denoted as $d_{ul,l}$, may differ even within a uniform DynTDD system. Based on this observation, we propose the following remark:

Remark 1. *In DynTDD systems, if the tuple of DoF* $(d_{ul,1}, ..., d_{ul,K_{ul}}, d_{dl,1}, ..., d_{dl,K_{dl}})$ *is feasible for interference alignment according to the conditions outlined in theorem 7, and there exists a non-uniform distribution of DoF at the receivers (DL UEs) and/or transmitters (UL UEs), then the resulting sum DoF will be equal to or greater than the sum DoF achieved when assuming a feasible uniform DoF distribution.*

4.5 Numerical Results

In Table 4.1 we evaluate the DoF of a uniform system ($N_{ul,l} = N_{ul}$, $N_{dl,k} = N_{dl}$, $d_{ul,l} = d_{ul}$, $d_{dl,k} = d_{dl}$, $r_{kl} = r$) with $N_{ul} = 6$, $N_{dl} = 4$, $K_{dl} = 4$ and $K_{ul} = 2$, for the different conditions established in this chapter. In the following, we describe each element in Table 4.1, where a generic tuple $(d_{dl}, d_{ul}, d_{tot})$ denotes the uniform DoF of a DL UE, an UL UE, and the overall UL+DL sum DoF:

- $(d_{p,dl}, d_{p,ul}, d_{p,tot})$ considering Theorem 5 in the centralized case, i.e. considering (only) the proper (necessary) interference alignment feasibility conditions for a centralized design,

- $(d_{c,dl}, d_{c,ul}, d_{c,tot})$ considering the combined method, with DL UE DoF as in equation (4.13), and the UL UE DoF as in equation (4.14) (with the corresponding optimized n_F, n_G shown in Table 4.1 and denoted as n_{F_c}, n_{G_c}), i.e. this concerns a feasible centralized approach in which there is an optimized partitioning of the ZF roles among all Tx/Rx: each interference link is either zero-forced by the Tx or the Rx involved (but the resulting Tx depend on the Rx and vice versa, the Tx/Rx design requires an iterative algorithm),

- $(d_{r,dl}, d_{r,ul}, d_{r,tot})$ considering Rx side ZF only as in (4.13) with $n_F = K_{ul}$, i.e. all ZF is done by the Rx only (closed-form solutions, non-iterative, hence can be considered a distributed approach),

- $(d_{t,dl}, d_{t,ul}, d_{t,tot})$ considering Tx side ZF only as in(4.14) with $n_G = K_{dl}$, i.e. all ZF is done by the Tx only (closed-form solutions, non-iterative, hence can be considered a distributed approach),

- $(d_{T7,dl}, d_{T7,ul}, d_{T7,tot})$ considering Theorem 7, i.e. the exactly maximally feasible DoF in a centralized approach (requires an iterative Tx/Rx design).

In Algorithm 2, we offer pseudo-code to facilitate comprehension of the process for obtaining numerical results showcased in Tables 4.1 and 4.2

Algorithm 2 Procedure for Obtaining Numerical Results in Tables 4.1 and 4.2

For $K_{dl} = 3$ and $K_{ul} = 2$:

1) For a given system dimension $N_{dl,1}$, $N_{dl,2}$, $N_{dl,3}$, $N_{ul,1}$ and $N_{ul,2}$

I)For a combinations of data streams $(d_{dl,1}, d_{dl,2}, d_{dl,3}, d_{ul,1}, d_{ul,2})$ that gives the maximum DoF which satisfy the proper condition

i) Test if the following conditions are satisfied:

Distributed method condition
Combined method condition
Unilateral ZF condition
The necessary and sufficient condition

ii) If not satisfied reduce the $d_{dl,k}$and/or $d_{ul,l}$ until the conditions are satisfied

iii) Indicate the maximum feasible DoF for each condition

In Algorithm 3, we provide pseudo-code outlining the procedure we followed to verify the necessary and sufficient condition stated in Theorem 7.

Algorithm 3 Pseudo code to check the necessary and sufficient condition in Theorem 7

For a given dimension K_{dl}, K_{ul}, $N_{dl,1}, ..., N_{dl,K_{dl}}$, $N_{ul,1}, ..., N_{ul,K_{ul}}$, $d_{dl,1}, ..., d_{dl,K_{dl}}$, $d_{ul,1}, ..., d_{ul,K_{ul}}$ and $r_{k,l}$:

1) Set $\boldsymbol{H}_{k,l}$: Define $\boldsymbol{A}_{k,l}^{(1)}$, $\boldsymbol{A}_{k,l}^{(2)}$, $\boldsymbol{B}_{k,l}^{(1)}$ and $\boldsymbol{B}_{k,l}^{(2)}$ with respects to:

I)$\boldsymbol{H}_{k,l}^{(1)} = \boldsymbol{B}_{k,l}^{(1)H} \boldsymbol{A}_{k,l}^{(1)}$ and $rank(\boldsymbol{A}_{k,l}) = rank(\boldsymbol{B}_{k,l}) = r_{k,l}$, that amounts to choose:

i) $n_{k,l}$ rows equal to zero in $\boldsymbol{A}_{k,l}^{(1)}$, and $\boldsymbol{B}_{k,l}^{(1)}$ with the complementary $r_{k,l} - n_{k,l}$ rows equal to zero, which amounts to satisfy :

a)$N_{ul,l} - d_{dl,k} \geq r_{k,l} - min(r_{k,l} - n_{k,l}, d_{ul,l})$ so $= rank(\boldsymbol{A}_{k,l}) = r_{k,l}$
b)$N_{dl,k} - d_{ul,l} \geq r_{k,l} - min(r_{k,l} - n_{k,l}, d_{dl,k})$ so $= rank(\boldsymbol{B}_{k,l}) = r_{k,l}$

2) Construct the Jacobian matrix $\boldsymbol{J}$ and $\boldsymbol{J}_H$ from $\boldsymbol{A}_{k,l}^{(1)}$, $\boldsymbol{A}_{k,l}^{(2)}$, $\boldsymbol{B}_{k,l}^{(1)}$ and $\boldsymbol{B}_{k,l}^{(2)}$

check if $rank[\boldsymbol{J}\boldsymbol{J}_H] = rank(\boldsymbol{J})$

For the application of Theorem 7, we perform an algorithm that allows us to check the rank of the matrices $\boldsymbol{J}$ and $\boldsymbol{J}_J$ depending on the variables N_{ul}, N_{dl}, d_{ul}, d_{dl} and $r_{k,l}$, when given the IC matrix $\boldsymbol{H}_{k,l}$ with random coefficients that must satisfy the conditions mentioned in Appendix E. We test all possible combinations regarding the values of n_{kl} and also the possible positions of the zero rows in $\boldsymbol{A}_{kl}^{(1)}$ and $\boldsymbol{B}_{kl}^{(1)}$in (E.1)(the details of these variables are mentioned in Appendix E).

Table 4.1: DoF per user as a function of the rank of any cross-link channel with $N_{ul} = 6$, $N_{dl} = 4$, $K_{ul} = 2$ and $K_{dl} = 4$.

rank of the IC	0	1	2	3	4
$(d_{p,dl},d_{p,ul},d_{p,tot})$	(4,6,28)	(3,4,20)	(2,4,16)	(2,2,12)	(2,2,12)
$(d_{c,dl},d_{c,ul},d_{c,tot})$	(4,6,28)	(3,4,20)	(2,2,12)	(2,2,12)	(2,2,12)
$(n_{F,c},n_{G,c})$	(1,2)	(1,2)	(1,2)	(1,2)	(1,2)
$(d_{r,dl}, d_{r,ul}, d_{r,tot})$	(4,6,28)	(2,6,20)	(2,1,10) $_{(0,6,12)^*}$	(2,1,10) $_{(0,6,12)^*}$	(2,1,10) $_{(0,6,12)^*}$
$(d_{t,dl}, d_{t,ul}, d_{t,tot})$	(4,6,28)	(4,2,20)	(1,2,8) $_{(4,0,16)^*}$	(1,2,8) $_{(4,0,16)^*}$	(1,2,8) $_{(4,0,16)^*}$
$(d_{T7,dl}, d_{T7,ul}, d_{T7,tot})$	(4,6,28)	(3,4,20)	(2,3,14)	(2,2,12)	(2,2,12)

(*): the given DoF does not satisfy the conditions in (3.1), if a negative DoF results from a formula, this DoF will be set to zero logically.

Considering Table 4.1 and the previously established interference alignment Feasibility conditions, the following observations can be made:

- The first line of Table 4.1 gives the proper condition, which represents an upper bound for the DoF, that is not necessarily reachable regarding the interference alignment feasibility,

- The necessary and sufficient condition in Theorem 7 (sixth line of Table 4.1) precisely defines the feasible DoF. Comparing it to the results of the combined method (second line of Table 4.1), derived from the proper condition in the centralized case, reveals an interesting alignment as long as the combined method is written in terms of the problem dimension. Specifically, the combined method matches the DoF given by Theorem 7, especially in low-rank channel scenarios.

To analyze the observations given in Remark 1, we give Tables 4.2 and 4.3, in which we consider a MIMO IBMAC-IC, and we evaluate the DoF for $K_{ul} = 2$ and $K_{dl} = 4$ of the two systems $N_{ul} = 3$, $N_{dl} = 4$, and $N_{ul} = 3$, $N_{dl} = 6$ respectively. In these tables, we evaluate the different conditions as in table 4.1.

Table 4.2: DoF per user as a function of the rank of cross-link channel with $N_{ul} = 3$, $N_{dl} = 4$, $K_{ul} = 2$ and $K_{dl} = 4$.

Rank of the IC	0	1	2	3
$(d_{p,dl},d_{p,ul},d_{p,tot})$	(4,3,22)	(3,2,16)	(3,1,14)	((3,2,2,2),1,11)**
$(d_{c,dl},d_{c,ul},d_{c,tot})$	(4,3,22)	(3,1,14)	(2,1,10)	(2,1,10)
$(n_{F,c},n_{G,c})$	(1,2)	(1,2)	(2,0)	(2,0)
$(d_{r,dl}, d_{r,ul}, d_{r,tot})$	(4,3,22)	(2,3,14)	(2,1,10)	(2,1,10)
$(d_{t,dl}, d_{t,ul}, d_{t,tot})$	(4,3,22)	(4,0,16)*	(4,0,16)*	(4,0,16)*
$(d_{T7,dl}, d_{T7,ul}, d_{T7,tot})$	(4,3,22)	((3,3,2,2),2,14)**	((3,3,2,2),1,12)**	((3,2,2,2),1,11)**

Table 4.3: DoF per user as a function of the rank of any cross-link channel with $N_{ul} = 3$, $N_{dl} = 6$, $K_{ul} = 2$ and $K_{dl} = 4$.

Rank of the IC	0	1	2	3
$(d_{p,dl},d_{p,ul},d_{p,tot})$	(6,3,30)	((6,5,5,5),2,25)**	((6,5,5,5),1,23)**	(5,1,22)
$(d_{c,dl},d_{c,ul},d_{c,tot})$	(6,3,30)	(5,1,22)	(4,1,18)	(4,1,18)
$(n_{F,c},n_{G,c})$	(1,2)	(1,2)	(2,0)	(2,0)
$(d_{r,dl}, d_{r,ul}, d_{r,tot})$	(6,3,30)	(4,3,18)	(2,3,14)	(0,3,6)*
$(d_{t,dl}, d_{t,ul}, d_{t,tot})$	(6,3,30)	(6,0,24)*	(6,0,24)*	(6,0,24)*
$(d_{T7,dl}, d_{T7,ul}, d_{T7,tot})$	(6,3,30)	(5,1,22)	((5,5,4,4),1,20)**	(4,1,18)

(*): the given DoF does not satisfy the conditions in (3.1), if a negative DoF results from a formula, this DoF will be set to zero logically
(**): The given DoF represents a non-uniform DoF at DL UEs, of the form $((d_{dl,1}, d_{dl,2}, d_{dl,3}, d_{dl,4}), d_{ul}, d_{tot})$

In Table 4.2 we can conclude that all the given DoF by the combined method in equations (4.13) and (4.14), is feasible as long as this DoF satisfies the necessary and sufficient condition in Theorem 7. For Remark 1, we can observe, in Table 4.2 for $r = 2$ and when considering the condition in Theorem 7, that the non uniform tuple DoF $d_{ul,1} = d_{ul,2} = 1, d_{dl,1} = d_{dl,2} = 3, d_{dl,3} = d_{dl,4} = 2$, which gives a sum DoF equal to 12, is feasible. Otherwise, if we assume a uniform DoF (i.e. $d_{ul,1} = d_{ul,2}$ and $d_{dl,1} = d_{dl,2} = d_{dl,3} = d_{dl,4}$) we are limited to a feasible sum DoF equal to 10. The same observation applies to Table 4.3 when $r = 2$, considering the condition stated in Theorem 7. This condition specifies that the non-uniform tuple DoF $d_{ul,1} = d_{ul,2} = 1, d_{dl,1} = d_{dl,2} = 5, d_{dl,3} = d_{dl,4} = 4$, resulting in a total DoF sum of 20, is feasible. Alternatively, if we consider uniform DoF (where $d_{ul,1} = d_{ul,2}$ and $d_{dl,1} = d_{dl,2} = d_{dl,3} = d_{dl,4}$), the achievable total DoF is constrained to 18. Exploring various combinations of data streams received and transmitted by users can be

intriguing. This exploration could potentially enhance the total DoF and consequently, the data transmission rate, especially in high SNR scenarios.

4.6 Closing Remarks

In this enlightening chapter, we navigated the intricate terrain of interference channels, specifically focusing on the realistic scenario of reduced-rank interference channel matrices. This departure from the conventional full-rank channel matrix assumption was pivotal, considering the multifaceted interactions with the environment, such as absorption, reflection, and scattering caused by surrounding objects.
Central to our discussions were the various interference alignment conditions: the proper conditions, essential for establishing a robust framework, and the necessary and sufficient conditions, which provide the exact feasible DoF. Through meticulous analysis, we explored optimization instances, aiming to discern the optimal division of ZF work between reception and transmission. These endeavors shed light on the intricate balance between efficiency and feasibility in interference alignment strategies.
The numerical results, our guiding compass, meticulously evaluate these diverse conditions, illuminating the gaps between them and delineating the limits of each model. This critical assessment not only highlighted the strengths and weaknesses of different approaches but also provided the maximum feasible DoF concerning interference alignment.

Chapter 5

Feasibility Condition of interference alignment for the MIMO IBMAC-IC – Distributed case

5.1 Overview

In the upcoming chapter, we delve into the dynamic landscape of distributed scenarios within wireless communication systems, a departure from the rigid constraints of centralized approaches. Here, each Tx and Rx operates with the local Channel State Information (CSI) of channels directly connected to it. This decentralized setup stands in stark contrast to the centralized paradigm, where a central unit holds the responsibility of possessing global CSI. This fundamental shift in perspective liberates our study assumptions, allowing us to explore communication scenarios more attuned to real-world complexities. The heart of our exploration lies in reduced-rank interference channel matrices, where the full-rank scenario emerges as a special case. By directly engaging with these reduced rank matrices, we unlock the door to a global perspective.
We start with the establishment of necessary conditions, which intriguingly double as sufficient conditions. This duality arises from the feasibility of corresponding Tx/Rx designs, captured through linear zero-forcing equations. As we unravel these fundamental equations, we gain deeper insights into the intricacies of interference alignment, paving the way for more informed decision-making in the design of communication systems. We push the boundaries further, seeking to optimize the division of zero-forcing interference between reception and transmission.

5.2 System Model

In our exploration of the MIMO DynTDD system discussed in Chapter 4, we ensure uniformity in the system configuration, encompassing both DL and UL cells, as well as

users and base stations involved in interference interactions. The factorization of the interference channel provided in equation (4.1) and the interference alignment equation in (2.2) enable us to derive the following new zero-forcing equations.

$$\boldsymbol{U}_{dl,k}^{H}\boldsymbol{B}_{k,l}\boldsymbol{A}_{k,l}^{H}\boldsymbol{V}_{ul,l}=0 \tag{5.1}$$

In the distributed scenario, our system can be split into two zero-forcing systems, ensuring interference alignment by meeting one of the following equations:

$$\boldsymbol{U}_{dl,k}^{H}\boldsymbol{B}_{k,l}=0,\forall l\in\boldsymbol{I}_{dl,k} \tag{5.2a}$$

or

$$\boldsymbol{A}_{k,l}^{H}\boldsymbol{V}_{ul,l}=0,\forall k\in\boldsymbol{I}_{ul,l} \tag{5.2b}$$

5.3 Distributed Solution Exploiting the Low-Rank Channel Factorization

As opposed to the centralized case, in the distributed case, each Tx/Rx disposes of at most local CSI, i.e. of the channels directly connected to it. In both distributed and centralized scenarios, the fundamental rule remains unchanged for the establishment of the proper condition: the number of variables must equal or exceed the count of non-linear equations in (5.2) for a feasible solution. The conditions required for the distributed solutions discussed in this section are not only necessary but also sufficient, as they align with linear ZF equations and ensure the feasibility of the corresponding Tx/Rx designs. In this case the global proper condition (4.2) reduces to :

Theorem 8. ***Global Proper Condition for interference alignment Feasibility in a Reduced MIMO IBMAC-IC*** *For reduced-rank MIMO channels, if the tuple of DoF* $(d_{ul,1},...,d_{ul,K_{ul}},d_{dl,1},...,d_{ul,K_{dl}})$ *is achievable through interference alignment, then it must satisfy the global proper condition:*

$$\sum_{l=1}^{K_{ul}}d_{ul,l}(N_{ul,l}-d_{ul,l})+\sum_{k=1}^{K_{dl}}d_{dl,k}(N_{dl,k}-d_{dl,k})\geq\sum_{l=1}^{K_{ul}}\sum_{k=1}^{K_{dl}}r_{k,l}\,\min(d_{dl,k},d_{ul,l}) \tag{5.3}$$

The corresponding local proper conditions become:

Theorem 9. ***Local Proper Condition for interference alignment Feasibility in a Reduced MIMO IBMAC-IC*** *For reduced-rank MIMO channels, if the tuple of DoF* $(d_{ul,1},...,d_{ul,K_{ul}},d_{dl,1},...,d_{ul,K_{dl}})$ *is achievable through interference alignment, then it must satisfy the local proper condition:*

$$\begin{aligned}&\forall k,l:\boldsymbol{z}_{k,l}^{R}+\boldsymbol{z}_{k,l}^{T}=r_{k,l}\,,\\&\forall l:\quad N_{ul,l}-d_{ul,l}\geq\textstyle\sum_{k\in\boldsymbol{I}_{ul,l}}\boldsymbol{z}_{k,l}^{T}\\&\forall k:\quad N_{dl,k}-d_{dl,k}\geq\textstyle\sum_{l\in\boldsymbol{I}_{dl,k}}\boldsymbol{z}_{k,l}^{R}\end{aligned} \tag{5.4}$$

This represents a generalization of [40] in which we considered the special case in which either $\boldsymbol{z}_{k,l}^R = r_{k,l}$, $\boldsymbol{z}_{k,l}^T = 0$, or $\boldsymbol{z}_{k,l}^T = r_{k,l}$, $\boldsymbol{z}_{k,l}^R = 0$. In other words, the interference of a particular UE-to-UE link is handled completely by either the Tx or the Rx. However, the handling of all UE-to-UE links is still partitioned between UL and DL UEs. The ZF of any particular UE-to-UE link can also be shared between Tx and Rx, as considered here. The first line in (5.4) can be interpreted as:

$$\begin{aligned} &\boldsymbol{B}_{k,l}^H \boldsymbol{U}_{dl,k} \text{ has } \boldsymbol{z}_{k,l}^R \text{ rows of zeros} \\ &\boldsymbol{A}_{k,l}^H \boldsymbol{V}_{ul,l} \text{ has } \boldsymbol{z}_{k,l}^T \text{ rows of zeros} \end{aligned} \tag{5.5}$$

where the zero rows in the two factors are complementary so that (2.2) is satisfied.

5.3.1 Uniform Scenario

As for the centralized scenario, we introduce the optimization instances $n_{F,k} = |\boldsymbol{I}_{dl,k}|$ and $n_{G,l} = |\boldsymbol{I}_{ul,l}|$. Hence $n_{F,k}$ (resp.$n_{G,l}$) denote the number of UL (resp. DL) UEs for which the cross-link interference is canceled by the kth DL UE (resp. the lth UL UE). If we consider the distributed solution based on low-rank channel factorizations, then for the uniform asymmetric case we obtain:

$$d_{dl} \leq N_{dl} - n_F r \tag{5.6a}$$
$$d_{ul} \leq N_{ul} - n_G r \tag{5.6b}$$

As in the centralized case, to ensure the cancellation of all the cross-link interference equation (4.12) should be satisfied. For the uniform symmetric case, we get $n_F = n_G = \frac{K}{2}$, and (5.6a), (5.6b) become:

$$d \leq N - \frac{K}{2} r \ . \tag{5.7}$$

5.4 Distributed Solution Based on Fixed Tx/Rx Factors

When the selections $(\mathbf{1}_{k,l}^R, \mathbf{1}_{k,l}^T) = (1,0)$ or $(0,1)$ are applied to all links, then in general the design of Tx and Rx is coupled. This coupling can be broken if either $(\mathbf{1}_{k,l}^R, \mathbf{1}_{k,l}^T) = (1,0)$ is applied to all links, or $(\mathbf{1}_{k,l}^R, \mathbf{1}_{k,l}^T) = (0,1)$ is applied to all links. In this case we get $\forall k, l$:

$$\begin{aligned} &\text{either } \boldsymbol{z}_{k,l}^R = \min(d_{ul,l}, r_{k,l}) \\ &\text{or } \boldsymbol{z}_{k,l}^T = \min(d_{dl,k}, r_{k,l}) \end{aligned} \tag{5.8}$$

where of course (4.5c), (4.5d) continue to apply. When the Rx handles all the ZF, then the Tx can be designed separately, e.g. based on the UE-BS channels, and vice versa.

5.5 Numerical Results

In the presented numerical results, our focus lies on evaluating the distributed method. This particular approach holds our interest due to its representation of a practical and achievable scenario. To truly understand the potential improvements this method could offer, it is imperative to compare it with the necessary and sufficient conditions in the centralized scenario. This condition provides a precise characterization of the feasible DoF. By juxtaposing the distributed method against these interference alignment conditions, we can discern the method's effectiveness and gain valuable insights into its capabilities.

In Tables 5.1 and 5.2, for two different system dimensions $N_{ul} = 3$, $N_{dl} = 6$ and $N_{ul} = 3$, $N_{dl} = 4$ respectively, we present the proper condition in Theorem 5 alongside the necessary and sufficient condition in Theorem 8, similar to the approach employed in Table 4.1, Table 4.2 and Table 4.3. Additionally, we introduce the DoF denoted as $(d_{d,dl}, d_{d,ul}, d_{d,tot})$, which pertains specifically to the distributed method. In this context, the DL UE DoF is calculated according to (5.6a), and the UL UE DoF follows (5.6b), with the respective optimized parameters n_F and n_G detailed in Table 5.1 and denoted as $n_{F,d}$ and $n_{G,d}$. Notably, this distributed method entails a unique approach where the Tx/Rx filters are solely dependent on the low-rank channel factors on their respective sides. Moreover, the filter designs are closed-form and non-iterative. Through an optimized allocation of ZF roles among the Txs and Rxs, this methodology maximizes efficiency. The results presented in these tables provide a comprehensive overview of the outcomes obtained through the distributed method, highlighting its effectiveness and the innovative strategies employed in its implementation.

Table 5.1: DoF per user as a function of the rank of any cross-link channel with $N_{ul} = 3$, $N_{dl} = 6$, $K_{ul} = 2$ and $K_{dl} = 4$.

Rank of the IC r	0	1	2	3
$(d_{p,dl},d_{p,ul},d_{p,tot})$	(6,3,30)	((6,5,5,5),2,25)	((6,5,5,5),1,23)	(5,1,22)
$(d_{d,dl},d_{d,ul},d_{d,tot})$	(6,3,30)	(5,1,22)	(2,3,14)or $_{(4,0,16)^*}$	$_{(3,0,12)^*}$
$(n_{F,d},n_{G,d})$	(1,2)	(1,2)	(1,2) or (2,0)	(1,2)
$(d_{T7,dl}, d_{T7,ul}, d_{T7,tot})$	(6,3,30)	(5,1,22)	((5,5,4,4),1,20)**	(4,1,18)

Table 5.2: DoF per user as a function of the rank of cross-link channel with $N_{ul} = 3$, $N_{dl} = 4$, $K_{ul} = 2$ and $K_{dl} = 4$.

Rank of the IC r	0	1	2	3
$(d_{p,dl},d_{p,ul},d_{p,tot})$	(4,3,22)	(3,2,16)	(3,1,14)	((3,2,2,2),1,11)**
$(d_{d,dl},d_{d,ul},d_{d,tot})$	(4,3,22)	(3,1,14)	(0,3,6)*	(0,3,6)*
$(n_{F,d},n_{G,d})$	(1,2)	(1,2)	(2,0)	(1,2)
$(d_{T7,dl}, d_{T7,ul}, d_{T7,tot})$	(4,3,22)	((3,3,2,2),2,14)**	((3,3,2,2),1,12)**	((3,2,2,2),1,11)**

(*): the given DoF does not satisfy the conditions in (3.1), if a negative DoF results from a formula, this DoF will be set to zero logically
(**): the given DoF represents a non-uniform DoF at DL UEs, of the form $((d_{dl,1}, d_{dl,2}, d_{dl,3}, d_{dl,4}), d_{ul}, d_{tot})$

DoF derived through the distributed method presents a feasible configuration for interference alignment within the given model. This assertion finds validation in Table 5.1 and Table 5.2, where the DoF obtained from the distributed method is equal to or less than the precise feasible DoF indicated by the necessary and sufficient condition outlined in Theorem 7. Significantly, these numerical results shed light on an important observation: the distributed solution does not demonstrate sub-optimality concerning the centralized optimal solution, particularly when the rank of the interference channel matrix is less or equal to the received/transmitted data stream. This finding underscores the efficiency and effectiveness of the distributed approach at low rank channel matrix, showcasing its ability to achieve a feasible DoF for interference alignment without compromising optimality.

5.6 Closing Remarks

In conclusion, exploring distributed methods in our study has unveiled intriguing avenues in the interference alignment. Our focus on local CSI knowledge has allowed us to delve into the intricacies of these decentralized approaches. By establishing interference alignment conditions, we have deciphered the optimal dimensions of a system, considering factors such as the number of antennas and interfering/interfered UEs and the number of data streams.
The numerical results vividly illustrate the disparities in DoF between centralized and distributed methodologies. This revelation serves as a testament to the potential efficiency of distributed methods. What is particularly striking is the demonstration of how a distributed approach, while inherently feasible, can match the efficacy of its centralized counterpart. This finding holds immense promise, especially in real-world applications where implementing centralized methods might be hindered by a plethora of constraints. Now armed with interference alignment conditions that precisely define our system's dimensions, including antennas, data streams, and users, we are ready to shift to the next chapter. Where we delve into the strategic design of beamformers for DL and UL UEs,

as well as the BSs. These beamformers are pivotal in ensuring interference alignment and maximizing overall data rates.

Part III

Optimizing Beamforming Design: Enhancing Signal Focusing and Interference Alignment

Chapter 6

The Beamforming Design for Interference Alignment and Sum Rate Optimization

6.1 Overview

Beamformers at transmission and reception are signal-processing techniques in wireless communication. At transmission, beamforming adjusts signal properties to focus energy in a specific direction. At reception, it processes incoming signals to extract desired information while minimizing interference. These methods enhance signal quality and system performance. Weighted Minimum Mean Square Error (WMMSE) beamformers are advanced signal-processing algorithms used in wireless communication systems. They optimize the beamforming vectors at both Tx and Rx points to minimize the mean square error between the desired signal and the received signal while considering channel conditions and interference. To optimize the power allocation at the BS, we use the water-filling method that maximizes the system's capacity by allocating more resources to channels with lower interference or noise levels.
In this chapter, we focus on designing beamformers for DL and UL UEs, initially ensuring interference elimination through ZF. We then employ WMMSE beamformers at the user equipment level to maximize sum rates. For DL BSs, WMMSE beamformers are applied, alongside the water-filling method for optimized power allocation. These techniques collectively enhance system efficiency by eliminating interference and optimizing power usage.

6.2 System Model

In our comprehensive exploration of the MIMO DynTDD system, as meticulously detailed in Chapter 4, we uphold a coherent and steadfast approach to configuring the

system.
Additionally, we introduce a crucial dimension to our study. Recognizing the pivotal role of sum rates as a metric for evaluating system performance in simulation results, we provide a precise formulation of these rates for both the UL and DL channels. For this system, the achievable rate for the UL user l is given as:

$$\begin{aligned}\boldsymbol{R}_{ul,l} = \log\det\Bigg(&\boldsymbol{I}_{M_{ul}} + \boldsymbol{H}_l^{UL}\boldsymbol{V}_{ul,l}\boldsymbol{V}_{ul,l}^H(\boldsymbol{H}_l^{UL})^H \\ &\Bigg(\sum_{i=1,i\neq l}^{K_{ul}} \boldsymbol{H}_i^{UL}\boldsymbol{V}_{ul,i}\boldsymbol{V}_{ul,i}^H(\boldsymbol{H}_i^{UL})^H + \sigma_{ul,l}^2\boldsymbol{I}_{M_{ul}}\Bigg)^{-1}\Bigg)\end{aligned} \tag{6.1}$$

In our study we consider a ZF precoders $\boldsymbol{V}_{ul,l}$ at each UL UE given as:

$$\boldsymbol{V}_{ul,l} = \sqrt{\frac{p_{ul,l}}{\mathrm{Tr}(\boldsymbol{G}_{z,l}\boldsymbol{G}_{z,l}^H)}}\boldsymbol{G}_{z,l} \tag{6.2}$$

The beamformer at the l^{th} UL UE, denoted by $\boldsymbol{G}_{z,l}$, is obtained by applying the ZF process that satisfies (2.2). This process is typically iterative, but for certain special cases, it can be obtained in closed form. Section 6.3 provides a detailed description of the process for obtaining $\boldsymbol{G}_{z,l}$ in such special systems.

The achievable rate for the DL user k is given as:

$$\begin{aligned}\boldsymbol{R}_{dl,k} = \log\det\Bigg(&\boldsymbol{I}_{N_{dl,k}} + \boldsymbol{H}_k^{DL}\boldsymbol{V}_{dl,k}\boldsymbol{V}_{dl,k}^H(\boldsymbol{H}_k^{DL})^H\Bigg(\sum_{j=1,j\neq k}^{K_{dl}}\boldsymbol{H}_k^{DL} \\ &\boldsymbol{V}_{dl,j}\boldsymbol{V}_{dl,j}^H(\boldsymbol{H}_k^{DL})^H + \sum_{l=1}^{K_{ul}}\boldsymbol{H}_{k,l}\boldsymbol{V}_{ul,l}\boldsymbol{V}_{ul,l}^H\boldsymbol{H}_{k,l}^H + \sigma_{dl,k}^2\boldsymbol{I}_{N_{dl,k}}\Bigg)^{-1}\Bigg)\end{aligned} \tag{6.3}$$

In our study, we choose $\boldsymbol{V}_{dl,k}$ as the ZF transmit filter at the DL BS for the k^{th} DL UE (in this context, ZF beamformers are designed to mitigate interference among DL users, specifically addressing intracell interference.), which is computed as:

$$\boldsymbol{V}_{dl} = b\bar{\boldsymbol{V}}_{dl} = \Big[\boldsymbol{V}_{dl,1},\quad \boldsymbol{V}_{dl,2},\quad \ldots,\quad \boldsymbol{V}_{dl,K_{dl}}\Big] \tag{6.4a}$$

$$\bar{\boldsymbol{V}}_{dl} = \boldsymbol{H}^H\boldsymbol{F}\Big(\boldsymbol{F}^H\boldsymbol{H}\boldsymbol{H}^H\boldsymbol{F}\Big)^{-1}, \tag{6.4b}$$

$$b = \sqrt{\frac{\sum_{k=1}^{K_{dl}} p_{dl,k}}{\mathrm{Tr}(\bar{\boldsymbol{V}}_{dl}\bar{\boldsymbol{V}}_{dl}^H)}} \tag{6.4c}$$

where $\boldsymbol{H} \in \mathbb{C}^{\sum_{k=1}^{K_{dl}} \boldsymbol{N}_{dl,k} \times M_{dl}}$ contains the different DL channel matrices stacked row-wise and $\boldsymbol{F} \in \mathbb{C}^{\sum_{k=1}^{K_{dl}} \boldsymbol{N}_{dl,k} \times \sum_{k=1}^{K_{dl}} \boldsymbol{d}_{dl,k}}$ is blocked diagonal matrix, and are given such that:

$$\boldsymbol{H} = \begin{bmatrix} \boldsymbol{H}_1^{DL} \\ \vdots \\ \boldsymbol{H}_{K_{dl}}^{DL} \end{bmatrix} \tag{6.5}$$

$$\boldsymbol{F} = \begin{bmatrix} \boldsymbol{F}_{z,1} & \boldsymbol{0} & \dots & \boldsymbol{0} \\ \boldsymbol{0} & \boldsymbol{F}_{z,2} & \dots & \boldsymbol{0} \\ \vdots & & \ddots & \vdots \\ \boldsymbol{0} & \dots & \boldsymbol{0} & \boldsymbol{F}_{z,K_{dl}} \end{bmatrix} \tag{6.6}$$

The beamformer at the k^{th} DL UE, denoted by $\boldsymbol{F}_{z,k}$, is obtained through the ZF process satisfying (2.2). While this process is iterative in general, it can be in closed form for some special cases, and the detailed process to obtain $\boldsymbol{F}_{z,k}$ for such a special case is discussed in Section 6.3. In the WMMSE study, we sometimes use $\boldsymbol{U}_{dl,k} = \boldsymbol{F}_{z,k}$ to find the initial beams at the DL-BS.

6.3 The ZF precoders at UL UEs and the ZF decoders at DL UEs

In this section, we aim to delve into the intricate process of deriving the ZF precoders denoted as $\boldsymbol{G}_{z,l}$ and the ZF decoders denoted as $\boldsymbol{F}_{z,k}$, under specific closed-form scenarios. These closed-form solutions are pivotal as they enable us to fulfill a crucial requirement outlined in equation (2.2), the elimination of all interference links from the UL UEs to the DL UEs.

In our setup, we consider a system configuration with $N_{ul} = 3$, $N_{dl} = 6$, $K_{ul} = 2$ and $K_{dl} = 4$. The interference channel matrix has a rank $r = 2$, and the data streams at DL and UL are given such that: $d_{ul,1} = d_{ul,2} = 1$, $d_{dl,1} = d_{dl,2} = 5$, and $d_{dl,3} = d_{dl,4} = 4$. Now, let's explore on the step-by-step process of how we arrive at the closed-form expressions for $\boldsymbol{G}_{z,l}$ and $\boldsymbol{F}_{z,k}$:

Step 0: We generate interference channel matrices $\boldsymbol{H}_{11}, \boldsymbol{H}_{12}, \boldsymbol{H}_{21}, \boldsymbol{H}_{22}, \boldsymbol{H}_{31}, \boldsymbol{H}_{32}, \boldsymbol{H}_{41}$ and $\boldsymbol{H}_{42}$ with a rank of $r = 2$.

Step 1: The stream from UL UE 1 to DL UE 1 is canceled by UL UE 1. This involves performing Singular Value Decomposition (SVD) of the interference channel matrix $\boldsymbol{H}_{11}$, resulting in:

$$\left[\boldsymbol{U}_{t1}\boldsymbol{S}_{t1}\boldsymbol{V}_{t1}\right] = SVD(\boldsymbol{H}_{11}). \tag{6.7}$$

$\boldsymbol{S}_{t1}$[1] is given such that:

$$\boldsymbol{S}_{t1} = \begin{bmatrix} 0 & 0 & 0 \\ 0 & \beta_{1,1} & 0 \\ 0 & 0 & \beta_{1,2} \\ 0 & 0 & 0 \\ 0 & 0 & 0 \\ 0 & 0 & 0 \end{bmatrix} \tag{6.8}$$

After obtaining the SVD of the interference channel matrix $\boldsymbol{H}_{11}$ and denoting the non-zero singular values by $\beta_{1,1}$ and $\beta_{1,2}$, we set $\boldsymbol{V}_{N1} = \boldsymbol{V}_{t1}$ and use it to transmit from Tx 1 (UL UE 1). This results in the following updated interference channel matrices:

$$\boldsymbol{H}_{N1,k1} = \boldsymbol{H}_{k1}\boldsymbol{V}_{N1}, \forall k \in [1, ..., K_{dl}] \tag{6.9}$$

The resulting $\boldsymbol{H}_{N1,11}$ has zeros at the first column, thus the interference from the UL UE 1 to the DL UE 1 is canceled by the UL UE 1.

Step 2: we perform interference cancellation from UL UE 2 to DL UE 2. This is achieved by performing the SVD of the interference channel matrix $\boldsymbol{H}_{22}$, which yields:

$$\left[\boldsymbol{U}_{t2}\boldsymbol{S}_{t2}\boldsymbol{V}_{t2}\right] = SVD(\boldsymbol{H}_{22}). \tag{6.10}$$

where the positions of the two non-zero singular values of $\boldsymbol{S}_{t2}$ are as those of $\boldsymbol{S}_{t1}$.
Then we take $\boldsymbol{V}_{N2} = \boldsymbol{V}_{t2}$ and apply it to Tx 2 (UL UE 2), so the new interference channel matrices become:

$$\boldsymbol{H}_{N2,k2} = \boldsymbol{H}_{k2}\boldsymbol{V}_{N2}, \forall k \in [1, ..., K_{dl}] \tag{6.11}$$

[1]This distribution of singular values is used to dedicate the first effective antennas to the reception/-transmission of the useful signal

The resulting $\boldsymbol{H}_{N2,22}$ has zeros at the first column, thus the interference from the UL UE 2 to the DL UE 2 is canceled by UL UE 2.

Step 3: To cancel the stream from UL UE 2 to DL UE 1, we obtain the new channel matrix $\boldsymbol{H}_{N2,12}$ after completing step 2. Then, we calculate the SVD of the first column of $\boldsymbol{H}_{N2,12}$, denoted as $\boldsymbol{H}_{N2p,12}$. This step allows us to remove the interference caused by UL UE 2 on DL UE 1:

$$\left[\boldsymbol{U}_1\boldsymbol{S}_1\boldsymbol{V}_1\right] = SVD(\boldsymbol{H}_{N2p,12}). \tag{6.12}$$

Then we take $\boldsymbol{U}_1^H$ and apply it to Rx 1 (DL UE 1), so the new interference channel matrices become:

$$\boldsymbol{H}_{n1,1l} = \boldsymbol{U}_1^H\boldsymbol{H}_{Nl,1l}, \forall l \in [1, ..., K_{ul}] \tag{6.13}$$

$\boldsymbol{S}_1$ [1] is given such that:

$$\boldsymbol{S}_1 = \begin{bmatrix} 0 & 0 & 0 & 0 & 0 & \gamma_1 \end{bmatrix}^T \tag{6.14}$$

with γ_1 is the non-zero singular value of $\boldsymbol{H}_{N2p,12}$.
The resulting $\boldsymbol{H}_{n1,12}$ has $d_{dl,1}$ zeros at the first column, thus the interference from the UL UE 2 to the DL UE 1 is canceled at the DL UE 1.

Step 4: To cancel the stream from UL UE 1 to DL UE 2, we use the new channel matrix from UL UE 1 to DL UE 2 obtained after step 1, denoted by $\boldsymbol{H}_{N1,21}$. Then, we consider the first column of $\boldsymbol{H}_{N1,21}$, which corresponds to the stream from UL UE 1 to DL UE 2, denoted by $\boldsymbol{H}_{N1p,21}$. We apply the SVD to $\boldsymbol{H}_{N1p,21}$:

$$\left[\boldsymbol{U}_2\boldsymbol{S}_2\boldsymbol{V}_2\right] = SVD(\boldsymbol{H}_{N1p,21}). \tag{6.15}$$

where the positions of the non-zero singular value of $\boldsymbol{S}_2$ is as that of $\boldsymbol{S}_1$.
Then we take $\boldsymbol{U}_2^H$ and apply it to Rx 2 (DL UE 2), so the new interference channel matrices become:

$$\boldsymbol{H}_{n2,2l} = \boldsymbol{U}_2^H\boldsymbol{H}_{Nl,2l}, \forall l \in [1, ..., K_{ul}] \tag{6.16}$$

The resulting $\boldsymbol{H}_{n2,21}$ has $d_{dl,2}$ zeros at the first column, thus the interference from the UL UE 1 to the DL UE 2 is canceled at the DL UE 2.

Step 5: we address the interference coming from both UL UE 1 and UL UE 2 towards DL UE 3. To cancel these two streams, we perform the SVD of the matrix $\boldsymbol{H}_{c,3}$ which

is formed by concatenating the interference channels from UL UE 1 and UL UE 2 to DL UE 3:

$$\boldsymbol{H}_{c,3} = \begin{bmatrix} h_{N1,31}^{11} & h_{N1,31}^{21} & h_{N1,31}^{31} & h_{N1,31}^{41} & h_{N1,31}^{51} & h_{N1,31}^{61} \\ h_{N2,32}^{11} & h_{N2,32}^{21} & h_{N2,32}^{31} & h_{N2,32}^{41} & h_{N2,32}^{51} & h_{N2,32}^{61} \end{bmatrix}^T \tag{6.17}$$

such that $h_{N1,31}^{ji}$ represents the element of $\boldsymbol{H}_{N1,31}$ at the i^{th} column and the j^{th} line:

$$\left[\boldsymbol{U}_3 \boldsymbol{S}_3 \boldsymbol{V}_3\right] = SVD(\boldsymbol{H}_{c,3}) \tag{6.18}$$

$\boldsymbol{S}_3$ [1] is given such that:

$$\boldsymbol{S}_3 = \begin{bmatrix} 0 & 0 & 0 & 0 & \gamma_{3,1} & 0 \\ 0 & 0 & 0 & 0 & 0 & \gamma_{3,2} \end{bmatrix}^T \tag{6.19}$$

with $\gamma_{3,1}$ and $\gamma_{3,2}$ are the non-zero singular values of $\boldsymbol{H}_{c,3}$.
Then we take $\boldsymbol{U}_3^H$ and apply it to Rx 3 (DL UE 3), so the new interference channel matrices become:

$$\boldsymbol{H}_{n3,3l} = \boldsymbol{U}_3^H \boldsymbol{H}_{Nl,3l}, \forall l \in [1, ..., K_{ul}] \tag{6.20}$$

After applying the cancellation schemes in Steps 1-5, the resulting interference channel matrices $\boldsymbol{H}_{n3,31}$ and $\boldsymbol{H}_{n3,32}$ have a total of $d_{dl,3}$ zeros at the first column. As a result, the interference from UL UE 1 and UL UE 2 to the DL UE 3 is effectively canceled at the DL UE 3.

Step 6: we aim to cancel the interference from UL UE 1 and UL UE 2 at DL UE 4. To achieve this, we follow a similar approach as in Step 5 by considering the SVD of a matrix denoted as $\boldsymbol{H}_{c,4}$ which is similar to $\boldsymbol{H}_{c,3}$ with considering $\boldsymbol{H}_{N1,41}$ and $\boldsymbol{H}_{N2,42}$:

$$\left[\boldsymbol{U}_4 \boldsymbol{S}_4 \boldsymbol{V}_4\right] = SVD(\boldsymbol{H}_{c,4}). \tag{6.21}$$

After obtaining the SVD of the matrix $\boldsymbol{H}_{c,4}$ in the previous step, we place the two non-zero singular values of $\boldsymbol{S}_4$ in the same positions as those of $\boldsymbol{S}_3$. Then, we apply the Hermitian transpose of $\boldsymbol{U}_4$ to the received signal at DL UE 4, denoted as Rx 4. Consequently, the interference channel matrices are updated as follows:

$$\boldsymbol{H}_{n4,4l} = \boldsymbol{U}_4^H \boldsymbol{H}_{Nl,4l}, \forall l \in [1, ..., K_{ul}] \tag{6.22}$$

The resulting $\boldsymbol{H}_{n4,41}$ and $\boldsymbol{H}_{n4,42}$ have $d_{dl,4}$ zeros at the first column, thus the interference from the UL UE 1 and from UL UE 2 to the DL UE 4 are canceled at the DL UE 4.

Finally, $\boldsymbol{F}_{z,1} = \boldsymbol{U}_1[:, 1 : d_{dl,1}]$, $\boldsymbol{F}_{z,2} = \boldsymbol{U}_2[:, 1 : d_{dl,2}]$, $\boldsymbol{F}_{z,3} = \boldsymbol{U}_3[:, 1 : d_{dl,3}]$ and $\boldsymbol{F}_{z,4} = \boldsymbol{U}_4[:, 1 : d_{dl,4}]$; $\boldsymbol{G}_{z,1} = \boldsymbol{V}_{N1}[:, 1 : d_{ul,1}]$ and $\boldsymbol{G}_{z,2} = \boldsymbol{V}_{N2}[:, 1 : d_{ul,2}]$.

To gain a deeper insight into the derivation of ZF beamformers $\boldsymbol{F}_{z,k}$ and $\boldsymbol{G}_{z,l}$ for DL and UL UEs in a closed-form scenario, we explore an additional dimension of the system. We provide the necessary steps to obtain these beamformers. Subsequently, both of these systems are included in the simulations for analysis.

In this scenario, we consider a system where $N_{ul} = 3$, $N_{dl} = 4$, $K_{ul} = 2$, and $K_{dl} = 4$, and the interference channel matrix has a rank of $r = 2$. We assume that the data streams are distributed as $d_{ul,1} = d_{ul,2} = 1$, $d_{dl,1} = d_{dl,2} = 3$, and $d_{dl,3} = d_{dl,4} = 2$. The subsequent steps outline the process of obtaining $\boldsymbol{G}_{z,l}$ and $\boldsymbol{F}_{z,k}$ in closed-form scenarios.

Step 0: We generate interference channel matrices $\boldsymbol{H}_{11}, \boldsymbol{H}_{12}, \boldsymbol{H}_{21}, \boldsymbol{H}_{22}, \boldsymbol{H}_{31}, \boldsymbol{H}_{32}, \boldsymbol{H}_{41}$ and $\boldsymbol{H}_{42}$ with a rank of $r = 2$.

Step 1: The stream from UL UE 1 to DL UE 1 is canceled by UL UE 1. This involves performing SVD of the interference channel matrix $\boldsymbol{H}_{11}$, resulting in:

$$\left[\boldsymbol{U}_{t1}\boldsymbol{S}_{t1}\boldsymbol{V}_{t1}\right] = SVD(\boldsymbol{H}_{11}). \tag{6.23}$$

$\boldsymbol{S}_{t1}$ [1] is given such that:

$$\boldsymbol{S}_{t1} = \begin{bmatrix} 0 & 0 & 0 \\ 0 & \beta_{1,1} & 0 \\ 0 & 0 & \beta_{1,2} \\ 0 & 0 & 0 \end{bmatrix} \tag{6.24}$$

After obtaining the SVD of the interference channel matrix $\boldsymbol{H}_{11}$ and denoting the non-zero singular values by $\beta_{1,1}$ and $\beta_{1,2}$, we set $\boldsymbol{V}_{N1} = \boldsymbol{V}_{t1}$ and use it to transmit from Tx 1 (UL UE 1). This results in the following updated interference channel matrices:

$$\boldsymbol{H}_{N1,k1} = \boldsymbol{H}_{k1}\boldsymbol{V}_{N1}, \forall k \in [1, ..., K_{dl}] \tag{6.25}$$

The resulting $\boldsymbol{H}_{N1,11}$ has zeros at the first column, thus the interference from the UL UE 1 to the DL UE 1 is canceled by the UL UE 1.

Step 2: we perform interference cancellation from UL UE 2 to DL UE 2. This is achieved by performing the SVD of the interference channel matrix $\boldsymbol{H}_{22}$, which yields:

$$\left[\boldsymbol{U}_{t2}\boldsymbol{S}_{t2}\boldsymbol{V}_{t2}\right] = SVD(\boldsymbol{H}_{22}). \tag{6.26}$$

where the positions of the two non-zero singular values of $\boldsymbol{S}_{t2}$ are as those of $\boldsymbol{S}_{t1}$.
Then we take $\boldsymbol{V}_{N2} = \boldsymbol{V}_{t2}$ and apply it to Tx 2 (UL UE 2), so the new interference channel matrices become:

$$\boldsymbol{H}_{N2,k2} = \boldsymbol{H}_{k2}\boldsymbol{V}_{N2}, \forall k \in [1, ..., K_{dl}] \tag{6.27}$$

The resulting $\boldsymbol{H}_{N2,22}$ has zeros at the first column, thus the interference from the UL UE 2 to the DL UE 2 is canceled by UL UE 2.

Step 3: To cancel the stream from UL UE 2 to DL UE 1, we obtain the new channel matrix $\boldsymbol{H}_{N2,12}$ after completing step 2. Then, we calculate the SVD of the first column of $\boldsymbol{H}_{N2,12}$, denoted as $\boldsymbol{H}_{N2p,12}$. This step allows us to remove the interference caused by UL UE 2 on DL UE 1:

$$\left[\boldsymbol{U}_1\boldsymbol{S}_1\boldsymbol{V}_1\right] = SVD(\boldsymbol{H}_{N2p,12}). \tag{6.28}$$

$\boldsymbol{S}_1$[1]is given such that:

$$\boldsymbol{S}_1 = \begin{bmatrix} 0 & 0 & 0 & \gamma_1 \end{bmatrix}^T \tag{6.29}$$

with γ_1 is the non-zero singular value of $\boldsymbol{H}_{N2p,12}$.
Then we take $\boldsymbol{U}_1^H$ and apply it to Rx 1 (DL UE 1), so the new interference channel matrices become:

$$\boldsymbol{H}_{n1,1l} = \boldsymbol{U}_1^H\boldsymbol{H}_{Nl,1l}, \forall l \in [1, ..., K_{ul}] \tag{6.30}$$

The resulting $\boldsymbol{H}_{n1,12}$ has $d_{dl,1}$ zeros at the first column, thus the interference from the UL UE 2 to the DL UE 1 is canceled at the DL UE 1.

Step 4: To cancel the stream from UL UE 1 to DL UE 2, we use the new channel matrix from UL UE 1 to DL UE 2 obtained after step 1, denoted by $\boldsymbol{H}_{N1,21}$. Then, we consider the first column of $\boldsymbol{H}_{N1,21}$, which corresponds to the stream from UL UE 1 to DL UE 2, denoted by $\boldsymbol{H}_{N1p,21}$. We apply the SVD to $\boldsymbol{H}_{N1p,21}$:

$$\left[\boldsymbol{U}_2\boldsymbol{S}_2\boldsymbol{V}_2\right] = SVD(\boldsymbol{H}_{N1p,21}). \tag{6.31}$$

where the positions of the non-zero singular value of $\boldsymbol{S}_2$ is as that of $\boldsymbol{S}_1$. Then we take $\boldsymbol{U}_2^H$ and apply it to Rx 2 (DL UE 2), so the new interference channel matrices become:

$$\boldsymbol{H}_{n2,2l} = \boldsymbol{U}_2^H \boldsymbol{H}_{Nl,2l}, \forall l \in [1, ..., K_{ul}] \tag{6.32}$$

The resulting $\boldsymbol{H}_{n2,21}$ has $d_{dl,2}$ zeros at the first column, thus the interference from the UL UE 1 to the DL UE 2 is canceled at the DL UE 2.

Step 5: we address the interference coming from both UL UE 1 and UL UE 2 towards DL UE 3. To cancel these two streams, we perform the singular value decomposition (SVD) of the matrix $\boldsymbol{H}_{c,3}$ which is formed by composing the interference channels from UL UE 1 and UL UE 2 to DL UE 3:

$$\boldsymbol{H}_{c,3} = \begin{bmatrix} h_{N1,31}^{11} & h_{N1,31}^{21} & h_{N1,31}^{31} & h_{N1,31}^{41} \\ h_{N2,32}^{11} & h_{N2,32}^{21} & h_{N2,32}^{31} & h_{N2,32}^{41} \end{bmatrix}^T \tag{6.33}$$

such that $h_{N1,31}^{ji}$ represents the element of $\boldsymbol{H}_{N1,31}$ at the i^{th} column and the j^{th} line:

$$\left[\boldsymbol{U}_3\boldsymbol{S}_3\boldsymbol{V}_3\right] = SVD(\boldsymbol{H}_{c,3}) \tag{6.34a}$$

$$\boldsymbol{S}_3 = \begin{bmatrix} 0 & 0 & \gamma_{3,1} & 0 \\ 0 & 0 & 0 & \gamma_{3,2} \end{bmatrix}^T \tag{6.34b}$$

with $\gamma_{3,1}$ and $\gamma_{3,2}$ are the non-zero singular values of $\boldsymbol{H}_{c,3}$.
Then we take $\boldsymbol{U}_3^H$ and apply it to Rx 3 (DL UE 3), so the new interference channel matrices become:

$$\boldsymbol{H}_{n3,3l} = \boldsymbol{U}_3^H \boldsymbol{H}_{Nl,3l}, \forall l \in [1, ..., K_{ul}] \tag{6.35}$$

After applying the cancellation schemes in Steps 1-5, the resulting interference channel matrices $\boldsymbol{H}_{n3,31}$ and $\boldsymbol{H}_{n3,32}$ have a total of $d_{dl,3}$ zeros at the first column. As a result, the interference from UL UE 1 and UL UE 2 to the DL UE 3 is effectively canceled at the DL UE 3.

Step 6: we aim to cancel the interference from UL UE 1 and UL UE 2 at DL UE 4. To achieve this, we follow a similar approach as in Step 5 by considering the SVD of a matrix denoted as $\boldsymbol{H}_{c,4}$ which is similar to $\boldsymbol{H}_{c,3}$ with considering $\boldsymbol{H}_{N1,41}$ and $\boldsymbol{H}_{N2,42}$:

$$\left[\boldsymbol{U}_4\boldsymbol{S}_4\boldsymbol{V}_4\right] = SVD(\boldsymbol{H}_{c,4}). \tag{6.36}$$

After obtaining the SVD of the matrix $\boldsymbol{H}_{c,4}$ in the previous step, we place the two non-zero singular values of $\boldsymbol{S}_4$ in the same positions as those of $\boldsymbol{S}_3$. Then, we apply the Hermitian transpose of $\boldsymbol{U}_4$ to the received signal at DL UE 4, denoted as Rx 4. Consequently, the interference channel matrices are updated as follows:

$$\boldsymbol{H}_{n4,4l} = \boldsymbol{U}_4^H \boldsymbol{H}_{Nl,4l}, \forall l \in [1, ..., K_{ul}] \tag{6.37}$$

The resulting $\boldsymbol{H}_{n4,41}$ and $\boldsymbol{H}_{n4,42}$ have $d_{dl,4}$ zeros at the first column, thus the interference from the UL UE 1 and from UL UE 2 to the DL UE 4 are canceled at the DL UE 4.

Finally, $\boldsymbol{F}_{z,1} = \boldsymbol{U}_1[:, 1 : d_{dl,1}]$, $\boldsymbol{F}_{z,2} = \boldsymbol{U}_2[:, 1 : d_{dl,2}]$, $\boldsymbol{F}_{z,3} = \boldsymbol{U}_3[:, 1 : d_{dl,3}]$ and $\boldsymbol{F}_{z,4} = \boldsymbol{U}_4[:, 1 : d_{dl,4}]$; $\boldsymbol{G}_{z,1} = \boldsymbol{V}_{N1}[:, 1 : d_{ul,1}]$ and $\boldsymbol{G}_{z,2} = \boldsymbol{V}_{N2}[:, 1 : d_{ul,2}]$.

6.4 The WMMSE Beamformers

The derivation of the WMMSE beamformer for a MIMO Broadcast Channel system is provided previously in [43] and [44]. In our study, we have leveraged the WMMSE filter framework proposed in [43] and have extended it to account for the unique characteristics of the DynTDD system. This allowed us to derive optimized beamformers at DL $\boldsymbol{V}_{dl,1}$ ... $\boldsymbol{V}_{dl,K_{dl}}, \boldsymbol{U}_{dl,1}$ ... $\boldsymbol{U}_{dl,K_{dl}}$ and at UL $\boldsymbol{V}_{ul,1}$ ... $\boldsymbol{V}_{ul,K_{ul}}, \boldsymbol{U}_{ul,1}$ ... $\boldsymbol{U}_{ul,K_{ul}}$ which maximize the weighted sum rate. The maximization problem can be written at the DL as:

$$\begin{aligned} &\max_{\boldsymbol{v}} \sum_{k=1}^{K_{dl}} \alpha_k \boldsymbol{R}_{dl,k}; \\ &s.t. \quad \sum_{k=1}^{K_{dl}} \mathrm{Tr}(\boldsymbol{V}_{dl,k}\boldsymbol{V}_{dl,k}^H) \leq P_{DL-BS} \end{aligned} \tag{6.38}$$

with α_k defines the priority for the DL user k in the system, P_{DL-BS} is the power budget at the DL BS, and $\boldsymbol{R}_{dl,k}$ is the rate of user k which is written as shown in (6.3).

The MSE-matrix for user k given that the MMSE-receive filter is applied can be written as:

$$\begin{aligned}\boldsymbol{E}_{dl,k} &= (\boldsymbol{I}_{d_{dl}} - \boldsymbol{U}_{dl,k}^H \boldsymbol{H}_k^{DL} \boldsymbol{V}_{dl,k})(\boldsymbol{I}_{d_{dl}} - \boldsymbol{U}_{dl,k}^H \boldsymbol{H}_k^{DL} \boldsymbol{V}_{dl,k})^H \\ &+ \sum_{j=1, j\neq k}^{K_{dl}} \boldsymbol{U}_{dl,k} \boldsymbol{H}_k^{DL} \boldsymbol{V}_{dl,j} \boldsymbol{V}_{dl,j}^H (\boldsymbol{H}_k^{DL})^H \boldsymbol{U}_{dl,k}^H \\ &+ \sum_{l=1}^{K_{ul}} \boldsymbol{U}_{dl,k} \boldsymbol{H}_{k,l} \boldsymbol{G}_l \boldsymbol{G}_l^H \boldsymbol{H}_{k,l}^H \boldsymbol{U}_{dl,k}^H + \sigma_k^2 \boldsymbol{U}_{dl,k}^H \boldsymbol{U}_{dl,k},\end{aligned} \tag{6.39}$$

So the MMSE receive filter at user k is given as:

$$\boldsymbol{U}_{dl,k}^{MMSE} = \boldsymbol{J}_{dl,k}^{-1} \boldsymbol{H}_k^{DL} \boldsymbol{V}_{dl,k} \tag{6.40a}$$

$$\boldsymbol{J}_{dl,k} = \textstyle\sum_{j=1}^{K_{dl}} \boldsymbol{H}_k^{DL} \boldsymbol{V}_{dl,j} \boldsymbol{V}_{dl,j}^H (\boldsymbol{H}_k^{DL})^H + \sum_{l=1}^{K_{ul}} \boldsymbol{H}_{k,l} \boldsymbol{V}_{ul,l} \boldsymbol{V}_{ul,l}^H \boldsymbol{H}_{k,l}^H + \sigma_{dl,k}^2 \boldsymbol{I} \tag{6.40b}$$

Using this MMSE receiver, the corresponding MSE matrix is given by:

$$\boldsymbol{E}_{dl,k}^{mmse} = \boldsymbol{I}_{d_{dl,k}} - \boldsymbol{V}_{dl,k}^H (\boldsymbol{H}_k^{Dl})^H \boldsymbol{J}_{dl,k}^{-1} \boldsymbol{H}_k^{DL} \boldsymbol{V}_{dl,k} \tag{6.41}$$

We denote $\boldsymbol{W}_{dl,k}$ as a constant weight matrix associated with user k, such that:

$$\boldsymbol{W}_{dl,k} = \boldsymbol{E}_{dl,k}^{mmse^{-1}} \tag{6.42}$$

The precoder at DL user k is given such that:

$$\bar{\boldsymbol{V}}_{dl} = \left(\boldsymbol{H}^H \boldsymbol{U} \boldsymbol{W} \boldsymbol{U}^H \boldsymbol{H} + \mu_{dl} \boldsymbol{I}_{M_{dl}} \right)^{-1} \boldsymbol{H}^H \boldsymbol{U} \boldsymbol{W} \tag{6.43a}$$

$$b_{dl} = \sqrt{\frac{P_{DL-BS}}{\mathrm{Tr}(\bar{\boldsymbol{V}}_{dl} \bar{\boldsymbol{V}}_{dl}^H)}} \tag{6.43b}$$

$$\boldsymbol{V}_{dl}^{WMMSE} = b_{dl} \bar{\boldsymbol{V}}_{dl} = \begin{bmatrix} \boldsymbol{V}_{dl,1}, & \boldsymbol{V}_{dl,2}, & \ldots, & \boldsymbol{V}_{dl,K_{dl}} \end{bmatrix} \tag{6.43c}$$

with μ_{dl} a regularization parameter given by:

$$\mu_{dl} = \frac{\mathrm{Tr}\left(\boldsymbol{W} \boldsymbol{U}^H \boldsymbol{U} \right)}{P_{DL-BS}} \tag{6.44}$$

The same approach used to obtain the WMMSE DL beamformers is applicable to derive the UL beamformers as well. Then at UL, the maximization of the sum rate is given by:

$$\begin{aligned} &\max_{\boldsymbol{v}} \boldsymbol{R}_{ul,l}, \\ &s.t. \quad \mathrm{Tr}(\boldsymbol{V}_{ul,l} \boldsymbol{V}_{ul,l}^H) \leq P_{ul,l} \end{aligned} \tag{6.45}$$

$P_{ul,l}$ is the power budget at the l^{th} UL UE, and $\boldsymbol{R}_{ul,l}$ is the rate of user l which is written as shown in (6.1). The MMSE receiver at the UL BS and the weighted matrix $\boldsymbol{W}_{ul,l}$ are given such that:

$$\boldsymbol{U}_{ul,l}^{MMSE} = \boldsymbol{J}_{ul,l}^{-1}\boldsymbol{H}_{l}^{UL}\boldsymbol{V}_{ul,l} \tag{6.46a}$$

$$\boldsymbol{J}_{ul,l} = \sum_{i=1}^{K_{ul}} \boldsymbol{H}_{i}^{UL}\boldsymbol{V}_{ul,i}\boldsymbol{V}_{ul,i}^{H}(\boldsymbol{H}_{i}^{UL})^{H} + \sigma_{ul}^{2}\boldsymbol{I}_{M_{ul}} \tag{6.46b}$$

$$\boldsymbol{E}_{ul,l}^{mmse} = \boldsymbol{I}_{d_{ul,l}} - \boldsymbol{V}_{ul,l}^{H}(\boldsymbol{H}_{l}^{Ul})^{H}\boldsymbol{J}_{ul,l}^{-1}\boldsymbol{H}_{l}^{UL}\boldsymbol{V}_{ul,l} \tag{6.46c}$$

$$\boldsymbol{W}_{ul,l} = \boldsymbol{E}_{ul,l}^{mmse^{-1}} \tag{6.46d}$$

So the precoder at the l^{th} UL user is:

$$\begin{aligned}\bar{\boldsymbol{V}}_{ul,l} = \Bigg((\boldsymbol{H}_{l}^{UL})^{H}\boldsymbol{U}_{ul,l}\boldsymbol{W}_{ul,l}\boldsymbol{U}_{ul,l}^{H}\boldsymbol{H}_{l}^{UL} + \\ \sum_{i=1}^{K_{dl}}(\boldsymbol{H}_{i,l})^{H}\boldsymbol{U}_{dl,i}\boldsymbol{W}_{dl,i}\boldsymbol{U}_{dl,i}^{H}\boldsymbol{H}_{i,l} + \mu_{ul,l}\boldsymbol{I}_{N_{ul,l}}\Bigg)^{-1}(\boldsymbol{H}_{l}^{UL})^{H}\boldsymbol{U}_{ul,l}\boldsymbol{W}_{ul,l}\end{aligned} \tag{6.47a}$$

$$b_{ul,l} = \sqrt{\frac{P_{ul,l}}{\mathrm{Tr}(\bar{\boldsymbol{V}}_{ul,l}\bar{\boldsymbol{V}}_{ul,l}^{H})}} \tag{6.47b}$$

$$\boldsymbol{V}_{ul,l}^{WMMSE} = b_{ul,l}\bar{\boldsymbol{V}}_{ul,l} \tag{6.47c}$$

with $\mu_{ul,l}$ a regularization parameter given by:

$$\mu_{ul,l} = \frac{\mathrm{Tr}\left(\boldsymbol{W}_{ul,l}\boldsymbol{U}_{ul,l}^{H}\boldsymbol{U}_{ul,l}\right)}{P_{ul,l}} \tag{6.48}$$

In Algorithm 4 we present a pseudo-code that serves as a comprehensive guide elucidating the sequential operations undertaken to attain optimized beamforming solutions through the WMMSE algorithm.

Algorithm 4 Pseudo code of WMMSE beamformers

Inputs:

Declare the interference channel matrices $\boldsymbol{H}_{k,l}$ of rank $r_{k,l}$

Initialization:

i. Calculate the ZF receiver beamformers at DL UEs $\boldsymbol{U}_{dl,k}^{(0)} = \boldsymbol{F}_{z,k}$,
ii. Calculate the ZF transmit beamformers at DL BS $\boldsymbol{V}_{dl,k}^{(0)}$ from equation (6.4),
iii. Calculate the transmit ZF beamformers at UL UE $\boldsymbol{V}_{ul,l}^{(0)}$ from equation (6.2),

Repeat until convergence:

i. Calculate/update the WMMSE receiver beamformers at DL UEs $\boldsymbol{U}_{dl,k}^{WMMSE^{(n)}}$ from equation (6.40),
ii. Update the WMMSE beamformers at DL BS $\boldsymbol{V}_{dl,k}^{WMMSE^{(n)}}$ from equation (6.43),
iii. Calculate/update the WMMSE receiver beamformers at UL BS $\boldsymbol{U}_{ul,l}^{WMMSE^{(n)}}$ from equation (6.46),
iv. Update to the WMMSE beamformers at UL UE $\boldsymbol{V}_{ul,l}^{WMMSE^{(n)}}$ from equation (6.47),
v. Calculate the sum rate at the UL and DL UEs $R_{ul,l}^{(n)}$ in (6.1) and $R_{dl,k}^{(n)}$ in (6.3)

6.4.1 Waterfilling algorithm

The subsequent section presents a method for applying the MIMO water-filling algorithm to broadband channels. The total rate at the DL, which takes into account the ZF between UL and DL UEs, as well as the ZF between the DL BS and DL UEs, can be expressed as:

$$\begin{aligned}\boldsymbol{R}_{dl} &= \sum_{k=1}^{K_{dl}} \log\det\left(\boldsymbol{I}_{N_{dl,k}} + \frac{1}{\sigma_n^2}(\boldsymbol{F}_{z,k}^H\boldsymbol{F}_{z,k})^{-1}\left(\boldsymbol{F}_{z,k}^H\boldsymbol{H}_k^{DL}\boldsymbol{V}_{dl,k}\boldsymbol{Q}_{dl,k}\boldsymbol{V}_{dl,k}^H(\boldsymbol{H}_k^{DL})^H\boldsymbol{F}_{z,k}\right)\right) \\ &= \sum_{k=1}^{K_{dl}} \log\det\left(\boldsymbol{I}_{N_{dl,k}} + \frac{1}{\sigma_n^2}\left(\boldsymbol{V}_{dl,k}^H(\boldsymbol{H}_k^{DL})^H\boldsymbol{F}_{z,k}(\boldsymbol{F}_{z,k}^H\boldsymbol{F}_{z,k})^{-1}\boldsymbol{F}_{z,k}^H\boldsymbol{H}_k^{DL}\boldsymbol{V}_{dl,k}\boldsymbol{Q}_{dl,k}\right)\right),\end{aligned} \tag{6.49}$$

with $\boldsymbol{Q}_{dl,k} = \boldsymbol{I}_{d_{dl,k}}$, and the DL transmit power constraint is $\sum_{k=1}^{K_{dl}} \mathrm{Tr}(\boldsymbol{Q}_{dl,k}\boldsymbol{V}_{dl,k}^H\boldsymbol{V}_{dl,k}) = P$, P is the power budget available at the DL BS.

Now, we consider the eigendecomposition of $\boldsymbol{V}_{dl,k}^H\boldsymbol{V}_{dl,k}$ given by:

$$\boldsymbol{V}_{dl,k}^H\boldsymbol{V}_{dl,k} = \tilde{\boldsymbol{X}}_{dl,k}\tilde{\boldsymbol{\Sigma}}_{dl,k}\tilde{\boldsymbol{X}}_{dl,k}^H \tag{6.50}$$

where $\tilde{\boldsymbol{X}}_{dl,k}\tilde{\boldsymbol{X}}_{dl,k}^H = \tilde{\boldsymbol{X}}_{dl,k}^H\tilde{\boldsymbol{X}}_{dl,k} = \boldsymbol{I}$, and $\tilde{\boldsymbol{\Sigma}}_{dl,k} = \tilde{\boldsymbol{\Sigma}}_{dl,k}^{1/2}\tilde{\boldsymbol{\Sigma}}_{dl,k}^{1/2}$ is a positive diagonal matrix. Let $\boldsymbol{Q}_{dl,k}^{'} = \tilde{\boldsymbol{\Sigma}}_{dl,k}^{1/2}\tilde{\boldsymbol{X}}_{dl,k}^H\boldsymbol{Q}_{dl,k}\tilde{\boldsymbol{X}}_{dl,k}\tilde{\boldsymbol{\Sigma}}_{dl,k}^{1/2}$ and $\boldsymbol{V}_{dl,k}^{'} = \boldsymbol{V}_{dl,k}\tilde{\boldsymbol{X}}_{dl,k}\tilde{\boldsymbol{\Sigma}}_{dl,k}^{-1/2}$. So with $\boldsymbol{Q}_{dl,k}^{'}$ and $\boldsymbol{V}_{dl,k}^{'}$ (6.49) could be written such that:

$$\boldsymbol{R}_{dl} = \sum_{k=1}^{K_{dl}} \log\det\left(\boldsymbol{I}_{N_{dl,k}} + \frac{1}{\sigma_n^2}\left(\boldsymbol{V}_{dl,k}^{'H}(\boldsymbol{H}_k^{DL})^H \boldsymbol{F}_{z,k}(\boldsymbol{F}_{z,k}^H\boldsymbol{F}_{z,k})^{-1}\boldsymbol{F}_{z,k}^H\boldsymbol{H}_k^{DL}\boldsymbol{V}_{dl,k}^{'}\boldsymbol{Q}_{dl,k}^{'}\right)\right) \quad (6.51)$$

with the DL transmit power constraint $\sum_{k=1}^{K_{dl}} \mathrm{Tr}(\boldsymbol{Q}_{dl,k}^{'}) = P$.

Then, we consider the following eigendecomposition:

$$\frac{1}{\sigma_n^2}\boldsymbol{V}_{dl,k}^{'H}(\boldsymbol{H}_k^{DL})^H \boldsymbol{F}_{z,k}(\boldsymbol{F}_{z,k}^H\boldsymbol{F}_{z,k})^{-1}\boldsymbol{F}_{z,k}^H\boldsymbol{H}_k^{DL}\boldsymbol{V}_{dl,k}^{'} = \boldsymbol{X}_{dl,k}\boldsymbol{\Sigma}_{dl,k}\boldsymbol{X}_{dl,k}^H. \quad (6.52)$$

where $\boldsymbol{X}_{dl,k}\boldsymbol{X}_{dl,k}^H = \boldsymbol{X}_{dl,k}^H\boldsymbol{X}_{dl,k} = \boldsymbol{I}$, and $\boldsymbol{\Sigma}_{dl,k} = \boldsymbol{\Sigma}_{dl,k}^{1/2}\boldsymbol{\Sigma}_{dl,k}^{1/2}$ is a positive diagonal matrix. We note $\boldsymbol{V}_{dl,k}^{''} = \boldsymbol{V}_{dl,k}^{'}\boldsymbol{X}_{dl,k}$ and $\boldsymbol{Q}_{dl,k}^{''} = \boldsymbol{X}_{dl,k}^H\boldsymbol{Q}_{dl,k}^{'}\boldsymbol{X}_{dl,k}$, then $\boldsymbol{V}_{dl,k}^{'}\boldsymbol{Q}_{dl,k}^{'}\boldsymbol{V}_{dl,k}^{'H} = \boldsymbol{V}_{dl,k}^{''}\boldsymbol{Q}_{dl,k}^{''}\boldsymbol{V}_{dl,k}^{''H}$.
So the sum rate at DL in (6.51) becomes:

$$\begin{aligned}\boldsymbol{R}_{dl} &= \sum_{k=1}^{K_{dl}} \log\det\left(\boldsymbol{I}_{N_{dl,k}} + \frac{1}{\sigma_n^2}\left(\boldsymbol{V}_{dl,k}^{"H}(\boldsymbol{H}_k^{DL})^H \boldsymbol{F}_{z,k}(\boldsymbol{F}_{z,k}^H\boldsymbol{F}_{z,k})^{-1}\boldsymbol{F}_{z,k}^H\boldsymbol{H}_k^{DL}\boldsymbol{V}_{dl,k}^{"}\boldsymbol{Q}_{dl,k}^{"}\right)\right) \\ &= \sum_{k=1}^{K_{dl}} \log\det\left(\boldsymbol{I}_{N_{dl,k}} + \boldsymbol{\Sigma}_{dl,k}\boldsymbol{Q}_{dl,k}^{"}\right),\end{aligned} \quad (6.53)$$

The constraint on the transmit power for DL becomes $\sum_{k=1}^{K_{dl}} \mathrm{Tr}(\boldsymbol{Q}_{dl,k}^{''}) = \sum_{k=1}^{K_{dl}} \mathrm{Tr}(\boldsymbol{Q}_{dl,k}^{'}\boldsymbol{X}_{dl,k}\boldsymbol{X}_{dl,k}^H) = \sum_{k=1}^{K_{dl}} \mathrm{Tr}(\boldsymbol{Q}_{dl,k}^{'}) = P$. Here, we have $\boldsymbol{Q}_{dl,k}^{''} = diag\{p_{k,1},\ldots,p_{k,d_{dl,k}}\}$ and $\boldsymbol{\Sigma}_{dl,k} = diag\{\sigma_{k,1},\ldots,\sigma_{k,d_{dl,k}}\}$, represents the power allocated to the k^{th} DL UE at the antennas with the i^{th} data stream. Therefore, the expression for (6.53) is:

$$\boldsymbol{R}_{dl} = \sum_{k=1}^{K_{dl}}\sum_{i=1}^{d_{dl,k}} \log(1+\sigma_{k,i}p_{k,i}). \quad (6.54)$$

with the power constraint $\sum_{k=1}^{K_{dl}}\sum_{i=1}^{d_{dl,k}} p_{k,i} = P$. We use the Kuhn–Tucker conditions to verify that the solution $\sum_{k=1}^{K_{dl}}\sum_{i=1}^{d_{dl,k}} p_{k,i} = \sum_{k=1}^{K_{dl}}\sum_{i=1}^{d_{dl,k}}\left[\lambda - \frac{1}{\sigma_{k,i}}\right]_+ = P$ is the assignment that maximizes the sum rate, where the optimal λ can be solved using bisection method. In section 6.6, the P mentioned here will be denoted as P_{DL-BS}.

6.5 Elaboration on Computational Complexity

The computation complexity associated with the determination of beamformers in this chapter encompasses various aspects that warrant elaboration:

- Considering the beamformers at the DL BS, denoted as $\boldsymbol{V}_{dl,k}$ in equation (6.4), their computational burden primarily stems from the inversion matrix complexity. This complexity scales proportionally with $\mathcal{O}((\sum_{k=1}^{K_{dl}} d_{dl,k})^2)$ for each beamformer.

- In the case of the WMMSE beamformers, their computational load is characterized by the complexity of matrix inversions. This complexity is composed of three main components, this cumulative complexity is expressed as $\mathcal{O}({N_{dl,k}}^3 + {d_{dl,k}}^3 + {M_{dl}}^3)$ for each iteration.

- Lastly, the ZF beamformers employed at UEs, denoted by $\boldsymbol{G}_{z,l}$ and $\boldsymbol{F}_{z,k}$, entail a computational overhead related to SVD. The complexity of this operation is expressed as $\mathcal{O}({N_{dl,k}}^2 N_{ul,l})$ for each step within the algorithm.

6.6 Simulation Results

In this section, we evaluate the sum rate of both DL and UL UEs across various scenarios that consider the rank of the MIMO IBMAC-IC and the beamformers implemented.

We start by evaluating the sum rate for the system $N_{ul} = 3$, $N_{dl} = 6$, $K_{ul} = 2, K_{dl} = 4, M_{dl} = 20$ and $M_{ul} = 4$. For this, we consider several cases of initialization of the beamformers and repeat the WMMSE algorithm in an iterative process to maximize the sum rate.

By Monte Carlo averaging over 100 channel realizations, we compute the sum rate at the UL and DL with $\boldsymbol{R}_{ul,l}$ of (6.1) and $\boldsymbol{R}_{dl,k}$ of (6.3), respectively. The direct channel matrices' elements are generated as independent and identically distributed (i.i.d.) Gaussian random variables $\mathcal{CN}(0,1)$, and the receive noise covariance is normalized such that $\boldsymbol{R}_{n_k n_k} = \boldsymbol{I}_{N_{dl,k}}$. In simulations without water-filling, we assume the same power at each UL UE, i.e., $P_{ul,1} = P_{ul,2} = P$, and a total power of $K_{dl}P$ at the DL BS, where $\sum_{k=1}^{K_{dl}} p_{dl,k} = K_{dl}P = P_{DL-BS}$ and $P = 10^{\frac{SNR}{10}}$.

In Fig. 6.1, we present the sum rate at the DL and UL UEs for two systems with $K_{ul} = 2, K_{dl} = 4, M_{dl} = 20$, and $M_{ul} = 4$. In Fig. 6.1a we consider $N_{ul} = 3$ and $N_{dl} = 6$ as number of antennas at UL and DL UE respectively, and $N_{ul} = 3$ and $N_{dl} = 4$ in Fig. 6.1b. We consider two cases for the interference channel rank between the UL UEs and the DL UEs, which is denoted as r:

- Reduced rank MIMO IBMAC-IC: $r = 2$ such that the DoF at each UL and DL UE is: $d_{ul,1} = d_{ul,2} = 1$ and $d_{dl,1} = d_{dl,2} = 5, d_{dl,3} = d_{dl,4} = 4$ for Fig. 6.1a, and $d_{ul,1} = d_{ul,2} = 1$, $d_{dl,1} = d_{dl,2} = 3$, $d_{dl,3} = d_{dl,4} = 2$ for the system in Fig. 6.1b.
  The procedure for acquiring $\boldsymbol{G}_{z,l}$ and $\boldsymbol{F}_{z,k}$ for both systems, is outlined in subsection 6.3,

- Full rank MIMO IBMAC-IC: $r = 3$ such that the DoF at each UL and DL UE is $d_{ul,1} = d_{ul,2} = 1$ and $d_{dl,1} = d_{dl,2} = d_{dl,3} = d_{dl,4} = 4$ for the system in Fig. 6.1a, and

$d_{ul,1} = d_{ul,2} = 1$, $d_{dl,1} = 3$, $d_{dl,2} = d_{dl,3} = d_{dl,4} = 2$, for the system in Fig. 6.1b.

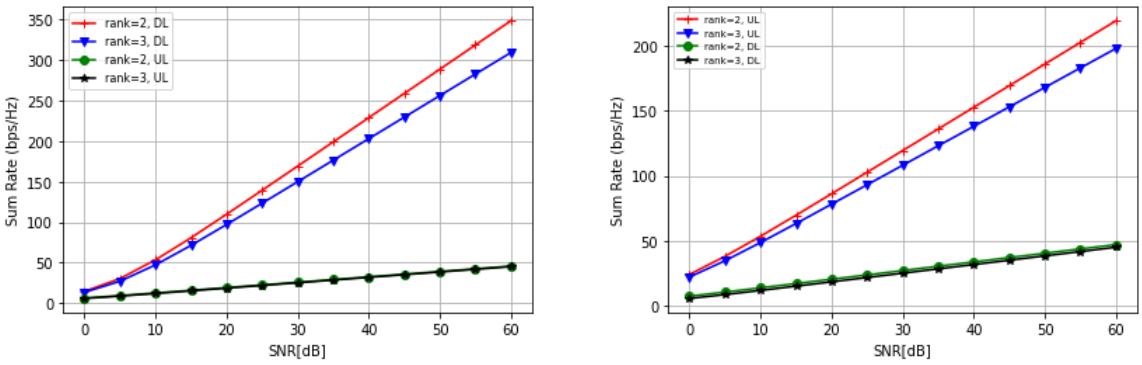

(a) $N_{ul} = 3$, $N_{dl} = 6$ (b) $N_{ul} = 3$, $N_{dl} = 4$

Figure 6.1: Sum rate performance with UE2UE ZF+ BS2UE ZF for $K_{ul} = 2$ and $K_{dl} = 4$.

In the simulation shown in Fig. 6.1, we examine the performance of the sum rate at UL and DL for two different ranks of the MIMO IBMAC-IC, namely $r = 2$ and $r = 3$. As depicted in Fig. 6.1a and Fig. 6.1b, the sum rate at UL is almost the same in both cases. This is because based on the interference alignment feasibility condition in Theorem 7, it is not possible to increase the DoF at UL UEs (and hence the rate at high SNR) for this system dimension, without violating interference alignment feasibility (Table 4.3 and Table 4.2). On the other hand, for the DL side, we can observe in Fig. 6.1a that at high SNR, the sum rate is higher for $r = 2$ compared to $r = 3$, which is also confirmed in the numerical results presented in Table 4.3. This can be explained by considering a non-uniform DoF at DL UEs (as suggested in Remark 1), which enables us to increase the sum rate at high SNR. The comment made about the outcome shown in Fig. 6.1a can also be applied to Fig. 6.1b when referencing Table 4.2

Prior to initiating the forthcoming simulations, we will first elaborate on each of the selected scenarios. By succinctly explaining these scenarios, we establish a clear framework, enhancing the interpretation and analysis of the ensuing simulation results:

- **init (UE2UE ZF + BS2UE ZF)**: The simulation calculates the sum rate during initialization with UE-to-UE ZF by utilizing UL UEs' precoders $\boldsymbol{G}_{z,l}$ and DL UEs' decoders $\boldsymbol{F}_{z,k}$, and the ZF precoders at the DL BS from (6.4) to consider the ZF between DL UEs,
- **init (UE EigR + BS2UE ZF)**: The simulation calculates the sum rate during initialization without UE-to-UE ZF by using UL UEs' precoders and DL UEs' decoders as the reception vectors obtained from the SVD of the direct channel matrices at the UL and DL sides, and the ZF precoders at the DL BS from equation (6.4) to consider the ZF between DL UEs,

- **init (UE2UE ZF + BS2UE ZF)+ WMMSE, iter=n**: This simulation starts with the initialization explained in the **init (UE2UE ZF + BS2UE ZF)** simulation, followed by running the WMMSE algorithm described in section 6.4, and returns the sum rate at the n^{th} iteration of the WMMSE algorithm,
- **init (UE EigR + BS2UE ZF)+ WMMSE, iter=n**: This simulation starts with the initialization explained in the **init (UE EigR + BS2UE ZF)** simulation, followed by running the WMMSE algorithm described in section 6.4, and returns the sum rate at the n^{th} iteration of the WMMSE algorithm.

In Fig. 6.2a and Fig. 6.2b, we explored two different initialization. Fig. 6.2a involved the initialization "init (UE2UE ZF + BS2UE ZF)". In Fig. 6.2b, we retained the UE-to-UE interference while limiting our consideration to ZF between the DL UEs for intracell interference, so the initialization "init (UE EigR + BS2UE ZF)". Each system served as an initialization for the WMMSE algorithm, and we plotted the sum rates for UL and DL UEs across different iterations: $1, 3, 10$, and 50.

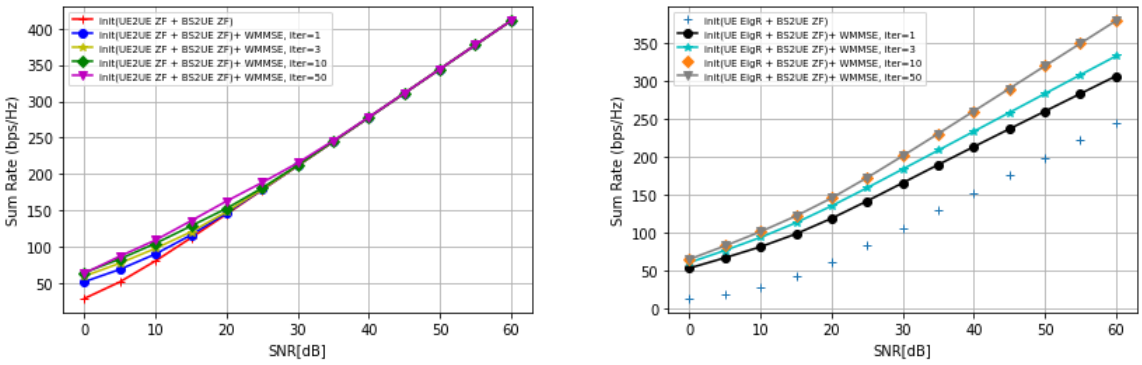

(a) init (UE2UE ZF + BS2UE ZF) (b) init (UE EigR + BS2UE ZF)

Figure 6.2: Sum rate performance with $N_{ul} = 3$, $N_{dl} = 6$, $K_{ul} = 2$, $K_{dl} = 4$ and $r = 2$

Upon comparing these two figures, a notable observation emerges. At high SNR, in Fig. 6.2a aligning UE-to-UE interference using ZF beamformers at both UL and DL UEs enabled performance comparable to that of the WMMSE algorithm even after 50 iterations. In contrast, Fig. 6.2b, where UE-to-UE interference was retained, indicates that this specific type of CLI significantly hampers the convergence of the WMMSE algorithm. Even after 50 iterations, the sum rate at $SNR = 60$ stood at 375 bits per second per Hertz (bps/Hz). In the same Signal-to-Noise Ratio (SNR) scenario, Fig. 6.2a yielded a total sum rate of 410 bps/Hz.

To underscore the influence of UE-to-UE interference on system performance, Fig. 6.3 is presented, where both types of initialization "init (UE2UE ZF + BS2UE ZF)" and "init (UE EigR + BS2UE ZF)" are combined and plotted alongside the WMMSE algorithm. For this simulation we assess the sum rate of the system with the following configuration: $N_{ul} = 3$, $N_{dl} = 4$, $K_{ul} = 2$, $K_{dl} = 4$, $M_{dl} = 14$, $M_{ul} = 4$, and $r = 2$, the DoF at each UL UE is $d_{ul,1} = d_{ul,2} = 1$, and at each DL UE, we have $d_{dl,1} = d_{dl,2} = 3$ and $d_{dl,3} = d_{dl,4} = 2$.

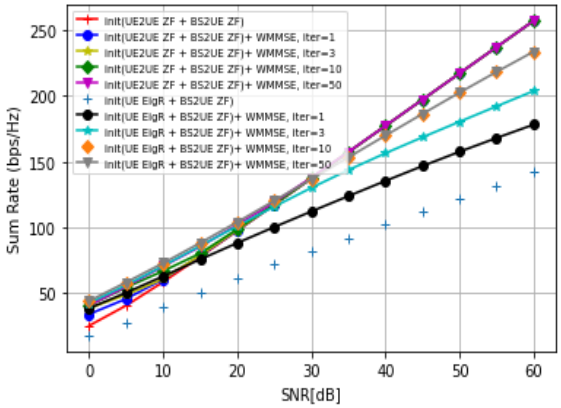

Figure 6.3: Sum rate performance with $N_{ul} = 3$, $N_{dl} = 4$, $K_{ul} = 2$, $K_{dl} = 4$ and $r = 2$.

Fig. 6.3 illustrates the impact of UE-to-UE interference on the performance of the DynTDD system. The total sum rate is depicted by considering two different initialization: "init (UE2UE ZF + BS2UE ZF)" and "init (UE EigR + BS2UE ZF)". Analyzing the simulation results presented in Fig. 6.3, it becomes evident that incorporating UE-to-UE ZF interference cancellation yields a substantial enhancement in the sum rate. Up to an SNR of $15dB$, the WMMSE algorithm effectively reduces the sum rate disparity between the "init (UE2UE ZF + BS2UE ZF)" and "init (UE EigR + BS2UE ZF)" initialization. However, at high SNR levels, the WMMSE algorithm struggles to bridge this gap, particularly with a low number of iterations. For instance, at a sum rate of $175bps/Hz$, the WMMSE algorithm without UE-to-UE ZF in the initialization requires an additional $18dB$, $8dB$, or $2dB$ of SNR for iter=1, 3, or 10, respectively, to achieve the performance of the "init (UE2UE ZF + BS2UE ZF)" initialization. Therefore, the proposed UE-to-UE ZF decoders and precoders effectively mitigate UE-to-UE interference, leading to a remarkable overall system performance improvement.

Now, in an attempt to optimize power allocation at the BS and enhance the overall sum rate, we explored the water-filling algorithm, as outlined in Section 6.4.1.

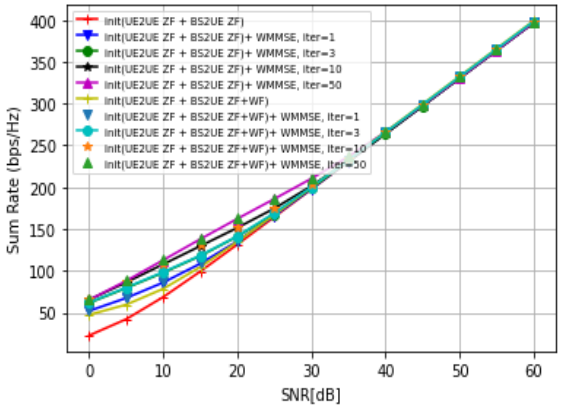

Figure 6.4: Sum rate performance with $N_{ul} = 3$, $N_{dl} = 6$, $K_{ul} = 2$, $K_{dl} = 4$ and $r = 2$

Fig. 6.4 presents a comparison of the average sum rate versus SNR for four different simulations: init (UE2UE ZF + BS2UE ZF), init (UE2UE ZF + BS2UE ZF+ WF), init (UE2UE ZF + BS2UE ZF)+ WMMSE, iter=n and init (UE2UE ZF + BS2UE ZF+ WF)+ WMMSE, iter=n, to evaluate the water-filling algorithm. The simulation results show the sum rate at initialization and the sum rate at different iterations (1st, 3rd, 10th, and 50th) of the WMMSE algorithm, indicating the convergence behavior of the algorithm. The comparison also shows that the WMMSE algorithm outperforms the ZF solution at low SNR, but the water-filling algorithm combined with the ZF can approach the performance of the WMMSE algorithm at low SNR.

6.7 Closing Remarks

In conclusion, our simulations in this chapter have underscored the critical significance of addressing User UE-to-UE interference in DynTDD systems. Failing to manage UE-to-UE interference results in a substantial degradation of system performance. Notably, our findings highlight the pivotal role of UE-to-UE interference alignment during initialization, which significantly accelerates the convergence of the WMMSE algorithm, reducing the required iterations.
Furthermore, our comparisons have shed light on the nuanced performance nuances at varying SNR. Specifically, the WMMSE algorithm outperforms the ZF solution, particularly at low SNR levels. Interestingly, our results demonstrate that incorporating the water-filling algorithm alongside ZF mitigates this performance gap, allowing it to approach the efficiency of the WMMSE algorithm in low SNR scenarios. These insights emphasize the importance of tailored strategies for interference alignment and pave the way for more efficient and adaptive DynTDD systems in real-world applications.

Part IV

Conclusions, Outlook and Appendices

Chapter 7

Conclusions and Future Directions

In the course of this thesis, an in-depth exploration into the phenomenon of cross-link interference (CLI) in Dynamic Time Division Duplexing (DynTDD) systems was undertaken. Our primary focus lies on understanding the interference between User Equipement (UE)s in these systems. Regarding Base Station (BS)s interference, we operated under the assumption that the BS possessed an ample number of antennas to receive and manage signals amid interference. The motivation behind our research was rooted in the urgent necessity to fully exploit DynTDD's capabilities by addressing the challenges posed by CLI. Through meticulous analysis, innovative methodologies, and an unwavering commitment to expanding the existing boundaries of knowledge, our thesis aims to make a significant contribution to this field.

We begin by addressing the query: how should we dimension a system to ensure the interference alignment? This involves determining the appropriate number of antennas for Downlink (DL) Uplink (UL) users, the number of data streams that DL users can receive and UL users can transmit, and considering the count of both interfered and interfering users within our system. This comprehensive assessment is crucial for devising a solution to interference alignment, where the term "solution" denotes the strategic design of beamformers for both UL and DL users. Answering this question necessitated determining the conditions under which interference alignment was feasible. To achieve this, we scrutinized various conditions: the proper (necessary) conditions representing an upper limit for feasible Degree of Freedom (DoF), necessary and sufficient conditions offering precise characterizations of feasible DoF, and sufficient conditions that represented a subset of all possible feasible DoF. These conditions were contingent on a variable within our system: the rank of the interference channel matrix.

Our investigation began with a full-rank interference channel matrix, enabling a deep understanding of this type of interference and providing insights for handling reduced-rank cases. This analysis was crucial because practical scenarios often deviate from ideal conditions due to environmental factors such as absorption, reflection, and scattering caused by surrounding objects. When examining interference alignment conditions, we considered two scenarios. Firstly, the centralized scenario involved a central design unit equipped with knowledge about all involved channels. Secondly, we delved into distributed scenar-

ios within wireless communication systems, where each transmitter and receiver operated with the local Channel State Information (CSI) of directly connected channels. We explored these scenarios by optimizing the Zero Forcing (ZF) work distribution between UL and DL users and subsequently evaluated their performance numerically.
Having determined the correct sizing for our system, we proceeded to design beamformers. For closed-form cases, shared ZF beamformers at UL and DL users were defined to align UE-to-UE interference. Additionally, the Weighted Minimum Mean Square Error (WMMSE) algorithm at the DL BS, UL UEs, and DL UEs was utilized to optimize beamformers by minimizing the mean square error between the desired and received signals while considering channel conditions and interference. The water-filling algorithm was also incorporated for optimized power allocation. This consideration of beamformers was rigorously evaluated through sum rate simulations, varying the Signal-to-Noise Ratio (SNR). The results underscored the significance of tailored strategies for interference alignment and indicated the potential of the water-filling algorithm alongside ZF to approach the efficiency of the WMMSE algorithm in low SNR scenarios.
By confronting the challenges of interference in DynTDD, we are pioneering solutions that have broad applicability across a spectrum of interference channels in diverse communication contexts. Our research not only signifies significant progress in DynTDD technology but also acts as a driving force for the development of innovative interference alignment strategies in various communication scenarios.

In the future trajectory of this thesis, there are several intriguing avenues for further exploration. One compelling area of study involves delving deeper into the reduced-rank scenario, aiming to establish the necessary and sufficient conditions for interference alignment feasibility. Unlike the current formulation, it would be valuable to express these conditions in terms of fundamental problem dimensions: the number of antennas, data streams, users, and the rank of the interference channel matrix. This shift in perspective could offer new insights into the intricate interplay of these factors and their impact on interference alignment.
Additionally, a promising direction for future research lies in the development of a comprehensive algorithm capable of generating ZF beamformers for both UL and DL users, ensuring interference alignment, from the correct system dimensions. One intriguing approach to addressing this challenge could involve leveraging reinforcement learning techniques. By employing reinforcement learning, we might uncover intelligent strategies for designing beamformers, enhancing the efficiency and adaptability of interference alignment in DynTDD systems.
Furthermore, there exists a compelling opportunity to apply the ZF beamformers derived in this thesis to real-world interference channels, as defined in the 3rd Generation Partnership Project (3GPP) standards. This practical application would not only validate the theoretical constructs developed in this research but also contribute to the refinement of interference alignment techniques in standardized communication systems. Such an endeavor holds the potential to bridge the gap between theoretical advancements and practical implementation, fostering advancements in the field of wireless communication.

Bibliography

[1] Andrea Goldsmith. *Wireless communications*. Cambridge university press, 2005.

[2] Praneeth Jayasinghe, Antti Tölli, and Matti Latva-aho. Bi-directional signaling strategies for dynamic tdd networks. In *2015 IEEE 16th International Workshop on Signal Processing Advances in Wireless Communications (SPAWC)*, pages 540–544. IEEE, 2015.

[3] Howard H Yang, Giovanni Geraci, Yi Zhong, and Tony QS Quek. Packet throughput analysis of static and dynamic tdd in small cell networks. *IEEE Wireless Communications Letters*, 6(6):742–745, 2017.

[4] Anubhab Chowdhury, Chandra R Murthy, and Ribhu Chopra. Dynamic tdd enabled distributed antenna array massive mimo system. In *2022 IEEE 12th Sensor Array and Multichannel Signal Processing Workshop (SAM)*, pages 131–135. IEEE, 2022.

[5] Zukang Shen, Alexey Khoryaev, Erik Eriksson, and Xueming Pan. Dynamic uplink-downlink configuration and interference management in td-lte. *IEEE Communications Magazine*, 50(11):51–59, 2012.

[6] Wun-Cheol Jeong. *Dynamic time division duplex and time slot allocation strategy for multimedia traffic in wireless applications*. The Pennsylvania State University, 2002.

[7] Rajpamal R Pethuraj. *Adaptive resource allocation strategies for dynamic heterogeneous traffic in TD-CDMA/TDD systems*. Oklahoma State University, 2006.

[8] Yoghitha Ramamoorthi and Abhinav Kumar. Energy efficiency in millimeter wave based cellular networks with dude and dynamic tdd. In *2020 International Conference on COMmunication Systems & NETworkS (COMSNETS)*, pages 670–673. IEEE, 2020.

[9] Tung T Vu, Duy T Ngo, Hien Quoc Ngo, and Tho Le-Ngoc. Full-duplex cell-free massive mimo. In *ICC 2019-2019 IEEE International Conference on Communications (ICC)*, pages 1–6. IEEE, 2019.

[10] Hieu V Nguyen, Van-Dinh Nguyen, Octavia A Dobre, Shree Krishna Sharma, Symeon Chatzinotas, Björn Ottersten, and Oh-Soon Shin. On the spectral and energy efficiencies of full-duplex cell-free massive mimo. *IEEE Journal on Selected Areas in Communications*, 38(8):1698–1718, 2020.

[11] Prince Anokye, Roger K Ahiadormey, and Kyoung-Jae Lee. Full-duplex cell-free massive mimo with low-resolution adcs. *IEEE Transactions on Vehicular Technology*, 70(11):12179–12184, 2021.

[12] Jalal Rachad, Ridha Nasri, and Laurent Decreusefond. Interference analysis in dynamic tdd system combined or not with cell clustering scheme. In *2018 IEEE 87th Vehicular Technology Conference (VTC Spring)*, pages 1–5. IEEE, 2018.

[13] YuNan Han, YongYu Chang, Jie Cui, and DaCheng Yang. A novel inter-cell interference coordination scheme based on dynamic resource allocation in lte-tdd systems. In *2010 IEEE 71st Vehicular Technology Conference*, pages 1–5. IEEE, 2010.

[14] Zhiheng Guo and Yongqiang Fei. On the cross link interference of 5g with flexible duplex and full duplex. In *2020 IEEE Wireless Communications and Networking Conference Workshops (WCNCW)*, pages 1–4. IEEE, 2020.

[15] Shaohe Lv, Weihua Zhuang, Xiaodong Wang, and Xingming Zhou. Scheduling in wireless ad hoc networks with successive interference cancellation. In *2011 Proceedings IEEE INFOCOM*, pages 1287–1295. IEEE, 2011.

[16] Islam Abu Mahady, Ebrahim Bedeer, Salama Ikki, and Halim Yanikomeroglu. Sum-rate maximization of noma systems under imperfect successive interference cancellation. *IEEE Communications Letters*, 23(3):474–477, 2019.

[17] Antoine Kilzi, Joumana Farah, Charbel Abdel Nour, and Catherine Douillard. Mutual successive interference cancellation strategies in noma for enhancing the spectral efficiency of comp systems. *IEEE Transactions on Communications*, 68(2):1213–1226, 2019.

[18] Long Suo, Hongyan Li, Shun Zhang, and Jiandong Li. Successive interference cancellation and alignment in k-user mimo interference channels with partial unidirectional strong interference. *China Communications*, 19(2):118–130, 2022.

[19] Chuan Ma, Weijie Wu, Ying Cui, and Xinbing Wang. On the performance of successive interference cancellation in d2d-enabled cellular networks. In *2015 IEEE Conference on Computer Communications (INFOCOM)*, pages 37–45. IEEE, 2015.

[20] Tingting Liu and Chenyang Yang. On the Feasibility of Linear Interference Alignment for MIMO Interference Broadcast Channels With Constant Coefficients. *IEEE Trans. Signal Processing*, May 2013.

[21] Óscar González, Carlos Beltrán, and Ignacio Santamaría. A Feasibility Test for Linear Interference Alignment in MIMO Channels With Constant Coefficients. *IEEE Trans. Information Theory*, March 2014.

[22] Meisam Razaviyayn, Gennady Lyubeznik, and Zhi-Quan Luo. On the Degrees of Freedom Achievable Through Interference Alignment in a MIMO Interference Channel. *IEEE Trans. Signal Processing*, Feb. 2012.

[23] Yongce Chen, Yan Huang, Yi Shi, Y Thomas Hou, Wenjing Lou, and Sastry Kompella. On dof-based interference cancellation under general channel rank conditions. *IEEE/ACM Transactions on Networking*, 28(3):1002–1016, 2020.

[24] Francesco Negro, Shakti Prasad Shenoy, Dirk TM Slock, and Irfan Ghauri. Interference alignment limits for k-user frequency-flat mimo interference channels. In *2009 17th European Signal Processing Conference*, pages 2445–2449. IEEE, 2009.

[25] Francesco Negro, Shakti Prasad Shenoy, Irfan Ghauri, and Dirk T.M. Slock. Interference alignment feasibility in constant coefficient MIMO interference channels. *Int'l Workshop Signal Processing Advances in Wireless Comm's (SPAWC)*, 2010.

[26] Sang-Woon Jeon, Kiyeon Kim, Janghoon Yang, and Dong Ku Kim. The Feasibility of Interference Alignment for MIMO Interfering Broadcast–Multiple-Access Channels. *Trans. Wireless Comm's*, July 2017.

[27] Marios Kountouris and Nikolaos Pappas. Hetnets and massive mimo: Modeling, potential gains, and performance analysis. In *2013 IEEE-APS Topical Conference on Antennas and Propagation in Wireless Communications (APWC)*, pages 1319–1322. IEEE, 2013.

[28] Jeffrey G Andrews. Seven ways that hetnets are a cellular paradigm shift. *IEEE communications magazine*, 51(3):136–144, 2013.

[29] Kianoush Hosseini, Jakob Hoydis, Stephan Ten Brink, and Mérouane Debbah. Massive mimo and small cells: How to densify heterogeneous networks. In *2013 IEEE international conference on communications (ICC)*, pages 5442–5447. IEEE, 2013.

[30] Ansuman Adhikary, Ebrahim Al Safadi, and Giuseppe Caire. Massive mimo and inter-tier interference coordination. In *2014 Information Theory and Applications Workshop (ITA)*, pages 1–10. IEEE, 2014.

[31] Amitabha Ghosh, Nitin Mangalvedhe, Rapeepat Ratasuk, Bishwarup Mondal, Mark Cudak, Eugene Visotsky, Timothy A Thomas, Jeffrey G Andrews, Ping Xia, Han Shin Jo, et al. Heterogeneous cellular networks: From theory to practice. *IEEE communications magazine*, 50(6):54–64, 2012.

[32] Wuncheol Jeong and Mohsen Kavehrad. Cochannel interference reduction in dynamic-tdd fixed wireless applications, using time slot allocation algorithms. *IEEE Transactions on Communications*, 50(10):1627–1636, 2002.

[33] Jungnam Yun and Mohsen Kavehrad. Adaptive resource allocations for d-tdd systems in wireless cellular networks. In *IEEE MILCOM 2004. Military Communications Conference, 2004.*, volume 2, pages 1047–1053. IEEE, 2004.

[34] Illsoo Sohn, Kwang Bok Lee, and Young Sil Choi. Comparison of decentralized time slot allocation strategies for asymmetric traffic in tdd systems. *IEEE transactions on wireless communications*, 8(6):2990–3003, 2009.

[35] Yongce Chen, Yan Huang, Yi Shi, Y. Thomas Hou, Wenjing Lou, and Sastry Kompella. A General Model for DoF-based Interference Cancellation in MIMO Networks with Rank-deficient Channels. *IEEE Conf. on Computer Communications (INFOCOM)*, 2018.

[36] Kab Seok Ko, Bang Chul Jung, and Mijeong Hoh. Distributed Interference Alignment for Multi-Antenna Cellular Networks With Dynamic Time Division Duplex. *IEEE Communications Letters*, April 2018.

[37] W. Du, Z. Liu, , and F. Li. Interference Neutralization With Partial CSIT for Full-Duplex Cellular Networks. *IEEE Access*, April 2019.

[38] Z. Huo, N. Ma, and B. Liu. Joint User Scheduling and Transceiver Design for Cross-link Interference Suppression in MU-MIMO Dynamic TDD Systems. *3rd IEEE Int'l Conf. on Computer and Communications (ICCC)*, 2017.

[39] Yongce Chen, Shaoran Li, Chengzhang Li, Y. Thomas Hou, and Brian Jalaian. To Cancel or Not to Cancel: Exploiting Interference Signal Strength in the Eigenspace for Efficient MIMO DoF Utilization. *Conf. on Computer Comm's (INFOCOM)*, June 2019.

[40] Yohan Lejosne, Manijeh Bashar, Dirk Slock, and Yi Yuan-Wu. Decoupled, Rank Reduced, Massive and Frequency-Selective Aspects In MIMO Interfering Broadcast Channels. *Int'l Symp. Communications, Control and Sig. Proc. (ISCCSP)*, 2014.

[41] H.Q. Ngo, E.G. Larsson, and T.L. Marzetta. The Multicell Multiuser MIMO Uplink with Very Large Antenna Arrays and a Finite-Dimensional Channel. *IEEE Trans. on Communications*, June 2013.

[42] A.G. Burr. Capacity bounds and estimates for the finite scatterers MIMO wireless channel. *IEEE Journal on Selected Areas in Communications*, June 2003.

[43] Søren Skovgaard Christensen, Rajiv Agarwal, Elisabeth De Carvalho, and John M Cioffi. Weighted sum-rate maximization using weighted mmse for mimo-bc beamforming design. *IEEE Transactions on Wireless Communications*, 7(12):4792–4799, 2008.

[44] Qingjiang Shi, Meisam Razaviyayn, Zhi-Quan Luo, and Chen He. An iteratively weighted mmse approach to distributed sum-utility maximization for a mimo interfering broadcast channel. *IEEE Transactions on Signal Processing*, 59(9):4331–4340, 2011.

[45] L.T. Watson. Globally Convergent Homotopy Methods: A Tutorial. *Applied Mathematics and Computation*, May 1989.

[46] D.M. Malioutov, M. Çetin, and A.S. Willsky. Homotopy Continuation for Sparse Signal Representation. In *IEEE Int'l Conf. Acoust. Speech Sig. Proc. (ICASSP)*, 2005.

[47] R.A. Horn and C.R. Johnson. *Matrix Analysis*. Cambridge Univ. Press, 2 edition, 2013.

Appendix A

Determining Variable Count in Interference Alignment Equations

The interference alignment equation $\boldsymbol{U}_{dl,k}^{H}\boldsymbol{H}_{k,l}\boldsymbol{V}_{ul,l} = 0$ remains unaffected whether it's multiplied before or after by non-singular square mixing matrices. Thus, the true variables Tx/Rx can be disclosed by parameterizing the precoders $\boldsymbol{V}_{ul,l}$ and decoders $\boldsymbol{U}_{dl,k}$ in the following manner:

$$\boldsymbol{U}_{dl,k} = \begin{bmatrix} \boldsymbol{I}_{d_{dl,k}} \\ \bar{\boldsymbol{U}}_{dl,k} \end{bmatrix}, \boldsymbol{V}_{ul,l} = \begin{bmatrix} \boldsymbol{I}_{d_{ul,l}} \\ \bar{\boldsymbol{V}}_{ul,l} \end{bmatrix} \tag{A.1}$$

Here, matrices $\bar{\boldsymbol{U}}_{dl,k}$ and $\bar{\boldsymbol{V}}_{ul,l}$ are of dimensions $(N_{dl,k}-d_{dl,k})\times d_{dl,k}$ and $(N_{ul,l}-d_{ul,l})\times d_{ul,l}$ respectively. Therefore, the total number of variables corresponds to the total number of elements in matrices $\bar{\boldsymbol{U}}_{dl,k}$ and $\bar{\boldsymbol{V}}_{ul,l}$, which can be calculated as $\sum_{k=1}^{K_{dl}} d_{dl,k}(N_{dl,k} - d_{dl,k}) + \sum_{l=1}^{K_{ul}} d_{ul,l}(N_{ul,l} - d_{ul,l})$.

Appendix B

Proof of Theorem 3: Necessary and Sufficient Condition for interference alignment Feasibility in a Regular MIMO IBMAC-IC

Within this appendix, we delve into the intricate details of Theorem 3, where we rigorously establish the requisite and comprehensive condition for achieving the feasibility of interference alignment. To this end, we provide a detailed analysis of the interference by shedding light on the channel matrices and the Beamformers at Tx and Rx to find a solution for equation (2.2). We revisit the feasibility analysis framework of [22], [21], and [20]. From the analysis in [22],[21], we know that the linear interference alignment will be feasible for generic channel coefficients. An interference alignment solution for channels $\boldsymbol{H}_{k,l}$ in (2.2) will be feasible if and only if a perturbed interference alignment solution $\boldsymbol{U}_{dl,k} + d\boldsymbol{U}_{dl,k}$ and $\boldsymbol{V}_{ul,l} + d\boldsymbol{V}_{ul,l}$ exists for perturbed channels $\boldsymbol{H}_{kl} + d\boldsymbol{H}_{kl}$:

$$(\boldsymbol{U}_{dl,k}^{H} + d\boldsymbol{U}_{dl,k}^{H})(\boldsymbol{H}_{k,l} + d\boldsymbol{H}_{k,l})(\boldsymbol{V}_{ul,l} + d\boldsymbol{V}_{ul,l}) = 0 \, . \tag{B.1}$$

The "if" part follows from considering that (2.2) becomes a special case of (B.1) when the perturbations disappear. The "only if" part follows from the philosophy of homotopy methods [45], [46] in which the solution of any instance of the problem (here for the given channel matrices) can be obtained by an analytical continuation of the solution at any particular instance (which will correspond here to a particular choice of the channel matrices). The particular instance is typically chosen to allow analytical problem solvability. The analytical continuation works as long as a Jacobian appearing in the problem continues to have full rank. This Jacobian will appear here also. For arbitrarily small perturbations (as in the homotopy method), expanding the products in (B.1) and considering only first-order perturbations, we get:

$$\boldsymbol{U}_{dl,k}^{H}\boldsymbol{H}_{k,l}\, d\boldsymbol{V}_{ul,l} + d\boldsymbol{U}_{dl,k}^{H}\boldsymbol{H}_{k,l}\boldsymbol{V}_{ul,l} = -\boldsymbol{U}_{dl,k}^{H} d\boldsymbol{H}_{k,l}\, \boldsymbol{V}_{ul,l} \tag{B.2}$$

which need to be considered jointly for all interference links, and all Tx/Rx involved. (B.2) means that the feasibility of the bi-linear equations (2.2) is equivalent to the feasibility of the linear equations (B.2), which can be rewritten jointly in the form $\boldsymbol{J}\boldsymbol{x} = -\boldsymbol{b}$.

To identify the Jacobian $\boldsymbol{J}$, continue to consider link (k,l), for which we can obtain $\boldsymbol{J}_{kl}\boldsymbol{x}_{kl} = -\boldsymbol{b}_{kl} = -\text{vec}(\boldsymbol{U}_{dl,k}^H d\boldsymbol{H}_{k,l}\,\boldsymbol{V}_{ul,l})$ by taking vec(.) of both sides of (B.2):

$$\text{vec}(\boldsymbol{U}_{dl,k}^H \boldsymbol{H}_{k,l}\, d\boldsymbol{V}_{ul,l}) = (\boldsymbol{I}_{d_{ul,l}} \otimes \boldsymbol{U}_{dl,k}^H \boldsymbol{H}_{k,l})\,\text{vec}(d\boldsymbol{V}_{ul,l}) \tag{B.3a}$$

$$\text{vec}(d\boldsymbol{U}_{dl,k}^H \boldsymbol{H}_{k,l}\, \boldsymbol{V}_{ul,l}) = ((\boldsymbol{H}_{k,l}\boldsymbol{V}_{ul,l})^T \otimes \boldsymbol{I}_{d_{dl,k}})\,\text{vec}(d\boldsymbol{U}_{dl,k}^H) \tag{B.3b}$$

Then we get for link (k,l) the system $\boldsymbol{J}_{kl}\boldsymbol{x}_{kl} = -\boldsymbol{b}_{kl}$ with

$$\boldsymbol{x}_{kl} = \begin{bmatrix} \text{vec}(d\boldsymbol{V}_{ul,l})^T & \text{vec}(d\boldsymbol{U}_{dl,k}^H)^T \end{bmatrix}^T, \tag{B.4}$$

$$\boldsymbol{J}_{kl} = \begin{bmatrix} \boldsymbol{I}_{d_{ul,l}} \otimes \boldsymbol{U}_{dl,k}^H \boldsymbol{H}_{k,l} & (\boldsymbol{H}_{k,l}\boldsymbol{V}_{ul,l})^T \otimes \boldsymbol{I}_{d_{dl,k}}\,. \end{bmatrix} \tag{B.5}$$

Now, the ZF conditions in (2.2) are insensitive to pre or post-multiplication by non-singular square mixing matrices, or in other words, only the column spaces of the Rx/Tx filters $\boldsymbol{U}_{dl,k}$, $\boldsymbol{V}_{ul,l}$ matter. The actual available Rx/Tx variables are revealed by parameterizing the precoders and decoders as:

$$\boldsymbol{U}_{dl,k} = \begin{bmatrix} \boldsymbol{I}_{d_{dl,k}} \\ \bar{\boldsymbol{U}}_{dl,k} \end{bmatrix}, \boldsymbol{V}_{ul,l} = \begin{bmatrix} \boldsymbol{I}_{d_{ul,l}} \\ \bar{\boldsymbol{V}}_{ul,l} \end{bmatrix} \tag{B.6}$$

where $\bar{\boldsymbol{U}}_{dl,k}$ and $\bar{\boldsymbol{V}}_{ul,l}$ are matrices of size $(N_{dl,k} - d_{dl,k}) \times d_{dl,k}$ and $(N_{ul,l} - d_{ul,l}) \times d_{ul,l}$ respectively, and which represent the only part of the $\boldsymbol{U}_{dl,k}$, $\boldsymbol{V}_{ul,l}$ that need/can be perturbed. They represent the variables appearing in the proper conditions. For channels with a continuous Probability density function (pdf), this parameterization is possible w.p. 1 and furthermore guarantees the Rx/Tx filters to have a rank equal to their number of streams d. Now, as in [22],[21], we can simplify the selected channels and associated ZF Rx/Tx filters around which we consider the perturbation. In particular we consider $\bar{\boldsymbol{U}}_{dl,k} = \boldsymbol{0}$ and $\bar{\boldsymbol{V}}_{ul,l} = \boldsymbol{0}$. Now, the partitioning in $\boldsymbol{U}_{dl,k}$, $\boldsymbol{V}_{ul,l}$ leads to a corresponding channel partitioning:

$$\boldsymbol{H}_{kl} = \begin{bmatrix} \boldsymbol{H}_{kl}^{(1)} & \boldsymbol{H}_{kl}^{(2)} \\ \boldsymbol{H}_{kl}^{(3)} & \boldsymbol{H}_{kl}^{(4)} \end{bmatrix} = \begin{bmatrix} \boldsymbol{0}_{d_{dl,k} \times d_{ul,l}} & \boldsymbol{H}_{kl}^{(2)} \\ \boldsymbol{H}_{kl}^{(3)} & \boldsymbol{0}_{(N_{dl,k}-d_{dl,k}) \times (N_{ul,l}-d_{ul,l})} \end{bmatrix}. \tag{B.7}$$

Indeed, with $\bar{\boldsymbol{U}}_{dl,k} = \boldsymbol{0}$, $\bar{\boldsymbol{V}}_{ul,l} = \boldsymbol{0}$, the ZF condition (2.2) becomes $\boldsymbol{U}_{dl,k}^H \boldsymbol{H}_{k,l}\, \boldsymbol{V}_{ul,l} = \boldsymbol{H}_{kl}^{(1)} = \boldsymbol{0}$. On the other hand, with these same Rx/Tx filters, the interference alignment perturbation does not involve $\boldsymbol{H}_{kl}^{(4)}$ which we can hence take to be zero. Though the

introduction of zeros in $\boldsymbol{H}_{kl}$ may lead to rank reduction, this has no effect as long as the resulting $\text{rank}(\boldsymbol{H}_{kl}) \geq \max(d_{dl,k}, d_{ul,l})$. Now we get for the perturbed system feasibility:

$$\begin{bmatrix} \boldsymbol{I}_{d_{ul,l}} \otimes \boldsymbol{H}_{kl}^{(2)} & \boldsymbol{H}_{kl}^{(3)T} \otimes \boldsymbol{I}_{d_{dl,k}} \end{bmatrix} \begin{bmatrix} \text{vec}(d\bar{\boldsymbol{V}}_{ul,l}) \\ \text{vec}(d\bar{\boldsymbol{U}}_{dl,k}^{H}) \end{bmatrix} = -\text{vec}(d\boldsymbol{H}_{kl}^{(1)}). \tag{B.8}$$

By considering all links, we get the overall system $\boldsymbol{J}\boldsymbol{x} = -\boldsymbol{b}$:

$$\boldsymbol{x}^T = \begin{bmatrix} \text{vec}^T(d\bar{\boldsymbol{V}}_{ul,1}) \cdots \text{vec}^T(d\bar{\boldsymbol{V}}_{ul,K_{ul}}) \text{vec}^T(d\bar{\boldsymbol{U}}_{dl,1}^{H}) \cdots \ \text{vec}^T(d\bar{\boldsymbol{U}}_{dl,K_{dl}}^{H}) \end{bmatrix}, \tag{B.9}$$

$$\boldsymbol{b}^T == \begin{bmatrix} \text{vec}^T(d\boldsymbol{H}_{11}) \cdots \text{vec}^T(d\boldsymbol{H}_{1,K_{ul}}) \cdots \text{vec}^T(d\boldsymbol{H}_{K_{dl},K_{ul}}) \end{bmatrix}, \tag{B.10}$$

$$\boldsymbol{J} = \begin{bmatrix} \boldsymbol{J}_G \, \boldsymbol{J}_F \end{bmatrix} = \underbrace{\begin{bmatrix} \boldsymbol{I}_{d_{ul,1}} \otimes \boldsymbol{H}_{11}^{(2)} & \boldsymbol{0} & (\boldsymbol{H}_{11}^{(3)})^T \otimes \boldsymbol{I}_{d_{dl,1}} & \boldsymbol{0} \\ \vdots & \vdots & \vdots & \vdots \\ \boldsymbol{0} & \boldsymbol{I}_{d_{ul,K_{ul}}} \otimes \boldsymbol{H}_{1K_{ul}}^{(2)} & (\boldsymbol{H}_{1K_{ul}}^{(3)})^T \otimes \boldsymbol{I}_{d_{dl,1}} & \boldsymbol{0} \\ \vdots & \vdots & \vdots & \vdots \\ \boldsymbol{I}_{d_{ul,1}} \otimes \boldsymbol{H}_{K_{dl}1}^{(2)} & \boldsymbol{0} & \boldsymbol{0} & (\boldsymbol{H}_{K_{dl}1}^{(3)})^T \otimes \boldsymbol{I}_{d_{dl,K_{dl}}} \\ \vdots & \vdots & \vdots & \vdots \\ \boldsymbol{0} & \boldsymbol{I}_{d_{ul,K_{ul}}} \otimes \boldsymbol{H}_{K_{dl}K_{ul}}^{(2)} & \boldsymbol{0} & (\boldsymbol{H}_{K_{dl}K_{ul}}^{(3)})^T \otimes \boldsymbol{I}_{d_{dl,K_{dl}}} \end{bmatrix}}_{\boldsymbol{J}_G \qquad\qquad\qquad\qquad\qquad\qquad \boldsymbol{J}_F} \tag{B.11}$$

The dimensions of the submatrices that constitute the matrix $\boldsymbol{J}$ are specified as follows:

- The block $\boldsymbol{I}_{d_{ul,l}} \otimes \boldsymbol{H}_{kl}^{(2)}$ in $\boldsymbol{J}_G$ has dimensions $d_{ul,l}d_{dl,k} \times d_{ul,l}(N_{ul,l} - d_{ul,l})$,
- The block $(\boldsymbol{H}_{kl}^{(3)})^T \otimes \boldsymbol{I}_{d_{dl,k}}$ in $\boldsymbol{J}_F$ has dimensions $d_{ul,l}d_{dl,k} \times (N_{dl,k} - d_{dl,k})d_{dl,k}$,
- The dimensions for the matrix $\boldsymbol{J}_G$ are $\sum_{l=1}^{K_{ul}} \sum_{k=1}^{K_{dl}} d_{ul,l}d_{dl,k} \times \sum_{l=1}^{K_{ul}} (N_{ul,l} - d_{ul,l})d_{ul,l}$,
- The dimension for the matrix $\boldsymbol{J}_F$ are $\sum_{l=1}^{K_{ul}} \sum_{k=1}^{K_{dl}} d_{ul,l}d_{dl,k} \times \sum_{k=1}^{K_{dl}} (N_{dl,k} - d_{dl,k})d_{dl,k}$.

Appendix C

Proof of Theorem 4: Sufficient Condition for IA Feasibility in a Regular MIMO IBMAC-IC

For the ease of understanding of the following proof, we can divide $\boldsymbol{J}_F$ and $\boldsymbol{J}_G$ into sub-matrices $\boldsymbol{J}_{F_k}$ and $\boldsymbol{J}_{G_l}$ respectively, regarding the k^{th} receiver, such as:

$$\boldsymbol{J} = \begin{bmatrix} \boldsymbol{J}_{G_1} & \boldsymbol{J}_{F_1} & \mathbf{0} & \mathbf{0} & \mathbf{0} \\ \boldsymbol{J}_{G_2} & \mathbf{0} & \boldsymbol{J}_{F_2} & \mathbf{0} & \mathbf{0} \\ \vdots & \vdots & & \ddots & \vdots \\ \boldsymbol{J}_{G_{K_{dl}}} & \mathbf{0} & \mathbf{0} & \mathbf{0} & \boldsymbol{J}_{F_{K_{dl}}} \end{bmatrix} \tag{C.1}$$

For each receiver $k \in [1, \ldots, K_{dl}]$, the matrices $\boldsymbol{J}_{F_k}$ and $\boldsymbol{J}_{G_l}$ are given by (C.2) and (C.3) respectively:

$$\boldsymbol{J}_{F_k} = \begin{bmatrix} \boldsymbol{J}_{F_{k1}}^T & \boldsymbol{J}_{F_{k2}}^T & \ldots & \boldsymbol{J}_{F_{kK_{ul}}}^T \end{bmatrix}^T \tag{C.2}$$

$$\boldsymbol{J}_{G_k} = \begin{bmatrix} \boldsymbol{J}_{G_{k1}} & \mathbf{0} & \ldots & \mathbf{0} \\ \mathbf{0} & \boldsymbol{J}_{G_{k2}} & \ldots & \mathbf{0} \\ \vdots & & \ddots & \vdots \\ \mathbf{0} & \ldots & \mathbf{0} & \boldsymbol{J}_{G_{kK_{ul}}} \end{bmatrix} \tag{C.3}$$

With $l \in [1, \ldots, K_{ul}]$, we have:

$$\boldsymbol{J}_{F_{kl}} = \boldsymbol{H}_{kl}^{(3)\,T} \otimes \boldsymbol{I}_{d_{dl,k}} \tag{C.4a}$$

$$\boldsymbol{J}_{G_{kl}} = \boldsymbol{I}_{d_{ul,l}} \otimes \boldsymbol{H}_{kl}^{(2)} \tag{C.4b}$$

We prove here that for any system $(N_{dl,k}, N_{ul,l}, d_{dl,k}, d_{ul,l})$ satisfying Theorem 4, the associated matrix $\boldsymbol{J}$ to this system can be transformed to a permutation matrix with a rank equal to the number of rows of $\boldsymbol{J}$, i.e. $\boldsymbol{J}$ is a full row matrix, thus the IA is feasible. This transformation can be done following the coming steps acting on $\boldsymbol{J}_F$ then on $\boldsymbol{J}_G$ side, we call this proof as *Diagonal Shift method*:

- **Building Diagonals on $\boldsymbol{J}_F$**:
  - *First diagonal:* On the given matrix $\boldsymbol{J}$ at $\boldsymbol{J}_F$, we choose the longest diagonal*** from the 1^{st} element of $\boldsymbol{J}_{F_1}$ and we put to zero the other elements in the rows including this diagonal, we note the number of elements of this diagonal as n_1. If n_1 is equal or smaller than the number of rows of $\boldsymbol{J}_{F_1}$, we set the variable sh to 0 or 1 respectively,
  - *Second diagonal:* We choose the longest diagonal from the element at the 1^{st} column and the $(sh \times d_{dl,2} + 1)^{th}$ row of $\boldsymbol{J}_{F_2}$, i.e. the diagonal is shift down by $sh \times d_{dl,2}$ elements. We put to zero the other elements in the rows including this diagonal. We note the number of elements of this diagonal as n_2. If n_2 is equal or smaller than the number of rows of $\boldsymbol{J}_{F_2}$, we don't increment sh or we increment by 1 respectively,

    $\vdots$
  - K_{dl}^{th} *diagonal:* We choose the longest diagonal from the element at the 1^{st} column and the $(sh \times d_{dl,K_{dl}} + 1)^{th}$ row of $\boldsymbol{J}_{F_{K_{dl}}}$, i.e. the diagonal is shift down by $sh\, d_{dl,K_{dl}}$ elements.We put to zero the other elements in the rows including this diagonal.

- **Choosing elements from $\boldsymbol{J}_G$**:
  The following process is done for each $k \in [1, \ldots, K_{dl}]$:
  Whenever n_k, with $k \in [1, \ldots, K_{dl}]$, is smaller than the number of rows of $\boldsymbol{J}_{F_k}$ noted as m_k, we work on the $m_k - n_k$ remaining rows of $\boldsymbol{J}$ that don't include element from the previous chosen diagonals on $\boldsymbol{J}_{F_k}$.
  For those rows, we choose $m_k - n_k$ elements from $\boldsymbol{J}_{G_k}$. The column and row of each chosen element should be different from each other and also different from the previously selected element in $\boldsymbol{J}_{G_1}$, ... , $\boldsymbol{J}_{G_{k-1}}$.

***: Our longest diagonal should take n elements for a matrix $\boldsymbol{A} \in (m \times n)$ with $m \geq n$, it begins always at the 1^{st} column of $\boldsymbol{A}$:

- If the diagonal begins at the i^{th} row with $i \leq (m - n + 1)$, the diagonal will end at the n^{th} column and the $(i + n - 1)^{th}$ row;
- If the diagonal begins at i^{th} row with $i > (m - n + 1)$; the diagonal will be stopped at the $(m - i + 1)^{th}$ column and the m^{th} row and goes forward from $(m - i + 2)^{th}$ column and the 1^{st} row.

Appendix D

Proof of Theorem 6: Local Proper Condition for Interference Alignment Feasibility in a Reduced rank MIMO IBMAC-IC

Here we prove the constraints on $\boldsymbol{z}_{k,l}^R$, $\boldsymbol{z}_{k,l}^T$ appearing in (4.8), esp. for the case $(1_{k,l}^R, 1_{k,l}^T) = (1,1)$:

Case $r \leq \min(d_{dl}, d_{ul})$

(2.2) can be rewritten as

$$\boldsymbol{U}_{dl,k}^H \boldsymbol{B}_{k,l} \boldsymbol{A}_{k,l}^H \boldsymbol{V}_{ul,l} = 0\,. \tag{D.1}$$

An application of Sylvester's rank inequality to (D.1) yields

$$\operatorname{rank}(\boldsymbol{B}_k^H \boldsymbol{U}_{dl,k}) + \operatorname{rank}(\boldsymbol{A}_{k,l}^H \boldsymbol{V}_{ul,l}) \leq r_{k,l}\,. \tag{D.2}$$

We can choose $\boldsymbol{B}_k^H \boldsymbol{U}_{dl,k}$ to have $\boldsymbol{z}_{k,l}^R$ zero rows and $\boldsymbol{A}_k^H \boldsymbol{G}_{k,l}$ to have $\boldsymbol{z}_{k,l}^t$ zero rows so that $\boldsymbol{z}_{k,l}^R + \boldsymbol{z}_{k,l}^T = r_{k,l}$. The optimized values for $\boldsymbol{z}_{k,l}^R$, $\boldsymbol{z}_{k,l}^T$ depend on the other variables d_{dl}, d_{ul}, N_{ul}, N_{dl}, K_{ul} and K_{dl}. We see that when $r \leq \min(d_{dl}, d_{dl})$, the case $(1_{k,l}^R, 1_{k,l}^T) = (1,1)$ leads to a distributed design: the design of $\boldsymbol{U}_{dl,k}$ depends only on the factor $\boldsymbol{B}_{k,l}$ in $\boldsymbol{H}_{k,l}$ and not on $\boldsymbol{V}_{ul,l}$, and similarly $\boldsymbol{V}_{ul,l}$ only depends on $\boldsymbol{A}_{k,l}$.

Case $r \geq \max(d_{dl}, d_{ul})$

In this case $\boldsymbol{U}_{dl,k}^H \boldsymbol{H}_{k,l} \boldsymbol{V}_{ul,l}$ is a priori full rank, in the case of arbitrary Tx/Rx. Here we assume a uniformity of the number of zeros produced by the columns (beamformers) in $\boldsymbol{U}_{dl,k}$ and $\boldsymbol{V}_{ul,l}$. Let $\boldsymbol{U}_{dl,k}$ now produce $\boldsymbol{z}_{k,l}^R$ zeros in each row of the matrix product $\boldsymbol{U}_{dl,k}^H \boldsymbol{H}_{k,l} \boldsymbol{V}_{ul,l}$, i.e. in total it produces $d_{dl,k} \boldsymbol{z}_{k,l}^R$ zeros (the position of the zeros in each row may be different so that the number of non-zeros per column is also equal between all columns). Then let $\boldsymbol{V}_{ul,l}$ produce $\boldsymbol{z}_{k,l}^T$ zeros in each column, with the constraint that

we produce a total of $d_{dl,k}\boldsymbol{z}_{k,l}^R + d_{ul,l}\boldsymbol{z}_{k,l}^T = d_{dl,k}d_{ul,l}$ zeros. In this case, the design of $\boldsymbol{U}_{dl,k}$ and $\boldsymbol{V}_{ul,l}$ is clearly coupled.

Now, in the combination of the two cases above, care has to be taken with the limiting cases $\boldsymbol{z}_{k,l}^R = 0$ or $\boldsymbol{z}_{k,l}^T = 0$, corresponding to one-sided ZF. In that case we have linear ZF equations representing a number of ZF constraints equal to the rank of the matrix of coefficients, as mentioned in the discussion of the cases $(\mathbf{1}_{\boldsymbol{z}_{k,l}^R}, \mathbf{1}_{\boldsymbol{z}_{k,l}^T}) = (1_{k,l}^R, 1_{k,l}^T) = (1, 0)$ or $(0, 1)$. This results in the first condition appearing in (4.8).

Case $d_{dl} < r < d_{ul}$ or $d_{ul} < r < d_{dl}$

Consider w.l.o.g. the case $d_{dl} < r < d_{ul}$. In this case let $\boldsymbol{U}_{dl,k}$ produce $\boldsymbol{z}_{k,l}^R$ rows of zeros in $\boldsymbol{B}_{k,l}^H\boldsymbol{U}_{dl,k}$ as in the first case. Then for $\boldsymbol{V}_{ul,l}$ to produce $\boldsymbol{U}_{dl,k}^H\boldsymbol{H}_{k,l}\boldsymbol{V}_{ul,l} = 0$ imposes on it a number of ZF constraints of $\boldsymbol{z}_{k,l}^T = \text{rank}(\boldsymbol{U}_{dl,k}^H\boldsymbol{H}_{k,l}) = \min(d_{dl,k}, r_{k,l} - \boldsymbol{z}_{k,l}^R)$, [35, Lemma 1]. In this case $\boldsymbol{U}_{dl,k}$ is decoupled from $\boldsymbol{V}_{ul,l}$ but $\boldsymbol{V}_{ul,l}$ is coupled to $\boldsymbol{U}_{dl,k}$.

Appendix E

Proof of Theorem 7: Necessary and Sufficient Condition for Interference Alignment Feasibility in a Reduced rank MIMO IBMAC-IC

For the case of rank deficient interfering channels, we consider the channel factorization in (4.1), combined with the channel partitioning in (B.7), leading to:

$$\boldsymbol{A}_{kl}^{H} = \begin{bmatrix} \boldsymbol{A}_{kl}^{(1)} & \boldsymbol{A}_{kl}^{(2)} \end{bmatrix}, \; \boldsymbol{B}_{kl}^{H} = \begin{bmatrix} \boldsymbol{B}_{kl}^{(1)} & \boldsymbol{B}_{kl}^{(2)} \end{bmatrix}. \tag{E.1}$$

The matrix blocks $\boldsymbol{A}_{kl}^{(1)}$ and $\boldsymbol{B}_{kl}^{(1)}$ have dimensions $r_{kl} \times d_{ul,l}$ and $r_{kl} \times d_{dl,k}$ respectively. So (B.7) becomes:

$$\boldsymbol{H}_{kl} = \begin{bmatrix} \boldsymbol{O}_{d_{dl,k} \times d_{ul,l}} & \boldsymbol{B}_{kl}^{(1)H} \boldsymbol{A}_{kl}^{(2)} \\ \boldsymbol{B}_{kl}^{(2)H} \boldsymbol{A}_{kl}^{(1)} & \boldsymbol{B}_{kl}^{(2)H} \boldsymbol{A}_{kl}^{(2)} \end{bmatrix} \tag{E.2}$$

where again $\boldsymbol{H}_{kl}^{(4)} = \boldsymbol{B}_{kl}^{(2)H} \boldsymbol{A}_{kl}^{(2)}$ will not appear further in the analysis. Nevertheless, the structure in (4.1), (E.2) assumes that the following requirements are satisfied:

- To have $\boldsymbol{H}_{kl}^{(1)} = \boldsymbol{B}_{kl}^{(1)H} \boldsymbol{A}_{kl}^{(1)} = \boldsymbol{0}$, we can take $\boldsymbol{A}_{kl}^{(1)}$ with n_{kl} rows equal to zero, and $\boldsymbol{B}_{kl}^{(1)}$ with the complementary $r_{kl} - n_{kl}$ rows equal to zero.
- The channel model in (4.1) assumes $\text{rank}(\boldsymbol{A}_{kl}) = \text{rank}(\boldsymbol{B}_{kl}) = r_{kl}$.
- With $\text{rank}(\boldsymbol{A}_{kl}^{(1)}) = \min(r_{kl} - n_{kl}, d_{ul,l})$, $\boldsymbol{A}_{kl}^{(2)}$ should have the complementary rank to have $\text{rank}(\boldsymbol{A}_{kl}) = r_{kl}$. Hence the number of columns of $\boldsymbol{A}_{kl}^{(2)}$ needs to satisfy: $N_{ul,l} - d_{ul,l} \geq r_{kl} - \min(r_{kl} - n_{kl}, d_{ul,l})$,

- Same discussion for $\boldsymbol{B}_{kl}$, so we need to have $N_{dl,k} - d_{dl,k} \geq r_{kl} - \min(n_{kl}, d_{dl,k})$.

In what follows, we shall assume that all these conditions are met. On the other hand, in the rank deficient case, also the channel perturbation exhibits structure:

$$\mathrm{vec}(d\boldsymbol{H}_{kl}^{(1)}) = \mathrm{vec}(d\boldsymbol{B}_{kl}^{(1)H}\boldsymbol{A}_{kl}^{(1)}) + \mathrm{vec}(\boldsymbol{B}_{kl}^{(1)H}\, d\boldsymbol{A}_{kl}^{(1)}) \tag{E.3}$$

Now exploiting the channel structure in (E.2), $\boldsymbol{J}_G$ and $\boldsymbol{J}_F$ in (B.11) (with $\boldsymbol{J} = [\boldsymbol{J}_G \;\; \boldsymbol{J}_F]$) can be written as:

$$\boldsymbol{J}_G = \begin{bmatrix} & \\ \boldsymbol{I}_{d_{ul,1}} \otimes \boldsymbol{B}_{11}^{(1)H}\boldsymbol{A}_{11}^{(2)} & \boldsymbol{0} \\ \vdots & \vdots \\ \boldsymbol{0} & \boldsymbol{I}_{d_{ul,K_{ul}}} \otimes \boldsymbol{B}_{1K_{ul}}^{(1)H}\boldsymbol{A}_{1K_{ul}}^{(2)} \\ \vdots & \vdots \\ \boldsymbol{I}_{d_{ul,1}} \otimes \boldsymbol{B}_{K_{dl}1}^{(1)H}\boldsymbol{A}_{K_{dl}1}^{(2)} & \boldsymbol{0} \\ \vdots & \vdots \\ \boldsymbol{0} & \boldsymbol{I}_{d_{ul,K_{ul}}} \otimes \boldsymbol{B}_{K_{dl}K_{ul}}^{(1)H}\boldsymbol{A}_{K_{dl}K_{ul}}^{(2)} \end{bmatrix} \tag{E.4}$$

$$\boldsymbol{J}_F = \begin{bmatrix} & \\ (\boldsymbol{B}_{11}^{(2)H}\boldsymbol{A}_{11}^{(1)})^T \otimes \boldsymbol{I}_{d_{dl,1}} & \boldsymbol{0} \\ \vdots & \vdots \\ (\boldsymbol{B}_{1K_{ul}}^{(2)H}\boldsymbol{A}_{1K_{ul}}^{(1)})^T \otimes \boldsymbol{I}_{d_{dl,1}} & \boldsymbol{0} \\ \vdots & \vdots \\ \boldsymbol{0} & (\boldsymbol{B}_{K_{dl}1}^{(2)H}\boldsymbol{A}_{K_{dl}1}^{(1)})^T \otimes \boldsymbol{I}_{d_{dl,K_{dl}}} \\ \vdots & \vdots \\ \boldsymbol{0} & (\boldsymbol{B}_{K_{dl}K_{ul}}^{(2)H}\boldsymbol{A}_{K_{dl}K_{ul}}^{(1)})^T \otimes \boldsymbol{I}_{d_{dl,K_{dl}}} \end{bmatrix} \tag{E.5}$$

For $\boldsymbol{b}$ in $\boldsymbol{J}\,\boldsymbol{x} = -\boldsymbol{b}$, we consider the following vectorization:

$$\begin{aligned} &vec(d\boldsymbol{H}_{kl}^{(1)}) = vec(\boldsymbol{B}_{kl}^{(1)H}\, d\boldsymbol{A}_{kl}^{(1)}) + vec(d\boldsymbol{B}_{kl}^{(1)H}\, \boldsymbol{A}_{kl}^{(1)}) = \\ &(\boldsymbol{I}_{d_{ul,l}} \otimes \boldsymbol{B}_{kl}^{(1)H})\, vec(d\boldsymbol{A}_{kl}^{(1)}) + (\boldsymbol{A}_{kl}^{(1)T} \otimes \boldsymbol{I}_{d_{dl,k}})\, vec(d\boldsymbol{B}_{kl}^{(1)H}) \end{aligned} \tag{E.6}$$

Hence the vector $\boldsymbol{b}$ can be written as $\boldsymbol{b} = \boldsymbol{J}_H \boldsymbol{x}_H$ with:

$$\boldsymbol{J}_H = \underbrace{\begin{bmatrix} (\boldsymbol{I}_{d_{ul,1}} \otimes \boldsymbol{B}_{11}^{(1)H}) & \boldsymbol{0} & (\boldsymbol{A}_{11}^{(1)T} \otimes \boldsymbol{I}_{d_{dl,1}}) & \boldsymbol{0} \\ \vdots & \vdots & \vdots & \vdots \\ \boldsymbol{0} & (\boldsymbol{I}_{d_{ul,K_{ul}}} \otimes \boldsymbol{B}_{K_{dl}K_{ul}}^{(1)H}) & \boldsymbol{0} & (\boldsymbol{A}_{K_{dl}K_{ul}}^{(1)T} \otimes \boldsymbol{I}_{d_{dl,K_{dl}}}) \end{bmatrix}}_{\boldsymbol{J}_B \qquad\qquad\qquad\qquad\qquad\qquad \boldsymbol{J}_A} \tag{E.7}$$

$$\boldsymbol{x}_H^T = \begin{bmatrix} vec(d\boldsymbol{A}_{11}^{(1)})^T & \dots & vec(d\boldsymbol{A}_{K_{dl}K_{ul}}^{(1)})^T & vec(d\boldsymbol{B}_{11}^{(1)})^T & \dots & vec(d\boldsymbol{B}_{K_{dl}K_{ul}}^{(1)})^T \end{bmatrix} \tag{E.8}$$

For the purpose of further analysis, it may be of interest to note that we can write $\boldsymbol{J}$ as $\boldsymbol{J} = \boldsymbol{J}_H \boldsymbol{T}$ where $\boldsymbol{T}$ is given by :

$$\boldsymbol{T} = \begin{bmatrix} \boldsymbol{T}_A & 0 \\ 0 & \boldsymbol{T}_B \end{bmatrix} \tag{E.9}$$

$$\boldsymbol{T}_A = \begin{bmatrix} \boldsymbol{I}_{d_{ul,1}} \otimes \boldsymbol{A}_{11}^{(2)} & \boldsymbol{0} \\ \vdots & \vdots \\ \boldsymbol{0} & \boldsymbol{I}_{d_{ul,K_{ul}}} \otimes \boldsymbol{A}_{1K_{ul}}^{(2)} \\ \vdots & \vdots \\ \boldsymbol{I}_{d_{ul,1}} \otimes \boldsymbol{A}_{K_{dl}1}^{(2)} & \boldsymbol{0} \\ \vdots & \vdots \\ \boldsymbol{0} & \boldsymbol{I}_{d_{ul,K_{ul}}} \otimes \boldsymbol{A}_{K_{dl}K_{ul}}^{(2)} \end{bmatrix} \tag{E.10}$$

$$\boldsymbol{T}_B = \begin{bmatrix} \boldsymbol{B}_{11}^{(2)H} \otimes \boldsymbol{I}_{d_{dl,1}} & \mathbf{0} \\ \vdots & \vdots \\ \boldsymbol{B}_{1K_{ul}}^{(2)H} \otimes \boldsymbol{I}_{d_{dl,1}} & \mathbf{0} \\ \vdots & \vdots \\ \mathbf{0} & \boldsymbol{B}_{K_{dl}1}^{(2)H} \otimes \boldsymbol{I}_{d_{dl,K_{dl}}} \\ \vdots & \vdots \\ \mathbf{0} & \boldsymbol{B}_{K_{dl}K_{ul}}^{(2)H} \otimes \boldsymbol{I}_{d_{dl,K_{dl}}} \end{bmatrix} \tag{E.11}$$

Note the following dimensions:

- The blocks $(\boldsymbol{I}_{d_{ul,l}} \otimes \boldsymbol{B}_{kl}^{(1)H})$ in $\boldsymbol{J}_B$ has the dimension $d_{ul,l}d_{dl,k} \times d_{ul,l}r_{kl}$,
- The blocks $(\boldsymbol{A}_{kl}^{(1)T} \otimes \boldsymbol{I}_{d_{dl,k}})$ in $\boldsymbol{J}_A$ has the dimension $d_{ul,l}d_{dl,k} \times r_{kl}d_{dl,k}$,
- The blocks $\boldsymbol{I}_{ul,l} \otimes \boldsymbol{A}_{kl}^{(2)}$ in $\boldsymbol{T}_A$ has the dimension $d_{ul,l}r_{kl} \times d_{ul,l}(N_{ul,l} - d_{ul,l})$,
- The blocks $\boldsymbol{B}_{kl}^{(2)H} \otimes \boldsymbol{I}_{d_{dl,k}}$ in $\boldsymbol{T}_B$ has the dimension $r_{kl}d_{dl,k} \times (N_{dl,k} - d_{dl,k})d_{dl,k}$.

Now we define the augmented matrix $\boldsymbol{J}_J$ as:

$$\boldsymbol{J}_J = [\boldsymbol{J} \;\; \boldsymbol{J}_H] \tag{E.12}$$

The condition presented in [47, page 12] can be summarized as follows: a linear system, represented as $\boldsymbol{A}\boldsymbol{x} = \boldsymbol{b}$, is consistent (meaning it has at least one solution) if and only if the rank of the augmented matrix $[\boldsymbol{A} \;\; \boldsymbol{b}]$ is equal to the rank of $\boldsymbol{A}$. Therefore, the existence of a solution for our system $\boldsymbol{J}\boldsymbol{x} = \boldsymbol{b}$ implies that $\text{rank}([\boldsymbol{J} \;\; \boldsymbol{b}]) = \text{rank}(\boldsymbol{J})$. In the case of a rank-deficient channel, this condition can be expressed as $\text{rank}([\boldsymbol{J} \;\; \boldsymbol{J}_H\boldsymbol{x}_H]) = \text{rank}(\boldsymbol{J})$, which should hold for any vector $\boldsymbol{x}_H$. Consequently, this necessitates that $\text{rank}([\boldsymbol{J} \;\; \boldsymbol{J}_H]) = \text{rank}(\boldsymbol{J})$.